Aus dem Institut für Geflügelkrankheiten
des Fachbereichs Veterinärmedizin
der Freien Universität Berlin
in Kooperation mit dem
Forschungszentrum Borstel
Leibniz-Zentrum für Medizin und Biowissenschaften
Laborgruppe Immunbiologie

The contribution of mast cells to antiviral immune responses: Characterization and functional definition of receptor transporter protein 4 (RTP4)

Inaugural-Dissertation
zur Erlangung des Grades eines
Doktors der Veterinärmedizin
an der
Freien Universität Berlin

vorgelegt von
Diego Andrés Goyeneche Patiño
Tierarzt
aus Bogotá, Kolumbien.

Berlin, 2012

Journal-Nr.: 3608

Gedruckt mit Genehmigung
des Fachbereichs Veterinärmedizin
der Freien Universität Berlin

Dekan:	Univ.-Prof. Dr. Jürgen Zentek
Erster Gutachter:	Univ.-Prof. Dr. Hafez Mohamed Hafez
Zweiter Gutachter:	PD. Dr. Holger Heine
Dritter Gutachter:	Univ.-Prof. Dr. Susanne Hartmann

Deskriptoren (nach CAB-Thesaurus):
Mast cells, immune response, viral infections, interferon, G proteins

Tag der Promotion: 19.03.2013

A mis madres
y a mi Toto (R.I.P)

Table of contents

List of figures

Page.

List of Tables

Page.

List of abbreviations

Abbreviation	Term
2D-DIGE	2D-differential gel electrophoresis
5'ppp	5' triphosphorylated ends
7TM	Seven trans-membrane domain
aa	Aminoacids
Ab	Antibody
ADRP	Adipose differentiation-related protein
Ag	Antigen
AIM2	Absent in melanoma 2
AP-1	activator protein-1
APC	Allophycocyanin
APS	Ammonium persulfate
ATP	Adenosin triphosphate
BMDC	Bone marrow derived dendritic cells
BMM	Bone marrow derived macrophages
BMMC	Bone marrow derived mast cells
bp	Base pairs
BSA	Bovine serum albumin
CARD	Caspase activation and recruitment domain
CCL/CXCL	Chemokine ligand
CCL3	MIP1α
CCL4	MIP1β
CCL5	RANTES
CCR	Chemokine receptor
cDNA	Complementary DNA
ConA	Concanavaline A
CpG	C-phosphate-G dinucleotides
CX3CL1	Fractalkine
CXCL10	IP-10
CXCL12	SDF-1
CXCL8	IL-8
DAI	DNA dependent activator of IRFs
DAPI	4',6-diamidino-2-phenylindole, dihydrochloride
DC	Dendritic cell
DEPC	Diethyl pyrocarbonate

DMEM	Dulbeco's modified essential medium
DNA	Deoxyribonucleic acid
dNTPs	Deoxynucleoside triphosphates
dsDNA	Double-stranded DNA
dsRNA	Double-stranded RNA
DTT	Dithiothreitol
EE	Early endosome
EEA1	Early endosome antigen 1
ER	Endoplasmic reticulum
ERK	Extracellular signal-regulated kinase
ES	Embryonic stem cells
FADD	Fas-associated death domain
FCM	Flow cytometry
FCS	Fetal calf serum
FcεR1	Fragment crystallisable region epsilon receptor I
FITC	Fluorescein isothyocyanate
GAPDH	Glyceraldehyde 3-phosphate dehydrogenase
GAS	IFNγ-activated site
GDP	Guanosine diphosphate
GM- CSF	Granulocyte-macrophage colony stimulating factor
GPCR	G protein-coupled receptors
GTP	Guanosine triphosphate
HCV	Hepatitis C virus
HPRT	Hypoxanthine guanine phosphoribosyl transferase
IAV	Influenza A virus
IFN	Interferon
IFNAR	Interferon α/β receptor
Ig	Immunoglobulin
IKK	IκB kinase
IL	Interleukin
IL-1R	Interleukin 1 receptor
IMDM	Iscove´s modified DMEM medium
IO	Ionomycin
IP-10	IFNγ induce protein-10
IPS-1	IFNβ promoter stimulator 1
IRAK	IL-1R associated kinase
IRF	Interferon regulator factor
ISG	Interferon-stimulated genes
ISGF3	Interferon stimulated gene factor 3
ISRE	Interferon stimulated regulatory elements
IκB	inhibitor of kappa B
JAK1	Janus kinase 1
JNK	c-Jun N-terminal kinase
KO	Knockout

LAMP	Lysosomal associated membrane protein
LB	Lipid bodies
LGP2	Laboratory of genetics and physiology 2
LN	Lymph nodes
LPS	Lipopolysaccharide
LRR	Leucin rich region
LT	Leukotriene
MACS	Magnetic associated cells sorting
MAPK	Mitogen activated protein kinases
MC	Mast cells
M-CSF	Macrophage colony stimulating factor
MDA5	Melanoma differentiation associated factor 5
MDCK	Madin Darby canine kidney cells
MHC	Major histocompatibility complex
MIP1α/β	Macrophages inflammatory protein 1α or β
mRNA	Messenger RNA
MyD88	Myeloid differentiation primary response gene (88)
NALP3	NOD-like receptor family pyrin domain containing 3
NDV	Newcastle disease virus
NEMO	NF-kappa B essential modulator
NF-κB	Nuclear factor-kappa B
NK	Natural killer cells
NLR	NOD like receptor
NOD	Nucleotide-binding oligomerization domain
OAS1	2',5'-oligoadenylate synthetase 1
ODGP	N-Octyl-β-D-thioglucopyranoside
Oligo(dT)	Oligo deoxy-thymine nucleotides
OpR	Opioid receptors
OR	Odorant receptors
PAMP	Pathogen-associated molecular pattern
PBL	Peripheral blood lymphocytes
PBS	Phosphate buffered saline
PCR	Polymerase chain reaction
PDI	Protein disulfide isomerase
PE	Phycoerythrin
PFA	Paraformaldehyde
PG	Prostaglandin
PI3K	phosphoinositide 3-kinase
pIC	Polyinosinic polycytidylic acid
PMA	Phorbol 12-myristate 13-acetate
PRR	Pattern recognition receptor
qRT-PCR	Quantitative real time PCR
RANTES	Regulated upon activation, normal T cells expressed and secreted

RD	C-terminal repressor domain
RIG-I	Retinoic acid inducible gene I
RLR	RIG-I like receptors
RNA	Ribonucleic acid
RPMI	Roswell Park Memorial Institute medium
Rsad2	Radical S-adenosyl methionine domain containing 2
RT	Room temperature
RTP4	Receptor transporter protein 4
SBE	STAT3-binding elements
SCF	Stem cell factor
SDF	stromal cell-derived factor-1
SDS	Sodium dodecyl sulfate
SDS-PAGE	SDS-polyacrilamide-gel electrophoresis
SPF	Special pathogen free
ssRNA	Single-stranded RNA
ST2	Interleukin 1 receptor-like 1
STAT	Signal transducer and activator of transcription
STING	Stimulator of interferon genes
TAB	TAK1 kinase binding
TAK	TGFβ activated kinase
TANK	TRAF-associated NF-κB activator
TBK1	TANK-binding kinase 1
TBS	Tris buffered saline
TEMED	Tetra-methylethylenediamine
TGFβ	Transforming growth factor β
TIM23	Translocase of the inner mitochondrial membrane
TIR	Toll-interleukin 1 receptor
TIRAP	TIR domain containing adaptor protein
TLR	Toll like receptor
TNFα	Tumor necrosis factor alpha
TRADD	TNFR-associated death domain
TRAF	Tumor necrosis factor receptor associated factor
TRAM	Toll-receptor-associated molecule
TRIF	TIR-domain-containing adapter-inducing interferon-β
TYK2	Tyrosine kinase 2
VIPERIN	Virus inhibitory protein endoplasmic reticulum associated
WGA	Wheat germ agglutinin
WT	Wild type
ZBP1	Z-DNA binding protein 1

Symbol	Term
ºC	Degree Celsius
µl	Microliter
µm	Micrometers
µg	Micrograms
cm^2	Square centimeter
g	Gravities
HAU	Hemagglutinin units
hr	Hour
M	Molar
mg	Milligram
min	Minutes
ml	Milliliter
mm	Millimeter
mM	Millimol
ng	Nanograms
nmλ	Nanometers lambda
v.	Version
V	Volts
vg.	*Verbi gratia*

1. Introduction

MC have been classically implicated in acute inflammation and type I hypersensitivity responses such as allergy and asthma. However, recently MC have been discovered to be functionally versatile and to regulate both innate and adaptive immune responses (Galli *et al.*, 2010). Furthermore, they are recognized to contribute in restraining bacterial and parasitic infections improving host resistance. Moreover, some studies indicate that MC can serve as vaccine adjuvants promoting host protective responses.

Interestingly, although a number of reports indicate that mast cells regulate antiviral immune responses, it is still largely unknown by which means. Therefore, the first aim of this project was to characterize the viral-induced gene signature in MC. This with the purpose to identify MC mediators involved in antiviral immune responses.

Since the gene *rtp4* which codes for a member of the GPCR family of proteins was shown to be the second of the most overexpressed genes in virus-infected MC, the second aim of this work was to study the expression, cellular localization, interaction partners and functions of RTP4 in murine BMMC through biochemical and immunological approaches. This with the goal of investigating the direct and indirect anti-viral properties of this protein.

2. Literature review

2.1 Immunity

Immunity evolved as a system to confer protection against invasive microbes or harmful substances able to induce disease or injury. In this sense, the immune system is able to recognize viruses and to rapidly induce mechanisms focused to eliminate the thread and to maintain responses for future encounters (Abbas *et al.*, 2007).

2.1.1 Antiviral innate immune responses

Innate immunity is the first line of defense against virus and is characterized for being antigen (Ag) -independent, immediate and for not requiring previous contact with viral agents. Innate immunity comprises different mechanisms such as, mechanical protection by epithelial barriers; phagocytosis by neutrophils, macrophages and dendritic cells; neutralization of viral particles by complement and scavenging receptors present in secretions, tissues and blood; cytotoxic effects by natural killer (NK) cells; apoptosis induction; and viral recognition by cells bearing pattern recognition receptors (PRR), that rapidly stimulates the production of antiviral mediators for clearing infections (Stetson *et al.*, 2006; Koyama *et al.*, 2008; MacLachlan *et al.*, 2010).

2.1.1.1 Molecular mechanisms for viral recognition

Recognition of viruses is led by the innate immune system which is able, via PRRs, to sense a wide variety of microbial components. Microbial structures binding PRRs are also known as pathogen-associated molecular patterns (PAMP) and comprise different macromolecules such as, nucleic acids (viral triphosphate RNA and bacterial CpG repeats), carbohydrates, proteins, and lipid complexes (lipopolysaccharides and lipoproteins) (Akira *et al.*, 2006).

Several classes of PRRs including toll like receptors (TLR), retinoic acid inducible gene I (RIG-I) like receptors (RLR) and nucleotide-binding oligomerization domain (NOD)-like receptors (NLR), sense viral components like DNA, RNA and proteins. Recognition of viral ligands rapidly induces the production of immune mediators such as interferons (IFN) and proinflammatory cytokines (Kawai *et al.*, 2011).

2.1.1.2 Viral recognition through toll like receptors

Activation of TLRs is caused by viruses that utilize the endocytic pathway to enter the cells or during the viral budding event, when viral particles acquire their envelope from host cell membranes. During these processes viruses are recognized by endosomal receptors (Blasius *et al.*, 2010).

TLR molecules are found in cell membranes and in intracellular compartments. So far, 12 different TLRs have been reported to be present in mice and recognize components from bacteria, viruses, fungi and parasites. Only three members from the TLR family, which localize exclusively in cytoplasmic vesicles such as endoplasmic reticulum (ER) and endosomes, are said to detect viral products. TLR3, TLR7 and TLR9 recognize viral double-stranded RNA (dsRNA), single-stranded RNA (ssRNA) and DNA rich in CpG motifs, respectively (Hornung *et al.*, 2008). Although TLR8 has been described as a receptor for recognition of ssRNA in humans, its role in mouse is still unclear (Koyama *et al.*, 2008).

Structurally, TLRs consist of an ectodomain containing leucin rich repeats (LRR), which mediate the recognition of PAMPs, a transmembrane region and a cytosolic toll interleukin (IL) -1 receptor (IL-1R) (TIR) domain that triggers signaling (Figure 2-1) (Bowie *et al.*, 2000; Choe *et al.*, 2005).

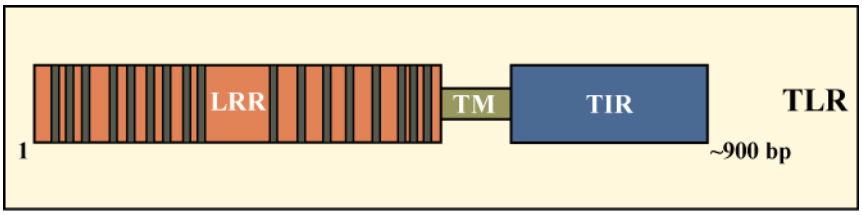

Figure 2-1: Structure of toll like receptors.
TLRs are constituted by 3 domains, the ectodomain containing leucine rich repeats (LRR), a transmembrane region (TM) and the cytosolic toll interleukin 1 receptor (TIR).

The virus-activated-TLR3 signals exclusively through the adaptor protein TIR-domain-containing adapter-inducing interferon-β (TRIF). TRIF associates with the tumor necrosis factor receptor associated factor (TRAF) 3, TRAF6 and with the receptor interacting protein (RIP) 1 and RIP3 (Jiang *et al.*, 2004).

TRAF3 also known as TRAF-associated NF-κB activator (TANK) activates TANK-binding kinase 1 (TBK1) and IKKε. The TBK1/IKKε complex then phosphorylates the interferon regulatory factor (IRF) 3 and IRF7, which are responsible of the induction of type I IFNs. TRAF6 and RIP1 activate the transcription factor NF-κB, via induction of the IKK complex. (Figure 2-2, A) (Fitzgerald *et al.*, 2003).

TLR7 and TLR9 signal through the recruitment of the adaptor protein myeloid differentiation primary response gene 88 (MyD88), which binds to the TIR domain of TLRs. Likewise, MyD88 recruits IL-1R associated kinase (IRAK) 4, which phosphorylates IRAK1 and IRAK2 that, in turn activates TRAF6 and TRAF3 (Akira *et al.*, 2006).

TRAF6 leads to the activation of the transforming growth factor β (TGFβ) activated kinase (TAK) 1. TAK1 together with the TAK1 kinase binding (TAB) 1, TAB2 and TAB3, activate the inhibitor of kappa B (IκB) kinase (IKK) complex, which consists of the kinases, IKKα, IKKβ and IKKγ, also known as NF kappa-B essential modulator (NEMO) (Xia *et al.*, 2009). The IKK complex phosphorylates IKKβ, which leads to the activation and translocation of the transcription factor nuclear factor kappa B (NF-κB) to the nucleus. Activation of NF-κB induces the expression of pro-inflammatory cytokines, such as IL-6, IL-12 and tumor necrosis factor alpha (TNFα). Additionally, TRAF6 also triggers the activation of the mitogen activated protein kinases (MAPK), via activation of the TAK1/TAB1/TAB2/TAB3 complex, which in turn, activates MAPK kinase (MAPKK) 3 and MAPKK6, resulting in the phosphorylation of 3 different types of kinases, c-Jun N-terminal kinase (JNK), the extracellular signal-regulated kinase (ERK) 1 and ERK-2 and p38 MAPK (Walsh *et al.*, 2008). These kinases mediate the activation of the transcription factor activator protein-1 (AP-1) that regulates the expression of cytokines and growth factors involved in proliferation, apoptosis, tumorigenesis and tissue morphogenesis (Figure 2-2 B) (Takeuchi *et al.*, 2007; Blasius *et al.*, 2010; Newton *et al.*, 2012).

TRAF3 activates the TBK1/IKKε complex which phosphorylates IRF3 and IRF7 thus resulting in the expression of type I interferons (Figure 2-2, B) (Oganesyan *et al.*, 2006; Sasai *et al.*, 2006).

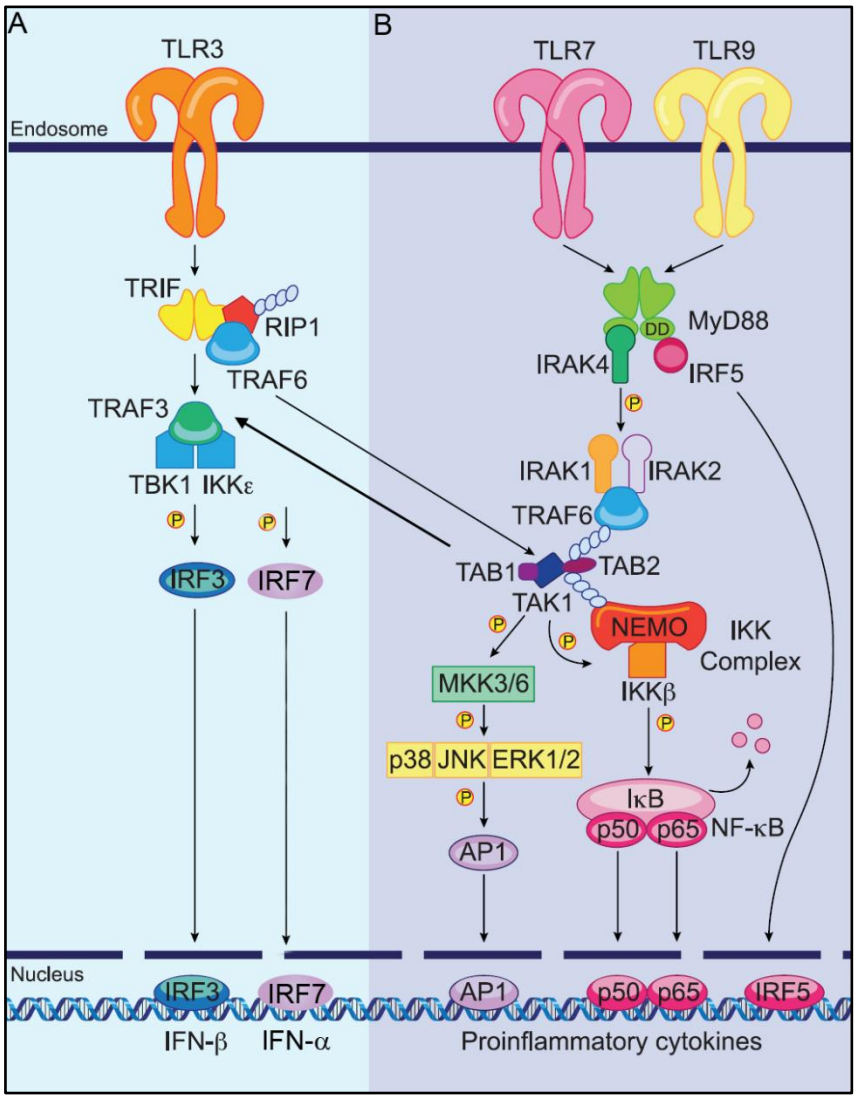

Figure 2-2: Activation of toll like receptors by viral particles and their signaling pathway.
Activated TLR3 **(A)** recruit the transcription factor TIR-domain-containing adapter-inducing interferon-β (TRIF), which associates with the transcription factors tumor necrosis factor receptor associated factor (TRAF) 3 and 6. The resulting complex mediate the activation of the transcription factors interferon regulatory factor (IRF) 3 and IRF7, which induce the expression of type I interferons. Activated TLR7 and TLR9 **(B)** signal through the recruitment of the adaptor protein myeloid differentiation primary response gene 88 (MyD88) that in turn recruits the IL-1R associated kinase (IRAK)-4. These kinase will mediate the activation of other kinases resulting in the activation of the transcription factors nuclear factor kappa B (NF-κB) and activator protein 1 (AP-1) responsible for the production of pro-inflammatory cytokines. Modified from Blasius *et al.*, 2010.

2.1.1.3 Viral recognition through RIG-I like receptors

Unlike TLRs, RLRs are located in the cytosol but not associated to intracellular compartments. This feature confers the advantage of sensing infected cells by the recognition of viral nucleic acids freely distributed within the cytoplasm. RLRs members belong to the family of the DEXD/H box RNA helicases which recognize and bind RNA. Expression of these receptors is maintained at low levels in resting and uninfected cells, but can be upregulated upon viral infection and IFN stimulation (Thompson *et al.*, 2011).

RLRs have evolved as sensors of specific virus families and only three members have been identified as major players in innate immunity: RIG-I, melanoma differentiation associated factor 5 (MDA5) and laboratory of genetics and physiology 2 (LGP2) (Andrejeva *et al.*, 2004; Yoneyama *et al.*, 2004; Rothenfusser *et al.*, 2005).

RIG-I has been reported as a sensor for hepacivirus and members of important viral families such as Paramayxoviridae, Rhabdoviridae, Orthimyxoviridae, Filoviridae, Arenaviridae, Bunyaviridae, Flaviviridae and Coronaviridae among others (Kato *et al.*, 2006; Pichlmair *et al.*, 2006; Loo *et al.*, 2011). MDA5 has been described to recognize murine norovirus and vaccinia virus and members of the Picornaviridae and Flaviviridae families. Although LGP2 has been reported to bind RNA, there is no conclusive evidence confirming the binding of this receptor to viral ligands (Fredericksen *et al.*, 2006; Loo *et al.*, 2011; McCartney *et al.*, 2011).

RLRs are able to differentiate between self and non-self RNA. RIG-I recognizes viral RNA, as short RNA fragments of up to 23 base pairs (bp), containing polyuridine motifs (poly-u/UC) and/or tagged with the 5' triphosphorylated ends (5'ppp) (Hornung *et al.*, 2006; Saito *et al.*, 2008). In addition, RIG also recognized AT-rich dsDNA, through the transcription into 5'ppp dsRNA by polymerase III. So far literature reports indicate that MDA5 recognizes viral RNA on the basis of high molecular weight dsRNA fragments (Kato *et al.*, 2008).

RLRs share the DExH-box helicase domain as a common structural feature, which is located centrally and is responsible for viral RNA recognition. In contrast, RIG-I and MDA5 possess two caspase activation and recruitment domains (CARD) at the N-terminal. RIG-I and LGP2 contain a C-terminal repressor domain (RD), which regulates and keeps the structural conformation of inactive or steady receptors (Figure 2-3) (Saito *et al.*, 2007).

RIG-I is the most studied RLR in terms of signaling and functionality. Autoregulation of RIG-I involves the interaction between the RD and CARD domains that in the absence of the ligand keeps the CARD domain unexposed avoiding its interaction with adaptor proteins and hence the activation of signaling pathways. Binding of the 5'ppp RNA with the RD of RIG-I induces receptor conformational changes, allowing CARD domains to become active and to multimerize with other RIG-I–CARD domains and to associate with the adaptor protein IFNβ promoter stimulator 1 (IPS-1), previously known as VISA or CARDIF. IPS-1 has been found to localize in the outer membrane of mitochondria and peroxisome membranes. Interaction with IPS-1 induces relocation of RIG-I to IPS-1 associated membranes where components of the downstream signaling pathways accumulate (Loo *et al.*, 2011).

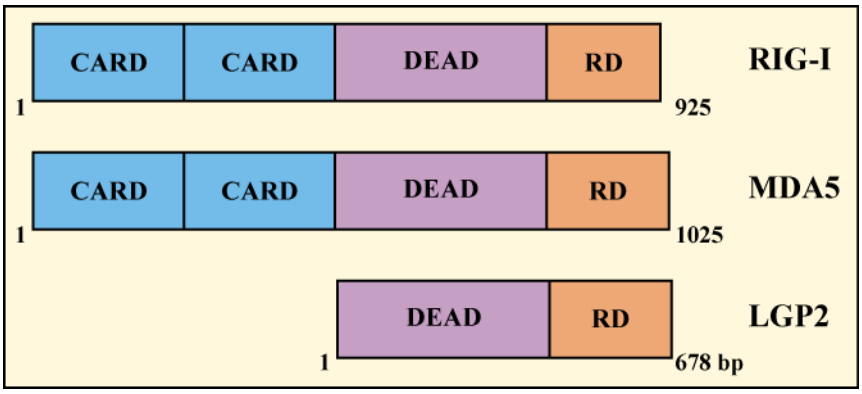

Figure 2-3: Structure of RIG-I like receptors.
The RLRs RIG-I and MDA5 are constituted by two caspase activation and recruitment domains (CARD), a DEAD domain containing the DExD/H-box helicase and the repressor domain (RD). The receptor LGP2 lacks of the CARD domain, preventing pathways signaling.

Activated IPS-1 recruits and interacts with TRAF3, which in turn associates with the Fas-associated death domain-containing protein (FADD) and RIP1 forming the complex, TRAF3-FADD-RIP1. This complex activates the group of kinases called NEMO, which phosphorylates IκB inducing its cleavage from the transcription factor NF-κB allowing its activation. Finally, translocation of NF-κB into the nucleus induces the transcription of proinflammatory genes. Additionally, activated IPS-1 recruits TANK, inducing the activation of the kinase TBK1 that phosphorylates and activates IRF3 and to a lesser extent IRF7.

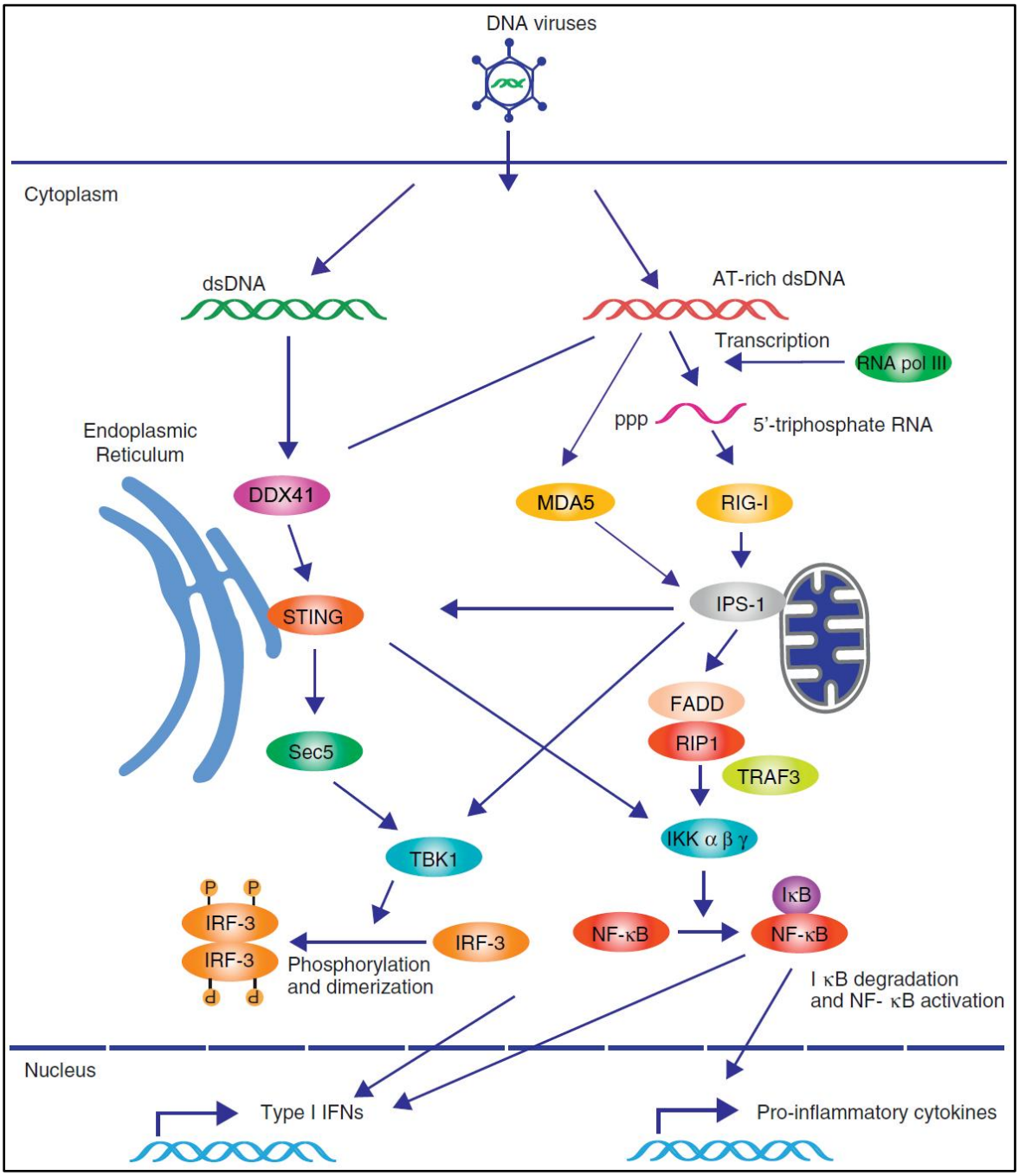

Figure 2-4: Activation of RIG-I like receptors by viral particles and their signaling pathway.
Viral binding to RLRs leads to the recruitment of the adaptor protein IPS-1, which mediates the activation of the transcription factors NFκB, IRF3 and IRF7 responsible for the expression of type I IFNs and pro-inflammatory cytokines. Modified from Barber *et al.*, 2011.

Translocation and accumulation in the nucleus of dimerized IRF3 and IRF7 induce the expression of IFNβ and IFNα, respectively. IPS-1 can also interact with the adaptor protein stimulator of interferon genes (STING) that was formerly described as a nucleic acid receptor. However, recent evidence suggests that STING associates with Sec5, a

component of the exocyst complex, which is able to recruit and activate TBK1, an intermediate in the activation of the transcription factor IRF3 (Figure 2-4). STING deficient mice infected with vesicular stomatitis virus were unable to induce type I IFNs, confirming its role in this kind of responses (Barral *et al.*, 2009; Barber, 2011; Ishikawa *et al.*, 2011; Bruns *et al.*, 2012).

2.1.1.4 Viral recognition by other receptors

NLRs are cytosolic proteins known to be involved in the recognition of many pathogen components and for having the potential to activate inflammasomes. Generally, NLRs are structurally conformed by a C-terminal of a LRR domain, a central nucleotide binding domain and an N-terminal containing CARD, as well as pyrin domains or baculovirus IAP repeats. Cryopyrin, also known as NOD-like receptor family pyrin domain containing 3 (NALP3), has been described as receptor for ssRNA and dsRNA (Davis *et al.*, 2011; Kersse *et al.*, 2011). Likewise another NLR, the absent in melanoma 2 (AIM2) receptor has been reported to sense cytosolic B-form-DNA. Activated NALP3 and AIM2 associate with the adaptor protein apoptosis-associated speck-like protein containing a caspase activating and recruiting domain (ASC) (Takeuchi *et al.*, 2007). This complex cleaves pro-IL-1β and pro-IL-18 leading to the secretion of their mature and active forms. IL-1 and IL-18 orchestrate the recruitment of immune cells to sites of infection/inflammation (Figure 2-5) (Barber, 2011; Rathinam *et al.*, 2012).

Z-DNA binding protein 1 (ZBP1), also known as DNA dependent activator of interferon regulatory factors (DAI), was the first cytosolic DNA receptor and was shown to recognize Z and B-DNA forms. Activation of DAI triggers signaling to type I IFNs. However in DAI knock-out mice, interferon responses were still elicited, implying the existence of other receptors involved in the recognition of microbial DNA and the consequent production of IFNs (Takaoka *et al.*, 2007; Wang *et al.*, 2008).

A screening of 59 members of the DExD/H-box helicase family revealed, that DDX41 through its DEAD domain, was the only protein that was able to sense viral and bacterial

DNA, independently of the length. Its activation induces signaling through the adaptor protein STING (Zhang *et al.*, 2011).

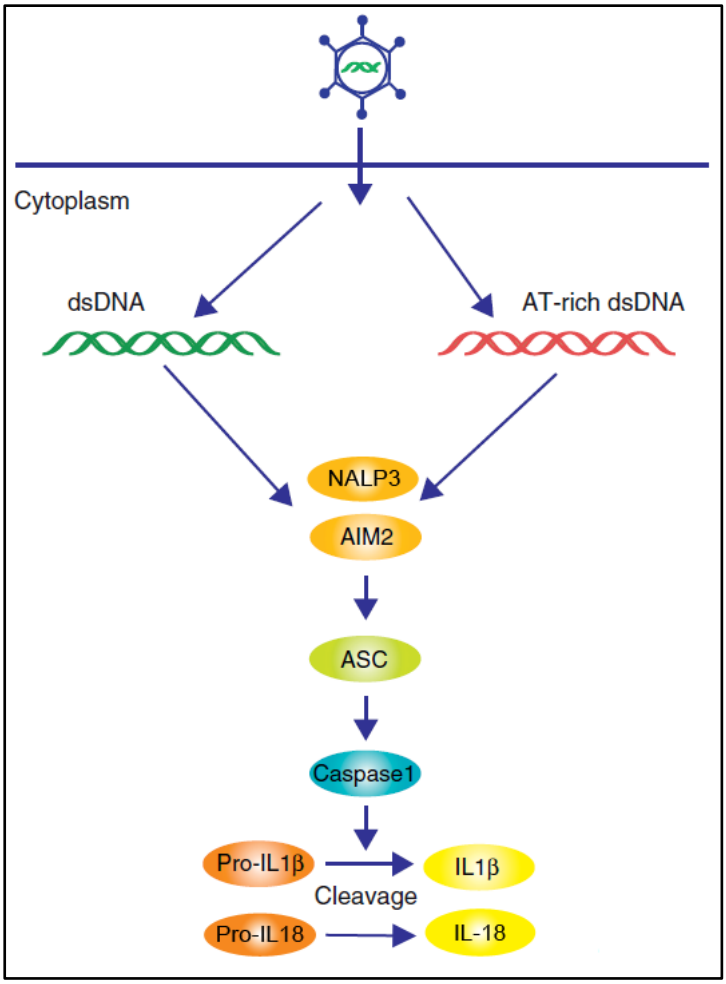

Figure 2-5: Activation of NOD like receptors by virus and their signaling pathways. Recognition of virus-derived nucleic acids by NOD-like receptor family pyrin domain containing 3 (NALP3) and the absent in melanoma 2 (AIM2) induce the recruitment of the adaptor protein ASC that mediates the activation of caspase 1, resulting in the cleavage and activation of the preforms for IL-1β and IL-18. Modified from Barber *et al*, 2011.

2.1.1.5 Interferons

Members of the IFN family of cytokines are involved in innate immune responses and have been well described for playing an essential role in antiviral immunity. IFNs are produced by almost all cell types but especially by immune cells, fibroblasts and endothelial cells (MacLachlan *et al.*, 2010; Murphy *et al.*, 2011). IFNs are divided in three classes; type I interferons with 12 members: IFNα, IFNβ, IFNε, IFNκ and IFNω. In

addition, IFNδ, IFNζ and IFNτ are detected only in pigs, ruminants and mice, respectively. Unique member of the type II interferon class is IFNγ, mainly produced by T and NK cells and participates in cell-mediated immune responses. Type III interferons have recently been discovered and include IFNλ1, 2 and 3 also known as IL-29, IL-28a and IL-28b, respectively. Although the type III interferons' structure is similar to the IL-10 family of cytokines, they belong to this group since they induce the expression of interferon stimulated genes (ISG) (Iversen *et al.*, 2010; Gonzalez-Navajas *et al.*, 2012).

2.1.1.6 Induction of type I interferons

From all the members of the IFN family, type I IFNs are the hallmark of antiviral responses. Type I IFNs are produced as a consequence of the activation of PPRs such as TLRs and RLRs by viral ligands. Type I IFNs signal through the IFNα/β receptor (IFNAR) which is composed of two subunits, IFNAR1 and IFNAR2 associated in their intracellular domains with Janus kinase 1 (JAK1) and tyrosine kinase 2 (TYK2). Activation of JAK1 and TYK2 leads to the recruitment and phosphorylation of signal transducers and activators of transcription (STAT) members. Activated STAT1 and STAT2 recruits IRF9, inducing the formation of the complex, STAT1-STAT2-IRF9, known also as IFN stimulated gene factor 3 (ISGF3). ISGF3 translocates into the nucleus where it binds to specific DNA sequences known as IFN-stimulated regulatory elements (ISRE) activating the transcription of a large number of ISG with antiviral and antimicrobial functions and ultimately mastering the antiviral responses (Honda *et al.*, 2005; Takaoka *et al.*, 2006; Onoguchi *et al.*, 2007; Sadler *et al.*, 2008).

Activation of IFNAR by type I IFNs induces no-less important signaling pathways that begin with the homodimerization of activated STAT1 and STAT3. Dimerized STAT1 translocates to the nucleus to bind to DNA sequences called IFNγ-activated site (GAS). Induction of GAS is a feature of the responses generated by IFNγ, however its activation by type I IFNs leads to the transcription of pro-inflammatory and apoptotic genes that contribute to the immune response. Alternatively, in the nucleus dimerized STAT3 binds to STAT3-binding elements (SBE), which contrary to GAS, will induce the transcription of anti-apoptotic genes and oncogenes (Figure 2-6) (Bonjardim, 2005; Sadler *et al.*, 2008; Gonzalez-Navajas *et al.*, 2012).

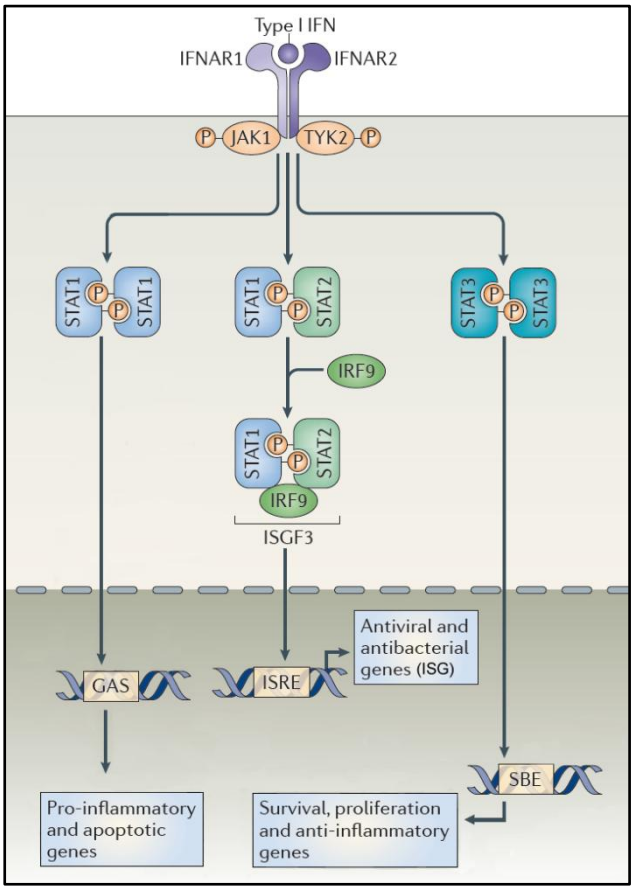

Figure 2-6: Signaling pathways through the Interferon receptor alpha.
Activated IFNAR by IFNα and IFNβ, induces the association and activation of Janus kinase 1 (JAK1) and tyrosine kinase 2 (TYK2). These kinases phosphorylate transcription factors belonging to the family of signal transducers and activators of transcription (STAT). Dimers of STAT1 and STAT2 bind to the interferon regulatory factor 9 (IRF9) forming the complex IFN stimulated gene factor 3 (ISGF3), which after translocation to the nucleus mediates the expression of interferon stimulated genes (ISG). Homodimers of STAT1 and STAT3 also bind to DNA sequences in the nuclear DNA to regulate the expression of pro-inflammatory, survival and apoptotic genes. Modified from Gonzalez-Navaja *et al*., 2012.

2.1.1.7 Modulatory functions of type I interferons

Following the production of type I interferons by infected cells, these cytokines act in an autocrine or paracrine manner affecting adjacent cells. IFNAR receptor activation leads to the transcription of more than 300 ISG. Some of these genes encode for PRRs, signaling proteins and transcription factors that amplify the IFNs production, through a positive feedback loop and establish the cellular "antiviral phenotype". ISG also codes for proteins involved in cytoskeletal remodeling, apoptosis induction and post-transcriptional modifications. However, the functions of a large group of ISG remain unknown (Stetson *et al.*, 2006; Noppert *et al.*, 2007).

Some ISG have been shown to play major roles in antiviral immune responses such as ISG15, Mx GTPases, OAS/RNaseL axis and VIPERIN (Schoggins *et al.*, 2011).

The interferon stimulated gene of 15 kDa (ISG15) is secreted in large amounts upon viral infection and has been shown to meditate antiviral responses by promoting the so called ISGylation. ISGylation resembles ubiquitylation, but instead of driving protein degradation, ISG15 prevents it. Substrates for ISG15 include products belonging to the same family of ISG, such as JAK1, STAT1, IRF3, RIG-I, and RNaseL. It has been reported that absence of ISG15 promotes IRF3 degradation and hence a lower production of IFNβ (Ritchie *et al.*, 2004; Chen *et al.*, 2011).

Mx GTPases are expressed in peripheral tissues and in different cells types like hepatocytes, endothelial and immune cells. They inhibit the replication of a wide variety of viruses by binding to nucleocapside proteins responsible for viral gene transcription. Mx GTPases locate in cell cytoplasm and nucleus and target viruses at different stages of maturation. Coxsackie and hepatitis virus are susceptible to the antiviral activity of Mx GTPases (Hefti *et al.*, 1999; Haller *et al.*, 2002; Sadler *et al.*, 2008).

The 2',5'-oligoadenylate synthetase 1 (OAS1) is constitutively expressed as an inactive monomer that is able to form homodimers, resulting in an active OAS1 tetramer. Monomers of OAS1 are activated by the binding of dsRNA, serving as PRRs. Tetramers of OAS1 activate the ribonuclease enzyme, RNaseL that mediates degradation of viral RNA. Degraded RNA activates the PRR RIG-I and MDA5 initiating the antiviral response. RNaseL deficient mice show an increased susceptibility to the infection with RNA viruses belonging to the Reoviridae, Togaviridae, Paramyxoviridae, Orthomyxoviridae families (Lin *et al.*, 2009; Kristiansen *et al.*, 2011).

The ISG *cig5* or *rsad2* encodes for the virus inhibitory protein endoplasmic reticulum associated (VIPERIN), a 42 kDa protein that disrupts lipids rafts in the cell membrane preventing the assembly of the viral envelope by decreasing the activity of the enzyme farnesyl diphosphate synthase, which is responsible for the synthesis of isoprenoid-derived

lipids used for viral membrane coating. VIPERIN also binds to lipid bodies preventing the assembly and budding of hepatitis C virus (HCV), since VIPERIN has an N-terminal amphipathic α-helix domain that is similar to the one present in HCV. The amphipathic domain is responsible for the association of the virus to the lipid bodies (Jiang *et al.*, 2008; Hinson *et al.*, 2009; Seo *et al.*, 2011).

2.1.2 Antiviral adaptive immune responses

Adaptive immunity includes responses that develop from previous encounters with viral agents and are characterized for being Ag specific, due to the ability of T cells to express a vast number of Ag receptors. Moreover these responses induce immunological memory, which enables the host to counteract rapidly and specifically to renewed exposures with the viral agent. Adaptive immune responses can be categorized in cell-mediated and humoral immune responses (Murphy *et al.*, 2011).

Cell-mediated immunity involves the capture of microbes by Ag-presenting cells (APC), their migration to lymphoid organs and the processing of microbial Ags that are presented to Ag-specific $CD4^+$ T lymphocytes. Recognition of Ags and molecules on the surface of APC by $CD4^+$ T cells induces their proliferation and differentiation into functional phenotypes of effector T cells. Production of cytokines by effector $CD4^+$ T cells mediates processes such as inflammation, macrophage activation, B cells proliferation and differentiation (Abbas *et al.*, 2007).

Alternatively cell-mediated immunity implicates the activities of $CD8^+$ T cells. This type of lymphocytes recognize cells expressing viral Ags in the context of the major histocompatibilty complex (MHC) I. Activation of $CD8^+$ T cells triggers the release via exocytosis of cytotoxic granules that leads to the lysis and/or apoptosis of virally-infected target cells (Abbas *et al.*, 2007).

Humoral immunity is mediated principally by circulating antibodies (Ab) produced by B cells. Expression of surface Ag-specific receptors enables B cells to recognize viral Ags and to differentiate into plasma cells, which are responsible for the secretion of Ag-specific Abs. The functional effects of these molecules comprise immune responses such as

neutralization of free-viral particles or toxins, viral opsonization and phagocytosis, viral lysis, inflammation and complement activation. Ag-specific Abs are produced by long-living plasma cells or by reactivation and proliferation of memory B cells (MacLachlan *et al.*, 2010).

2.2 Mast cells

Mast cells (MC) are part of the innate immune system, distributed along peripheral tissues, particularly, to those like mucosal tissues and skin that are exposed or in close contact with the environment. MC are also found in vascularized tissues, in proximity to blood vessels, nerves, smooth muscle cells, mucus-producing glands and hair follicles (Metcalfe *et al.*, 1997).

They have a major role in inflammatory and immediate allergic reactions due to their capacity of releasing potent inflammatory mediators. These mediators can be classified as follows: Preformed mediators, which are stored in cytoplasmic granules and are released through the process of degranulation and include vasoactive amines (histamine and serotonin), proteoglycans, proteases (chymase, tryptase and carboxypeptidase) and TNFα. The second category, *de novo* synthesized mediators, are produced in response to a wide variety of stimulus and include arachidonic acid metabolites (prostaglandins and leukotrienes), cytokines (TNFα, IL-1, IL-3, IL-4, IL-5, IL-6 and IL-10), chemokines (CCL2, CCL3, CCL4, CCL5, CCL11, CCL20, CXCL1, CXCL2, CXCL8, CXCL9, CXCL10 and CXCL11) and growth factors (vascular endothelial growth factor (VEGF), nerve growth factor (NGF), basic fibroblast growth factor (BFGF), granulocyte-macrophage colony stimulating factor (GM-CSF)) (Metcalfe *et al.*, 1997; Galli *et al.*, 2005; Kumar *et al.*, 2010; Amin, 2012).

2.2.1 Mast cell development and classification

MC originate from pluripotent hematopoietic cells in the bone marrow. They first circulate in the peripheral blood as immature progenitors. MC expansion, migration, differentiation and survival is controlled by cytokines and growth factors such as IL-3, IL-4, IL-9 and TGFβ (Amin, 2012). However, MC development strictly relies on stem cell factor (SCF),

also known as c-kit ligand, which binds to the c-kit receptor on the MC surface. SCF is produced by fibroblasts and endothelial cells. However, migration of MC progenitors ($CD34^+$ $c\text{-}kit^+$ cells) to connective and mucosal tissue is governed by the expression of membrane-bound SCF on stroma cells. The membrane-bound SCF promotes MC maturation and controls MC homeostasis in tissues, thanks to the stable expression of c-kit receptor during all the stages of MC development (Gurish *et al.*, 2006; Hu *et al.*, 2007).

Additionally, some studies indicate that homing is controlled by MC surface expression of integrins, which bind to adhesion molecules in different tissues/organs. In mice, the integrin $\alpha_4\beta_7$ is responsible for the migration of MC progenitors into the intestinal mucosa (Gurish *et al.*, 2001).

In rodents MC are classified according to the tissue where they reside: connective tissue mast cells (CTMC) and mucosal mast cells (MMC). In contrast, human mast cells are classified according to the type of proteases contained in their granules: MC containing tryptase (MC_T), found in lung alveolar septa and in the small intestine mucosa and usually in proximity to T cells. MC containing tryptase and chymase (MC_{TC}) found in skin, gastrointestinal tract, synovium and subcutaneous tissue (Metcalfe *et al.*, 1997; Kumar *et al.*, 2010; Amin, 2012).

2.2.2 Mast cells activation through the IgE high affinity receptor

One of the best described signaling pathway in MC is the one driven by the fragment crystallisable region epsilon receptor I (FcεRI) also known as immunoglobulin E (IgE) high affinity receptor, which is responsible for triggering the process of degranulation and for mediating type I hypersensitivity reactions. A good example of the role of this receptor is its involvement in the pathogenesis of allergic asthma (Metcalfe *et al.*, 1997; Bischoff, 2007).

Allergen-specific B cells, under the influence of IL-4, switch on the production of IgE which binds the FcεRI on the surface of connective and mucosal tissue MC. IgE together with allergens promote the cross-linking of the FcεRI activating signaling cascades. The γ chain of the FcεRI contains the cytoplasmic immunoreceptor tyrosine-based activation motif (ITAM), which is phosphorylated as a consequence of its interaction with Lyn, a member of Src kinases family. Lyn activates Syk, which in turn phosphorylates the adaptor

proteins LAT and NTAL/LAB/LAT2. Finally, adaptor proteins initiate signaling pathways driven by phospholipase Cγ (PLCγ), phosphoinositide 3-kinase (PI3K), Ras/Rho GTPases, Akt kinases, and MAPK (*vg.* p38, JNK and ERK) resulting in MC migration, proliferation, survival, degranulation and eicosanoid, chemokine and cytokine production (Galli *et al.*, 2005; Rommel *et al.*, 2007; Newton *et al.*, 2012).

FcεRI-engagement also induces degranulation by calcium signaling, either by the release of calcium from intracellular stores or by favoring extracellular calcium influx through channels that finally lead to the activation of PLCγ and hence the synthesis of new immune mediators (Galli *et al.*, 2005).

2.2.3 Mast cells and their role in immunity

Due to the arsenal of immune mediators released by activated MC, the influence of these cells in immune processes is wide.

MC promote inflammation by the release of pre-stored mediators like histamine and prostaglandin (PG) D_2, leading to enhanced vascular permeability and upregulation of adhesion molecules on endothelial cells that later allow other immune cells to adhere to the endothelium and to migrate to inflammatory sites. Likewise, the production and release of cytokines and chemokines supports the recruitment of other immune cells modulating their responses. For example, cytokines like IL-6 and TNFα stimulate migration of neutrophils that mediate pathogen clearance. MC-secreted TNFα together with IL-1 promotes migration of dendritic cells (DC), that recognize and uptake pathogens that after migration to peripheral lymphoid tissues, are presented in the form of Ags to T cells and hence start cell mediated immune responses. TNFα can also induce migration of effector/memory T cells which contribute to a faster and specific immune response (Dawicki *et al.*, 2007; Abraham *et al.*, 2010). The chemokines CXCL8 and CCL11 (eotaxin), have been reported to recruit NK cells and eosinophils (Vosskuhl *et al.*, 2010), respectively. In contrast to the pro-inflammatory roles of MC-mediators, release of IL-10 by MC contributes with the resolution of inflammation by locally inhibiting granulocytes, macrophages and T cells-mediated activities (Marshall, 2004; Galli *et al.*, 2008; Kumar *et al.*, 2010).

Further MC properties include: Ag uptake and presentation through MHC I and II, promotion of maturation and differentiation of DCs into a Th2 phenotype by the release of

MC-derived PGD_2, B cells isotype switching, via IL-4 and IL-13 and induction of antigen-specific $CD8^+$ T cell cytotoxicity (Stelekati *et al.*, 2009; Kumar *et al.*, 2010).

Allergy is the consequence of IgE-mediated type I hypersensitivity reactions in which MC play a central role, not only during the onset through the activation of the FcεRI, but also by causing structural tissue changes in chronic allergic reactions. In asthmatic allergy MC induce acute responses such as bronchial smooth muscle–contraction mediated by TNFα, IL-4, and IL-13 and proliferation of mucus-producing goblet cells via leukotriene (LT) C_4 release. During chronic allergy, MC induce airway remodeling characterized by smooth muscle hypertrophy, fibrosis and mucus hypersecretion through the release of tryptase and growth factors (Metz *et al.*, 2007; Amin, 2012).

MC also promote clearance of gram positive (*Streptococcus*, *Listeria*) and negative bacteria (*E. coli*, *K. pneumonia*, *P. aeruginosa*) by a variety of mechanisms that include phagocytosis, degranulation, production of reactive oxygen species, recruitment of immune cells, release of cytokines and antimicrobial peptides, such as cathelicidins which by disrupting membranes possess direct bactericidal activity (Di Nardo *et al.*, 2003; Dietrich *et al.*, 2010). Resistance to parasites, particularly to nematodes, is also conferred by MC by the signaling through specific IgE and the release of granule proteases (Abraham *et al.*, 2010).

2.2.4 Mast cells and their role in viral infections

Interestingly, besides of the functions described above, MC have been recently postulated as important players in the antiviral immune response, however their functional implications are not fully understood (Dawicki *et al.*, 2007; Galli *et al.*, 2010).

MC can be activated by viral products leading to degranulation and release of immune mediators. Early works showed that TLR3 agonists such as synthetic dsRNA, polyinosinic polycytidylic acid (pIC) activate MC (Kulka *et al.*, 2004; Matsushima *et al.*, 2004). In general, virus-activated MC acquire an antiviral phenotype, characterized by the secretion of type I interferons, cytokines and chemokines that promote recruitment of cells involved in the defense against virus. For example, stimulation of BMMC with Newcastle disease virus (NDV), promotes activation of TLR3 and the consequent expression of IFNβ and ISG, such as ISG15, CXCL10 (IFNγ induced protein-10 (IP-10)) and CCL5 (Regulated

upon activation, normal T cells expressed and secreted (RANTES)) that induce recruitment of $CD8^+$ T cells (Orinska *et al.*, 2005). Activation of MC with dengue virus through the receptor MDA5 leads to the production of IFNα, TNFα, and the chemokines CCL3 (macrophages inflammatory protein 1α (MIP1α)), CCL4 (MIP1β), CCL5, CXCL12 (stromal cell-derived factor-1 (SDF-1) and CX3CL1 (fractalkine)) involved in the recruitment of NK and NKT cells (King *et al.*, 2002; St John *et al.*, 2011; Brown *et al.*, 2012; Bruns *et al.*, 2012). Similar findings have been reported for MC infected with mammalian reovirus in which chemotaxis of NK and NKT cells is directed by MC-derived CXCL8 (IL-8) and CCL5, respectively (Burke *et al.*, 2008; McAlpine *et al.*, 2012).

Unlike activation through PRRs, Wang *et al*., (2012) showed that skin MC are able to recognize VV through different receptors namely CD48 or sphingosine-1-phosphate receptor (S1PR), which senses sphingomyelin intermediaries present on the enveloped membrane of virions. Activation of the S1PR on MC triggers degranulation and release of the antimicrobial peptide, cathelicidin, which was shown to be important in controlling the VV-viral load in MC. Degranulation has also been reported in MC upon infection with dengue virus (DV), the highly pathogenic H5N1 influenza virus, in which the release of tryptase, histamine and IFNγ generate severe lesions and hemorrhages in mouse lung tissue (Burke *et al.*, 2008; Hu *et al.*, 2012; McAlpine *et al.*, 2012).

However participation of MC is not always beneficial for the resolution of viral infections and host survival. In fact a number of reports show that activation of MC results in deleterious responses. For example, secretion of chymase, tryptase and VEGF is strongly produced in children infected with DV conferring the clinical manifestations of dengue hemorrhagic fever (Furuta *et al.*, 2012). In chickens infected with NDV, severe intestinal tissue damage was correlated with an increased number of infiltrating MC and tryptase content (Sun *et al.*, 2008). Similar findings have been reported for chickens infected with infectious bursal disease virus (IBDV) and severe tissue destruction of the Bursa of Fabricious (Wang *et al.*, 2009). Importantly, human blood cord-derived MC infected with human immunodeficiency virus-1 (HIV) and stimulated with ligands for TLR2, TLR4 and TLR9 , exhibit enhanced viral replication and apoptosis inhibition, supporting latent

infection and turning MC into HIV reservoirs (Bannert *et al.*, 2001; Sundstrom *et al.*, 2004).

Additionally, MC have been reported to be susceptible to infection with viruses like hantavirus (Guhl *et al.*, 2010), infectious bursal disease virus (IBDV) (Wang *et al.*, 2008), respiratory syncytial virus (RSV) (Shirato *et al.*, 2009) and sendai virus (Castleman *et al.*, 1990).

2.3 G protein coupled receptors

G protein-coupled receptors (GPCR) are the largest family of proteins embracing more than 500 members and the 4% of the human genome. They bridge the intracellular milieu with the extracellular environment and mediate responses influenced by ions, Ca^{+}, nucleotides, amines, peptides, lipids, photons and organic odorants. The wide variety of ligands reflects the multiplicity of functions these receptors exert. For example they are involved in: phagocytosis, degranulation, transduction of chemokines, hormones, and neurotransmitters signals, vision, olfactation and taste. GPCRs share a general mechanism of action in which the activation of the receptor by the ligand, is followed by the onset of signaling cascades governed mainly by G proteins, MAPK, or G proteins independent-signaling and receptor desensitization (Rosenbaum *et al.*, 2009).

Although GPCR vary in their sequences, their main feature is the conserved structure of seven transmembrane α-helical segments, spaced by alternating intracellular and extracellular loop regions. In fact, some authors suggest that a better name for these proteins might be “the family of the seven transmembrane domain receptors (7TM)”, also because a discrete number of GPCR family members do not interact with G proteins. Based on sequence similarities, GPCR can be classified in five different families: rhodopsin, secretin, glutamate, adhesion and frizzled/taste2 (Unal *et al.*, 2012). However, variations in the structure of transmembrane domains and extracellular loops, differential glycosylation and availability of di-sulphide bonds give rise to the variety and specificity of the so called, GPCR-binding pocket (ligand interaction site) contained in these receptors. Similarly, sequence differences in the intracellular loops, the transmembrane

α-helix 7 and the cytoplasmic tail, together with the rich chemical environment that surrounds GPCR, enable the interaction of these receptors with adaptor proteins that mediate activation of different signaling pathways (Katritch *et al.*, 2012).

Ligand-binding to GPCR entails conformational changes that regulate activation/inactivation and guarantee that receptor motifs are displayed properly for signaling. GPCR are coupled with heterotrimeric G proteins that consist of three subunits, Gα which associates to the heterodimer Gβγ; in basal states the subunit Gα is bound to guanine diphosphate (GDP) and upon ligand binding and receptor conformational changes, GDP is displaced allowing guanine triphosphate (GTP) to bind to the Gα subunit. This exchange results in dissociation of the GTP-bound Gα subunit from the heterodimer Gβγ. Free Gβγ interacts with effector proteins that lead to signaling through pathways such as, adenylyl cyclase, phospholipase C, Rho kinases and ion channels (Karnik *et al.*, 2003; Vines *et al.*, 2004; Kimple *et al.*, 2011). Deactivation or desensitization of GPCR is directed by mechanisms that include receptor phosphorylation, arrestin-mediated internalization towards late endosomes for ulterior degradation in lysosomal compartments or recycling endosomes that redirect the receptor to the plasma membrane. However, these events are conditional to the nature of the GPCR. Oligomerization states and intracellular localization tune the fate of the receptors (Hanyaloglu *et al.*, 2008; Magalhaes *et al.*, 2012).

2.3.1 Receptor transporter protein 4

A set of genes coding for accessory proteins belonging to the GPCR family and with possible roles in regulating the expression of odorant receptors (OR) was identified by Saito *et al*, (2004) upon screening of gene libraries derived from olfactory and vomeronasal organ neurons. These proteins were called receptor transporter proteins (RTP) and receptor expression enhancing proteins (REEP).

Mammalian protein-expression systems demonstrated that members of the RTP family like RTP1 and RTP2 and in less extent REEP1, induced the upregulation of OR expression. Likewise these proteins were confirmed to be located prominently in the olfactory and vomeronasal organ. In the same study, despite the fact that the receptor transporter protein-4 (RTP4), also known as 28 kD interferon-responsive gene (IFGR28) was not shown to improve the expression of OR it was found still to be expressed in mouse olfactory neurons

(Behrens *et al.*, 2006). This work was the basis for further studies on receptor co-expression with members of the RTP and REEP families.

RTP4 is a protein of 249 amino acids (aa), member of the 7TM family and classified as type III membrane protein (ER targeted). This protein has not been thoroughly characterized yet. However through bioinformatic tools functional motifs present in RTP4 were identified. RTP4 sequence shows the presence of phosphorylation motifs homologous to those found in proteins like casein kinase II and protein kinase C. The relevance and functional implications of these findings is still unknown.

Unlike OR, association of RTP4 with human bitter taste receptors increases the expression of these receptors on the cell surface (Behrens *et al.*, 2006). Similarly, RTP4 was shown to bind to heterodimers (μ and δ subunits) of opioid receptors (OpR), resulting in a decreased accumulation of the subunits μ-δ in the Golgi apparatus and enhancing cell surface localization by protection against ubiquitin-targeted degradation (Decaillot *et al.*, 2008).

Additionally, RTP4 was reported to be overexpressed in the endometrium, periphery blood lymphocytes (PBL) and *corpus luteum* of ewes in early pregnancy suggesting a role on the establishment of pregnancy (Gifford *et al.*, 2008).

The functional activities of RTP4 remain largely unknown, but it has been postulated that RTP4 could behave as a chaperone-like protein, promoting receptor folding and hence improving receptor trafficking towards the plasma membrane. In addition RTP4 binding to other receptor, could mask specific signal peptides involved in organelle retention, facilitating receptor transport mediated by specific vesicles/cargos (Saito *et al.*, 2004).

3. Materials and methods

3.1 Materials

3.1.1 Mice

Animal experiments were performed according to the guidelines and approval of the Schleswig-Holstein Ministry of Environment, Nature and Forestation.

C57BL/6J mice were purchased from The Jackson Laboratory, bred in the Animal Facility at the Forschungszentrum Borstel and used as wild-type (WT) animals.

Toll like receptor 2, 3, 4, 7, 9 knock-out mice (*tlr23479*$^{-/-}$) were kindly provided by Prof. Dr. Carsten Kirschning from the Institut für Medizinische Mikrobiologie, Universität Duisburg-Essen. Type I Interferon Receptor alpha chain deficient mice (*ifnar1*$^{-/-}$) were kindly provided by Prof. Dr. Rainer Zawatzky, from the Deutsches Krebsforschungszentrum. Adaptor protein MyD88 deficient mice (*myd88*$^{-/-}$) were supplied by Dr. Norbert Reiling from the Forschungszentrum Borstel and adaptor protein TRIF (*trif*$^{-/-}$) deficient mice were provided by Dr. Bruce Beutler, from the University of Texas, Southwestern Medical Centre.

3.1.2 RTP4 Deficient Mice Generation

The RTP4 deficient embryonic stem cells (ES) were purchased from University of California, Davis, Knockout Mouse Project (KOMP) Repository, which configured the targeting vector rtp4$^{tm1(KOMP)Vlcg}$ and electroporated the parental stem cells VGB6, isolated from C57BL/6NTac mice. RTP4 deficient ES were generated by utilizing a replacement vector containing: homologous regions for the *rtp4* gene at the 5' and 3' ends as substrate for the homologous recombination and a replacing sequence consisting of a cassette (ZEN-UB1) of two fused elements, the *lacZ* and *neo*, reporter and selection genes, respectively (Figure 3-1). After the introduction of the vector into mouse embryonic stem cells, homologous recombinant ES were selected with antibiotics and expanded in culture.

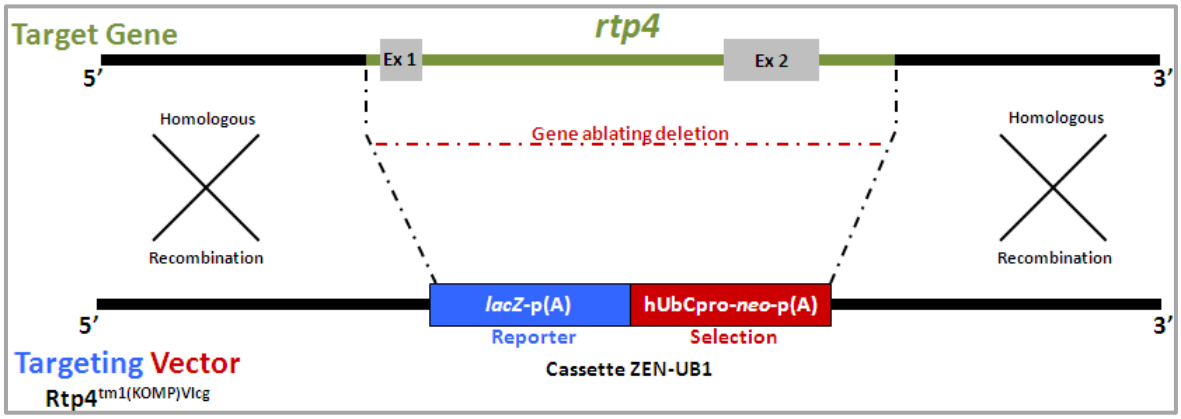

Figure 3-1: RTP4 gene targeting strategy.
The cassette (ZEN-UB1) that contains the reporter and selection genes *lacZ* and *neo* was used to replace the exon-containing sequence of the *rtp4* gene.

Blastocysts derived from an albino C57BL/6 strain (C57BL/6J-Tyr^{c-2J}/J) were microinjected with the recombined ES cells and then transferred to the uterus of a foster mother. The resulting offspring were mice with a different degree of chimerism, which resulted in different percentages of dark and white coats on these animals. The chimeric mice were then mated with WT animals in order to generate the germline of heterozygous mice for the *rtp4* gene (*rtp4*$^{+/-}$). The microinjection procedure as well as the germline generation was performed by GenOway, Lyon, France

The heterozygous animals were then interbred in order to generate homozygous mice for the *rtp4* gene (*rtp4*$^{-/-}$) on a C57BL/6 background.

3.1.3 Viruses

3.1.3.1 Newcastle disease virus

The lentogenic Newcastle disease virus strain chicken/Ulster/2C/68 (McFerran *et al.*, 1971) was obtained from Prof. R. Zawatzky (DKFZ, Heidelberg, Germany). The virus was propagated in embryonated chicken eggs by allantoic inoculation. After embryonic dead, the allantoic fluid was harvested and the virus was purified by ultracentrifugation (McGinnes *et al.*, 2006). The virus was quantified by hemagglutination assay (HA) using chicken red blood cells. One hemagglutination unit (HAU) is defined as the minimum amount of virus that induces agglutination of red blood cells (Donald *et al.*, 1954). NDV

stock titer contained 2400 HAU. Infection of BMMC with NDV virus was performed with 1 µl of the stock for a final concentration of 2.4 HAU/ml.

3.1.3.2 Influenza A virus

The influenza A virus (IAV) strain A/PR/8/34 (H1N1) (Taylor *et al.*, 1943) was obtained from ATCC, LGC standards (Middlesex, UK). The virus stock was propagated in Madin Darby canine kidney cells (MDCK), by dilution of the stock in DMEM complete medium and then added to cultured monolayers of MDCK cells. Supernatants from the cell culture were harvested daily and replaced with new DMEM complete medium until the cell monolayer exhibit 75% of cytopathic effect (Szretter *et al.*, 2006). IAV particles present in the supernatant were quantified by HA. The resultant HAU titer for the IAV-infected MDCK supernatant was 2048 HAU. Infection of BMMC with IAV was made using 10 µl of the supernatant stock for a final concentration of 20.4 HAU/ml.

3.1.4 Chemicals and reagents

Reagent	Company
2 - Mercaptoethanol (50 mM)	Gibco, Life Technologies GmbH, Darmstadt, Germany
Accutase	PAA Laboratories GmbH, Pasching, Austria
Acrylamide/Bis 29:1	Bio-Rad Laboratories, Hercules, USA
Anti PE microbeads	Miltenyi Biotec GmbH, Bergisch Gladbach, Germany
Ammonium persulfate	Amresco Inc, Cochran, USA
Bodipy 493/503	Life Technologies GmbH, Darmstadt, Germany
C-phosphate-G dinucleotides, ODN 1826	Invivogen, Tolouse, France
Chloroform, molecular grade	Carl Roth GmbH, Karlsruhe, Germany
Ciprofloxacin	Ratiopharm GmbH, Ulm, Germany
Complete Mini EDTA-Free, protease inhibitor cocktail	Roche Diagnostics GmbH, Mannheim, Germany
Coomassie blue dye	Fermentas GmbH, St. Leon-Rot, Germany
Concanavaline A	Sigma-Aldrich Co, St. Louis, USA
Deoxynucleoside triphosphate Set, PCR Grade	Roche Diagnostics GmbH, Mannheim, Germany
4',6-diamidino-2-phenylindole, dihydrochloride	Life Technologies GmbH, Darmstadt, Germany
Diethyl pyrocarbonate	Sigma-Aldrich Co, St. Louis, USA
DNP-HSA antigen	Sigma-Aldrich Co, St. Louis, USA

Dulbecco's modified medium	PAA Laboratories GmbH, Pasching, Austria
DuoSet® ELISA, mouse IL-6	R&D systems, Minneapolis, USA
DuoSet® ELISA, mouse osteopontin	R&D systems, Minneapolis, USA
Dynabeads® protein G	Life Technologies GmbH, Darmstadt, Germany
Ethanol, molecular grade	Carl Roth GmbH, Karlsruhe, Germany
Fetal bovine serum	Biochrom AG, Berlin, Germany
Gateway® pDEST 14 vector	Life Technologies GmbH, Darmstadt, Germany
Gateway®pDEST 40 vector	Life Technologies GmbH, Darmstadt, Germany
Gateway®pDEST 47 vector	Life Technologies GmbH, Darmstadt, Germany
Geneticin - G418 (50 mg/ml)	PAA Laboratories GmbH, Pasching, Austria
Glycine	Carl Roth GmbH, Karlsruhe, Germany
Goat serum	Dako Denmark A/S, Glostrup, Denmark
Granulocyte-macrophage colony stimulating factor (murine)	PeproTech, Inc, Rocky Hill, USA
High Pure PCR® product purification kit	Roche Diagnostics GmbH, Mannheim, Germany
IgE (Monoclonal) anti-dinitrophenyl clone SPE-7	Sigma-Aldrich Co, St. Louis, USA
Interleukin 3 (murine)	R&D systems, Minneapolis, USA
Iscove´s modified DMEM medium	PAA Laboratories GmbH, Pasching, Austria
Isopropanol, molecular grade	Carl Roth GmbH, Karlsruhe, Germany
L-Glutamine (200 mM)	PAA Laboratories GmbH, Pasching, Austria
Laemmli sample buffer	Bio-Rad Laboratories, Hercules, USA
LightCycler TaqMan master	Roche Diagnostics GmbH, Mannheim, Germany
Lipofectamine 2000	Life Technologies GmbH, Darmstadt, Germany
Lipopolysaccharide from *Salmonella enterica*	Brade, H., Forschungszentrum Borstel, Germany
Macrophage stimulating colony factor (murine)	PeproTech, Inc, Rocky Hill, USA
Minimum essential media, non essential amino acids (100x)	Gibco, Life Technologies GmbH, Darmstadt, Germany
Minimum Essential Media, Vitamins (100x)	Gibco, Life Technologies GmbH, Darmstadt, Germany
Mini-PROTEAN TGX gels, 12% acrylamide, 15 wells	Bio-Rad Laboratories, Hercules, USA
Mouse IP-10 module set ELISA	eBioscience, Frankfurt, Germany
Nitrocellulose Membrane	Bio-Rad Laboratories, Hercules, USA
N-Octyl-β-D-thioglucopyranoside	Merck KGaA, Darmstadt, Germany
Nucleospin plasmid quick pure	Machery-Nagel GmbH & Co, Dürel, Germany
p-max vector	Lonza Group Ltd, Basel, Switzerland

pDREAM 2.1 RTP4-FLAG vector	GeneScript Inc, Piscataway, USA
Penicillin-Streptomycin (100x)	PAA Laboratories GmbH, Pasching, Austria
Poly L-Lysine	Sigma-Aldrich Co, St. Louis, USA
Polyinosinic polycytidylic acid	Sigma-Aldrich Co, St. Louis, USA
Propidium iodide	Sigma-Aldrich Co, St. Louis, USA
Protein marker, precision plus, dual color standards	Bio-Rad Laboratories, Hercules, USA
Purelink, high pure plasmid midiprep kit	Life Technologies GmbH, Darmstadt, Germany
RNA extraction kit, RNeasy mini kit	Qiagen GmbH, Hilden, Germany
RnaseOUT recombinant ribonuclease inhibitor	Life Technologies GmbH, Darmstadt, Germany
Roswell Park Memorial Institute medium (RPMI)	Gibco, Life Technologies GmbH, Darmstadt, Germany
Roti-Blot	Carl Roth GmbH, Karlsruhe, Germany
S.O.C. medium	Life Technologies GmbH, Darmstadt, Germany
Sodium carbonate (7.5%)	Gibco, Life Technologies GmbH, Darmstadt, Germany
Sodium chloride	Merck KGaA, Darmstadt, Germany
Sodium dodecyl sulfate	Sigma-Aldrich Co, St. Louis, USA
Sodium pyruvate (100 mM)	Gibco, Life Technologies GmbH, Darmstadt, Germany
Stem cell factor (murine)	R&D systems, Minneapolis, USA
Sucrose	Sigma-Aldrich Co, St. Louis, USA
SuperScript™ III reverse transcriptase	Life Technologies GmbH, Darmstadt, Germany
ProteoExtract® subcellular proteome Extraction Kit	Merck KGaA, Darmstadt, Germany
N,N,N′,N′-Tetra-methylethylenediamine	Bio-Rad Laboratories, Hercules, USA
T4 DNA recombinant ligase	Roche Diagnostics GmbH, Mannheim, Germany
Tris	Carl Roth GmbH, Karlsruhe, Germany
Trypan blue 0.5% W/V	Biochrom AG, Berlin, Germany
Triton X-100	Sigma-Aldrich Co, St. Louis, USA
Trizol reagent	Life Technologies GmbH, Darmstadt, Germany
Tween 20	Sigma-Aldrich Co, St. Louis, USA
Universal probe library. Probe #11, 47 and 95	Roche Diagnostics GmbH, Mannheim, Germany
Vectashield	Vector Laboratories, Inc, Burlingame, USA.

3.1.5 Lab Supplies

Item	Company
Barrier tips Biospher (20, 200, and 1000 µl)	Sarstedt AG & Co, Nümbrecht, Germany
Cell culture flask (25, 75 cm^2)	Sarstedt AG & Co, Nümbrecht, Germany

Cell culture plates (6, 24, 96 wells)	Costar, Corning Inc, Corning, USA
Cells strainers (40 µm mesh)	BD, Franklin Lakes, USA
Centrifuge tubes (12, 15, 50 ml)	Sarstedt AG & Co, Nümbrecht, Germany
Confocal microscope slides (75 x 25 x 1 mm)	R. Langenbrinck, Emmendingen, Germany
Cover glass (60 x 24 x 0.16 mm)	R. Langenbrinck, Emmendingen, Germany
Cryotubes Vial	Nunc GmbH, Langenselbold, Germany
Diagnostic microscope slides 12 wells (well Ø5.2 mm)	Thermo Scientific, Braunschweig, Germany
LightCycler capillaries (20 µl)	Roche Diagnostics GmbH, Mannheim, Germany
LightCycler multiwell plate 96	Roche Diagnostics GmbH, Mannheim, Germany
Microcentrifuge tubes (0.1, 0.5, 1.5 and 2 ml)	Sarstedt AG & Co, Nümbrecht, Germany
FCM tubes	Sarstedt AG & Co, Nümbrecht, Germany
Filter paper	Whatman GmbH, Dassel, Germany
Needles	BD, Franklin Lakes, USA
Petri dishes	Sarstedt AG & Co, Nümbrecht, Germany
Pipette Tips (20, 200, 1000 and 1250 µl)	Sarstedt AG & Co, Nümbrecht, Germany
Serological pipettes (5,10,25 ml)	Sarstedt AG & Co, Nümbrecht, Germany
Plastic syringes (1, 5, 10 ml)	BD, Franklin Lakes, USA
Round microscope slides (Ø 12 x 0.13 mm)	Witeg Labortechnik GmbH, Wertheim, Germany
Square petri dishes	Falcon, BD, Franklin Lakes, USA

3.1.6 Antibodies

Antibody	Company
β-actin (mouse)	Sigma-Aldrich Co, St. Louis, USA
ADRP	Abcam, Cambridge, UK
Alexa 568 anti-rat IgG	Life Technologies GmbH, Darmstadt, Germany
Alexa 647 anti-rabbit IgG	Life Technologies GmbH, Darmstadt, Germany
CD 3ε	BD, Franklin Lakes, USA
CD4	BD, Franklin Lakes, USA
CD8a	Biolegend Inc, San Diego, USA
CD11b (Integrin α[M] chain)	Biolegend Inc, San Diego, USA
CD11c (Integrin α[x] chain)	BD, Franklin Lakes, USA
CD25 (IL-2 receptor α chain)	eBioscience, Frankfurt, Germany
CD44 (H-CAM)	BD, Franklin Lakes, USA
CD45R (B220)	BD, Franklin Lakes, USA
CD62L **(**L-selectin)	BD, Franklin Lakes, USA
CD49b (DX5)	Biolegend Inc, San Diego, USA

CD69 (Very early activation antigen)	BD, Franklin Lakes, USA
CD107a (LAMP-1)	Biolegend Inc, San Diego, USA
CD117 (c-Kit)	Biolegend Inc, San Diego, USA
F4/80	Ab Serotec, Düsseldorf, Germany
FcεRIa	Biolegend Inc, San Diego, USA
FLAG (N-DYKDDDDK-C)	Sigma Sigma-Aldrich Co, St. Louis, USA
GAPDH	Santa Cruz Biotechnology Inc, Santa Cruz, USA
Gr-1 (Ly6G)	BD, Franklin Lakes, USA
IgD	eBioscience, Frankfurt, Germany
IgM	BD, Franklin Lakes, USA
NK1.1 (Ly55)	eBioscience, Frankfurt, Germany
T1/ST2 (IL-33R)	MD Biosciences GmbH, Zurich Switzerland
IRDye 800CW Mouse IgG (H+L)	LI-COR, Lincoln, USA
IRDye 800CW Rabbit Rat IgG (H+L)	LI-COR, Lincoln, USA
IRDye 800CW Rat IgG (H+L)	LI-COR, Lincoln, USA
RTP4 (mouse)	Zawatzky, R., Deutsches Krebsforschungszentrum, Germany

3.1.7 Primers

Designed primers were acquired from Metabion GmbH, Martinsried, Germany, at a stock concentration of 100 µM. The primers listed below correspond to sequences matching with mouse genome.

Name	Sequence	Application
Oligo(dT)	FW: 5'- TTT TGT ACA AGC TTT TTT TTT TTT TTT TTT TTT TTT TTT TTT -3'	cDNA Synthesis
HPRT	FW: 5'- TCC TCC TCA GAC CGC TTT T-3' RW: 5'- CCT GGT TCA TCA TCG CTA ATC -3'	qRT-PCR
RTP4	FW: 5'- ACC AGC AGA CAG TGC TTG G -3' RW: 5'-CCT GAG CAG AGG TCC AAC TT -3'	qRT-PCR
VIP	FW: 5'- GCT TCA ACG TGG ACG AAG AC -3' RW: 5'- CCT CAA TTA GGA GGC ACT GG -3'	qRT-PCR

3.1.8 Solutions

3.1.8.1 Biochemistry and Molecular Biology Buffers

- **EDTA (500 ml)**
  EDTA 0.5 M
  pH 8.0

- **Blocking solution**
  Roti-Blot 20%
  PBS 10%
  H_2O
  For labeling with primary and secondary antibodies, 0.1% of Tween 20 must be added.

- **cDNA synthesis master mix**
  Buffer (5x) 5 µl
  dNTPs (2 mM) 5 µl
  DTT (0.1 M) 2.5 µl
  RNase inhibitor 1 µl
  Reverse Transcriptase 0.5 µl

- **dNTPs stock solution (2 mM)**
  RNase free H_2O 460 µl
  dATP, dCTP, dGTP, dTTp 10 µl each

- **Hypotonic Lyisis (HLM) Buffer**
  Tris HCl, pH 7.4, 20 mM
  EDTA 1 mM

- **1% ODGP lysis buffer (10 ml)**
  Tris HCl pH 7.5, 1 M 0.250 ml
  NaCl 3 M 0.250 ml
  ODGP 10% 1 ml
  H_2O 7.070 ml
  Protease inhibitor cocktail* 1.430 ml
  * Mini EDTA Free 7x stock

- **qRT-PCR mix**

Reagent	LightCycler system	
	Capillaries	96 Well plate
H_2O	4.9 µl	2.5 µl
Taq Man Master	2 µl	5 µl
Primer mix (10 µM)	1 µl	0.4 µl
Probe	0.1 µl	0.1 µl

- **Resolving gel buffer**
  Tris 1.5 M
  H_2O
  pH 8.8

- **RNase free water**
  DEPC water 0.1%
  H_2O
  Under a fume hood, mix the DEPC reagent overnight and the water and then autoclave.

- **Stacking gel buffer**
  Tris 0.5 M
  H_2O
  pH 6.8

- **SDS-PAGE running buffer**

Tris	25 mM
Glycine	192 mM
SDS	0.1 % (w/v)
H_2O	

- **TAE buffer 50x (1000 ml)**

Trizma Base	2 M
0.5M EDTA, pH8.0	100 ml
Acetic acid	57.2 ml

- **NuPAGE Transfer buffer**

NuPAGE transfer buffer (20x)	50 ml
Methanol	100 ml
Antioxidant	1 ml
H_2O	849 ml

3.1.8.2 Cell Culture Medium

- **DMEM complete medium**

DMEM	
Heat-inactivated FCS	10%
β-mercaptoethanol	50 µM
L-glutamine	2 mM
Penicillin	100 U/ml

- **Erythrocyte lysis buffer**

H_2O	
NH_4Cl	0.83%
Na_2CO_3	0.168%
EDTA	1 mM
pH 7.3, sterile filtrated	

- **IMDM complete medium**

IMDM	
Heat-inactivated FCS	10%
β-mercaptoethanol	50 µM
L-glutamine	2 mM
Penicillin	100 U/ml
Streptomycin	100 µg/ml
Non-essential amino acids	1%
Sodium pyruvate	1 mM

- **Luria Bertani (LB) Medium**

Tryptone	1%
Yeast extract	0.5%
NaCl	1%
H_2O	
pH 7.0	
For agar plates use 1.5% agar	

- **MACS buffer**
  PBS
  Heat-inactivated FCS 5%

- **Phosphate buffered saline (PBS)**
  H_2O
  Na_2HPO_4 3.2 mM
  KH_2PO_4 0.5 mM
  KCl 1.3 mM
  NaCl 135 mM
  pH 7.4

- **RPMI complete medium**
  RPMI - 1640
  Heat-inactivated FCS 10%
  β-mercaptoethanol 50 µM
  L-glutamine 2 mM
  Penicillin 100 U/ml
  Streptomycin 100 µg/ml

- **0.9% saline solution**
  H_2O
  NaCl 0.9%
  Filtered

3.1.8.3 Flow Cytometry (FCM) and Microscopy Buffers

- **Blocking solution for confocal microscopy**
  TBS
  Bovine serum albumin 5%
  Goat serum 2%

- **FCM buffer**
  PBS
  FCS 2%
  NaN_3 0.1%
  EDTA 2 mM
  pH 7.4 - 7.5

- **FCM flow**
  PBS
  NaN_3 0.1%
  Filtered

- **Paraformaldehyde 4%**
  H_2O
  PFA 4 %
  PBS 10x
  pH 7.4

- **Permeabilization buffer for confocal microscopy**
  PBS
  Triton X-100 0.25%
  Sodium citrate (stock 20% w/v) 0.2 %

- **Poly L-Lyisine coating solution**
  H_2O
  Poly L-lysine solution 1%

- **0.2% Propidium iodide FCM buffer**
  FCM buffer
  PI (stock 2 mg/ml) 0.05 %

- **Trypan blue**
  NaCl solution (0.9%)
  Trypan blue reagent 10 %

- **Tris Buffered saline (TBS)**
  H_2O
  Tris 10 mM
  NaCl 150 mM
  pH 7.4

3.1.9 Laboratory Equipment

Equipment	Description	Company
Bench centrifuge	Multifuge X3R	Thermo Fisher Scientific, Waltham, USA
Bench centrifuge	Rotina 46R	Hettich Lab technology, Tuttlingen, Germany
Confocal microscope	TCS SP5	Leica Microsystems GmbH, Wetzlar Germany
Culture microscope	CK40	Olympus, Tokyo, Japan
Electroporation system	Gene Pulser II	Bio-Rad Laboratories, Hercules, USA
ELISA reader	Inifinite M200	TECAN, Männedorf, Switzerland
Flow cytometer	FACS Calibur	BD, Franklin Lakes, USA
Image processor trans-illuminator	Universal Hood	Bio-Rad Laboratories, Hercules, USA
Incubator	Hera 150	Thermo Fisher Scientific, Waltham, USA
Infrared imaging system	Odyssey	LI-COR, Lincoln, USA
Magnet for immunoprecipitation	DynaMag™ Magnet	Life Technologies GmbH, Darmstadt, Germany
Magnetic Cell Sorting System	AutoMACS	Miltenyi Biotec GmbH, Bergisch Gladbach, Germany

Magnetic stirer	RH basic	IKA, Staufen, Germany
Microcentrifuge	Mikro 22	Hettich Lab technology, Tuttlingen, Germany
Microcentrifuge (refrigerated)	5415R	Eppendorf, Hamburg, Germany
Microplate washer	Fluido	Anthos, Heerhugowaard, Netherlands
Microwave oven	1026L	Privileg, Germany
Neubauer chamber	Bright improved	Brand GmbH, Wertheim, germany
pH Meter	MP 220	Mettler Toledo, Greifensee, Switzerland
Photometer	BioPhotometer	Eppendorf, Hamburg, Germany
Power supply	Power PAC basic	Bio-Rad Laboratories, Hercules, USA
Pipettes (10, 100, 1000 µl)	Eppendorf refference	Eppendorf, Hamburg, Germany
Power supply	Power PAC HC	Bio-Rad Laboratories, Hercules, USA
Precision balance	GF-300	A&D Instruments, Oxfordshire, United Kingdom
Protein electrophoresis	Mini-PROTEAN Tetra cell system	Bio-Rad Laboratories, Hercules, USA
Real Time thermocycler	Light Cycler 480	Roche Diagnostics GmbH, Mannheim, Germany
Real Time thermocycler	Light Cycler 2.0	Roche Diagnostics GmbH, Mannheim, Germany
Rotary shaker	Intelli Mixer 2M	LTF Labortechnik, Wasserburg, Germany
Safety cabinet	KR-200S	Kojair, Vilppula, Finland
Shaker	KS-260	IKA, Staufen, Germany
Spectrophotometer	Biophotometer	Eppendorf, Hamburg, Germany
Thermocycler	T3	Biometra, Göttingen, Germany
Transfer system (blotting)	XCell II Blot Module NuPAGE	Life Technologies GmbH, Darmstadt, Germany
Ultracentrifuge	L7-55	Beckman Coulter, Krefeld, Germany
Vortex	MS1 Minishaker	IKA, Staufen, Germany
Water bath	W6	Störk Tronik, Stuttgart , Germany

3.1.10 Software

Name	Use	Company
CLC Sequence Viewer, v. 6.5.2	Storing DNA, RNA, and proteins sequences	CLC bio, Aarhus, Denmark
David Bioinformatics Resource, v. 6.7	Analysis of microarrays data	National Institutes of Health, Bethesda, USA
Excel, v.14.0	Basic data analysis and figures design	Microsoft Inc, Redmond, USA
Finch T, v.1.4	Sequencing analysis	Geospiza Inc, Seatle, USA
FlowJo, v. 7.6.1	Flow cytometry data analysis	Tree Star, Inc, Ashland, USA
Leica Application Suite, LAS AF, v. 1.8.2	Acquisition and design for confocal microscopy	Leica Microsystems GmbH, Wetzlar, Germany
ImageJ	Quantification of band relative density	U.S. National Institutes of Health, Bethesda, USA
LightCycler 480 Software, v. 1.5	Acqisition and analysis of qRT-PCR	Roche Diagnostics GmbH, Mannheim, Germany
Odyssey, v. 2.1.12	Acquisition of Western blot data	LI-COR, Lincoln, USA
ProbeFinder, v. 2.45	Design of primers for qRT-PCR	Roche Diagnostics GmbH, Mannheim, Germany
SPSS, v.17	Statistical analysis	SPSS Inc, IBM Corp, Armonk, USA

3.2 Methods

3.2.1 Cell counting

Cells in suspension were mixed with the vital stain trypan blue in dilutions 1:10 or 1:20 depending on the cell density of the cultures. 10 µl of the dilution were placed in a Neubauer chamber and observed under the microscope. Cells acquiring the dye and appearing in blue color correspond to cells with altered cell membrane permeability and thus considered as dead cells. Live cells were refringent to the light and appeared bright. All experiments were conducted excluding dead cells.

3.2.2 Generation and culture of bone marrow derived mast cells (BMMC)

For the generation of BMMC (Razin *et al.*, 1984; Jensen *et al.*, 2006), mice from different genetic backgrounds (section 3.1.1 and 3.1.2) were euthanized with an overdose of CO_2 and superficially disinfected with 70% ethanol. The animals were aseptically dissected and the hind limbs were removed using sterile forceps and scissors. Tibia and femur were

cleared of the surrounding muscles and then the ends of the bones were cut in order to flush the medullary canal with ice-cooled PBS using a 26 gauge needle. Bone marrow cells were concentrated by centrifugation at 390 *g* for 5 min at 4ºC, treated with erythrocyte lysis solution for 15 minutes (min) at room temperature (RT), washed with PBS and finally cultured in 75 cm^2 tissue flasks. Cells were kept in IMDM complete medium, supplemented with murine recombinant SCF and IL-3 at doses of 10 ng/ml and 5 ng/ml, respectively, for 5 weeks at 37ºC and 7.5% CO_2. During the first week of culture, the cells were treated with ciprofloxacin hydrochloride at a concentration of 10 µg/ml to eliminate possible bacterial contamination. Once per week cells were collected, centrifuged and resuspended in fresh IMDM complete medium. In order to determine the correct differentiation of the progenitors into BMMC, aliquots of the cell cultures were analyzed by flow cytometry (FCM) for the expression of the maturation markers CD117, FcεR1a or ST2. Only cultures showing a purity higher than 90% were used for conducting experiments.

3.2.3 Generation and culture of bone marrow derived dendritic cells (BMDC)

After following the procedures described in the previous section for the isolation of bone marrow cells, these were resuspended in RPMI complete medium, counted using trypan blue and adjusted to a suspension of 3 x 10^6 cells in 10 ml of medium supplemented with 20 ng/ml of murine recombinant GM-CSF. Next, the cells were cultivated in Petri dishes during 7 days at 37ºC and 5% CO_2. On day 3, 10 ml of supplemented fresh medium were carefully added to the culture avoiding disturbance of the cells. On day 7, BMDC were detached and their maturity was assessed by FCM for the expression of the DC marker CD11c and for performing the experiments (Inaba *et al.*, 1992).

3.2.4 Generation and culture of bone marrow derived macrophages (BMM)

The procedure for the generation of BMM is similar to the one described for BMDC, with the difference that 10 x 10^6 cells were resuspended in 10 ml of RPMI complete medium supplemented with 20 ng/ml of M-CSF, seeded in a Petri dish and cultured for 7 days at 37ºC and 5% CO_2. On day 3, 10 ml of supplemented medium was added to the cultures. On

day 7, macrophages were detached from the dishes and their maturity evaluated by FCM, for the expression of the markers, CD11b and Gr1 (Weischenfeldt *et al.*, 2008).

3.2.5 Culture of cell lines

The Human Embryonic Kidney (HEK293T) cell line was cultured according to the specifications given by the provider. In general, cells were cultured in DMEM complete medium during 72 or 96 hr at 37ºC and 5% CO_2. Thereafter, the medium was collected and the cells were washed with PBS without altering the cell monolayer. Cells were then treated with Accutase for 5 min at 37ºC until detachment and then collected, washed with PBS and resuspended in complete medium.

3.2.6 Isolation of cells from primary and secondary immune organs

In order to isolate fresh B and T cells, WT mice were prepared for dissection as described in the previous section. With the help of forceps and scissors the spleen as well as the inguinal, superficial cervical, axillary, brachial and mesenteric lymph nodes (LN) were aseptically removed and collected in ice-cold PBS. Under sterile conditions, the spleen and separately the group of LN were placed on a cell strainer assembled to a 50 ml centrifuge. With the help of a 5 ml syringe's piston, the organs were carefully smashed and the cells were collected. Only splenic cells were resuspended in erythrocyte lysis buffer during 15 min at room temperature. All cells were washed with PBS by centrifugation at 390 *g*, counted and resuspended in MACS buffer. Cells from LN and spleen were subsequently used for isolation of B and T cells, respectively, using MACS (Section 3.2.8).

3.2.7 Detachment of adherent cells from cell culture flasks

Adherent primary cells (macrophages and dendritic cells) and cell lines were detached from the plastic surface of plates, dishes and cell culture flasks, by firstly removing the medium in which the cells were cultured, followed by a washing step with PBS in order to remove proteins that could inhibit the enzymatic action of the compound used for this aim. After removing the PBS, the cells were covered with Accutase (protease and collagenolytic

activity solution) and incubated during minimum 5 min at 37ºC and 5% CO_2. Detached cells were collected, washed with PBS and resuspended in the corresponding medium.

3.2.8 Purification of cell populations by magnetic associated cell sorting (MACS)

Cell populations can be purified from a heterogeneous cell mixture on the base of a differential expression of receptor markers. Hence, magnetic microbeads coupled with specific Abs against receptor markers are bound to the cells of interest, which later are separated in a MACS column and a magnetized separator that retain the labeled cells, which are considered as positive selected cell fraction. The flow- through fraction is collected as a negative fraction depleted of the labeled cells.

3.2.8.1 B cells separation

B cells and T cells were purified by negative selection, following the protocol of indirect magnetic labeling recommended by Miltenyi Biotec. Cells resuspended in MACS buffer at a concentration of 1 x 10^8 cells/ml were incubated with 1 µg/ml of the set of Phycoerythrin (PE) coupled Abs against the non-target populations (Table 3-1), during 15 min on ice and light protected. Light vortex was performed every 5 min. Next, cells were washed twice with ice-cold MACS buffer and resuspended at a concentration of 1 x 10^7 cells in 92 µl. Eight µl of anti-PE Abs coupled to microbeads were added to the cell suspension and then incubated for 15 min on ice and light protected. After incubation, cells were washed once and then resuspended in 2 ml of MACS buffer. Treated cells were separated using the AutoMACS machine and the program “DEPLETS”.

Table 3-1: List of antibodies used for cell isolation by MACS.

Cell type	Primary antibodies	Coupled microbeads
B cells	PE anti-CD11c PE anti-F480 PE anti-NK1.1 PE anti-CD8a PE anti-CD4	Anti PE
CD4$^+$ T cells	PE anti-B220 PE anti-CD11c PE anti-F480 PE anti-NK1.1 PE anti-CD8a	
CD8$^+$ T cells	PE anti-B220 PE anti-CD11c PE anti-F480 PE anti-NK1.1 PE anti-CD4	

3.2.9 Stimulation of mast cells for experimental procedures

As described in section 3.2.2, bone marrow cells are cultured for five weeks in the presence of IL-3 and SCF, which allow sustained proliferation and differentiation into mast cells. From this time point until the 8th week of culture, these mast cells were used for experiments.

The general procedure for using cells is described as follows: Five to 8 weeks cultured cells were harvested and transferred into 50 ml tubes. After 5 min of centrifugation at 390 *g*, the supernatant was discarded and the cell pellet reconstituted with fresh complete IMDM medium. Later, cell counting was performed using the trypan blue exclusion dye and then a suspension of cells was adjusted depending on the experimental needs (Table 3-2).

Table 3-2: Experimental conditions used for the stimulation of mast cells.

Application	Number of cells (10^6 cells)	Incubation time (hr)	Final volume (ml)	Culture Plate (N° wells)
qRT-PCR and microarrays	2	8	1	24
Western blot	2	24	1	24
Fractionation	5	24	2	6
Confocal Microscopy	1	24	1	24
Immunoprecipitation	5	24	2	6
ELISA	1	24	0.5	48

Then, cells were split into multi-well culture plates, where they received a growth-sustaining dose of 3 ng/ml of IL-3. BMMC were stimulated during different periods of time depending on the application. Table 3-3 lists the stimuli used in this work with their corresponding doses.

Table 3-3: Stimuli and dose used for cell culture.

Stimulus	Final concentration
CpG	3 µM
IAV	20.4 HAU/ml
IFNβ	5000 UI
LPS	100 g/ml
pIC	10 µg/ml
NDV	2.4 HAU/ml
Oleic acid	200 µM

3.2.10 Flow cytometry

Cells were analyzed for the expression of cell surface markers using FCM. For this, 2.5 - 5 x 10^5 cells were taken from cell suspensions, washed and resuspended in 100 µl of FACS buffer. Conjugated Abs with fluorescein isothyocyanate (FITC), phycoerythrin (PE) or allophycocyanin (APC) were added to the cell suspension in a concentration of 0.4 µg/ml, incubated for 30 min at 4ºC and light protected. The Abs used for the different objectives are described in the section 2.1.5. After incubation, cells were washed with FCM buffer containing 1 µg/ml of propidium iodide (PI) and then resuspended in 300 µl of FACS buffer. Samples were analyzed using the FACS Calibur flow cytometer and 20.000 cells were acquired for each condition.

Data files obtained from the experiments were analyzed using the software FlowJo v.7.6.1. The general procedure for FCM files comprised gating the cells according to their group size, eliminating cell debris and then excluding apoptotic/necrotic cells which are positive for PI. The final populations were gated depending on the cell markers and then their percentages were estimated.

3.2.10.1 Identification of cell subsets

Since primary and secondary immune organs contained a great variety of cell populations, different combinations of Abs were used for analyzing the cell phenotypes in spleen, lymph nodes, thymus and bone marrow. The following table shows the sets of Abs used for identifying the different cell subsets.

Table 3-4: Combination of antibodies for the identification of immune subsets.

Phenotype	Markers
$CD4^+$ T cells	APC-CD3 PE-CD4
Activated $CD4^+$ T cells	APC-CD4 PE-CD69
Effector memory $CD4^+$ T cells	APC-CD4 PE-CD44
Memory $CD4^+$ T cells	APC-CD4 PE-CD62L
$CD8^+$ T cells	APC-CD3 PE-CD8
Activated $CD8^+$ T cells	APC--CD8 PE-CD69
Effector memory $CD8^+$ T cells	APC-CD8 PE-CD44
Memory $CD8^+$ T cells	APC-CD8 PE-CD62L
B cells	APC-B220
Immature B cells	APC-B220 PE-IgM
Mature B cells	APC-B220 PE-IgD
Granulocytes	PE-Gr 1 PE-CD11b
NK cells	APC-CD3 PE-NK1.1
DC cells	APC-CD11c

Macrophages	PE-GR 1 PE-CD11b or PE- F4/80 PE-CD11b
Triple-positive thymocytes Triple-negative thymocytes	APC-CD3 APC-CD4 APC-CD8
$CD4^+$ thymocytes	APC-CD3 PE-CD4
$CD8^+$ thymocytes	APC-CD3 PE-CD8
Mast cells	APC- CD117 PE- T1/ST2 PE- FcεR1
Eosinophils	PE- CD11b PE- F4/80
Neutrophils	Gr1 CD117

3.2.10.2 Use of flow cytometry for assessment of mast cells degranulation

Degranulating mast cells were identified by the increased cell surface expression of the CD107a marker, which is the lysosomal associated membrane protein (LAMP-1). This protein resides in the membranes of cytolytic granules. When mast cells are induced to degranulate, LAMP-1 is mobilized to the cell surface upon granule exocytosis.

Matured BMMC were counted and 2 x 10^6 cells/ml were sensitized overnight with 5 µg/ml of mouse monoclonal IgE against the hapten dinitrophenyl (DNP) conjugated with bovine serum albumin (BSA). After 18 hr, sensitized cells were washed twice with fresh medium and then incubated for 30 min with 5, 10 and 20 ng of DNP-BSA Ag. As positive control for degranulation BMMC were treated with 100 ng/ml phorbol 12-myristate 13-acetate (PMA) and 1µM ionomycin (IO). Cells were washed and resuspended in 100 µl of FCM buffer together with anti-mouse CD107a at a concentration of 0.4 µg/ml. After 30 min of incubation cells were washed and resuspended in 300 µl of FCM buffer for flow cytometry.

3.2.11 Confocal microscopy

Since mast cells do not adhere to slides, round glass slides distributed in 24 wells plates were treated with a solution of 1% poly L-lysine in water, which is a positive-charged

amino acid that improves attachment of negatively charged cell membranes to slides. After 10 min of treatment, the solution was removed and 1 x 10^5 cells/300 µl were transferred into wells. Next, the plate was centrifuged for 5 min at 390 *g* and then incubated for 20 min at 37ºC and 5% CO_2. After attachment, the cells were fixed by the addition of 300 µl of a warm solution of 4% paraformaldehyde, incubated at 37ºC for 10 min, washed twice with TBS and permeabilized with 200 µl of 0.25% Triton X-100 for 10 min. Later, cells were washed 3 times with TBS, blocked with 5% BSA and 2% inactivated goat serum in TBS for 1 hr at RT and incubated with anti RTP4 (1:50) and anti ADRP (1:250) ON at 4ºC. After 3 washing steps with TBS the cells were incubated with the secondary Abs Alexa 568 anti-rat IgG (1:100), Alexa 647 anti-rabbit IgG (1:100) and DAPI (1 ng/ml) for cell nuclei staining. Cells were washed 3 times with TBS and then the slides were placed on rectangular microscope slides. 10 µl of the mounting medium Vectashield was used for ameliorating fading of fluorochromes. Slides were analyzed with the Leica TCS SP5 confocal microscope and the Leica LAS AF software.

3.2.12 Cytokine quantification in culture supernatants by ELISA

Cytokine quantification was done using the sandwich ELISA kits for IL-6 and osteopontin (DuoSet® ELISA, R&D Systems) and IP-10 (Module Set ELISA, eBioscience). Procedures were performed according to manufacturer's instructions. After 24 hr of cell stimulation, cell culture supernatants were collected in microcentrifuge tubes, centrifuged at full speed, to eliminate cell debris, and stored at -20ºC. 96-well microplates were coated with 50 µl of the capture antibody diluted in PBS solution, sealed and incubated overnight at 4ºC. After washing steps, microplates were blocked for 1 hr with the reagent diluent, provided in the kit, and then washed twice. 50 µl of samples and standards diluted in reagent diluent buffer were transferred to microplates and incubated for 2 hr at RT. After washing steps, 50 µl of the detection antibody, diluted in reagent diluent buffer, were added to wells and incubated for 2 hr. Microplates were washed and 50 µl of streptavidin-HRP diluted in reagent diluent buffer were added to wells. After 20 min of incubation, 50 µl of substrate solution (H_2O_2 - Tetramethylbenzidine) were split into wells and incubated for 20 min. Finally, microplate wells received 50 µl of stop solution. The optical density from each well was acquired using the Tecan ELISA reader set to 450 nmλ.

3.2.13 RNA isolation

For preparation of RNA, cells were collected from the cultures, centrifuged at 390 *g* and the resulting pellet was resuspended thoroughly in 1 ml of Trizol Reagent. 200 µl of chloroform were added and the tubes were vortexed and centrifuged at 13.000 *g* for 15 min and 4ºC. The upper clear phase resulting from centrifugation was collected and transferred to a new centrifugation tube. 500 µl of isopropanol were added and the tubes were vortexed, incubated for 10 min and centrifuged at 13.000 *g* for 15 min and 4ºC. The supernatant was discarded and 500 µl of 70% ethanol were used to wash the RNA pellet. After centrifugation of tubes at 7.500 *g* for 5 min and 4ºC, supernatant was removed and the RNA resuspended with 30 to 50 µl of RNAse free water. RNA samples were kept at -80ºC.

For some experiments, RNA isolation was performed using the Qiagen RNeasy mini kit. To this purpose, cells were collected, centrifuged as previously described and resuspended in 350 µl of the lysis buffer provided by the kit. The subsequent procedures were performed according to the instructions of the manufacturer. Isolated RNA was resuspended in 30 to 50 µl of RNAse free water.

RNA concentration and purity was determined by spectral absorption at A260 and A280 nmλ. For RNA purity, the ratio A260/A280 was calculated and RNA with ratio values between 1.7 and 2 were used for subsequent experiments.

3.2.14 Complementary DNA (cDNA) synthesis

For cDNA synthesis, 2 µg of mRNA in 10 µl of RNase free water were transferred in a 0.5 ml tube together with 200 ng of oligo(dT) primer, for a final volume of 11.5 µl. Samples were mixed, centrifuged and incubated for 10 min at 70ºC to perform the annealing of the oligo(dT) primers and the mRNA strand. Then, a master mix using the components of the SuperScript™ III Reverse Transcriptase kit, dNTPs and the RNase inhibitor was prepared and then distributed to the tubes. Samples were gently vortexed and then incubated during 1 hr at 37ºC. The incubation steps were performed using a thermocycler.

3.2.15 Analysis of gene expression by microarrays

Total RNA was sent to the Expression Core Facility at the Technische Universität München for microarray analysis. Gene expression was assessed using the array Affymetrix GeneChip Mouse Genome 430A 2.0, which allows the analysis of approximately 14.000 mouse genes.

3.2.16 Quantitative real-time polymerase chain reaction (qRT-PCR)

qRT-PCR was performed using the Light Cycler® system of Roche, either in capillaries or 96 wells plates format. All the assessments of gene expression included in this work comprised the use of hydrolysis probes also known as TaqMan probes. They consist of a modified oligonucleotide of a length of 8-9 nucleotides, bearing a fluorophore covalently attached to the 5'-end and a quencher to the 3'-end. When the quencher is close to the reporter, the fluorescence is suppressed. During the amplification step, the nuclease activity of the polymerase cleaves the probe, releasing the reporter dye that being no longer quenched is enabled to emit fluorescence. The fluorescence measured by the LightCycler system correlates with the accumulation of specific amplicons.

TaqMan probes and annealing primers were chosen based on the bioinformatics results of the software ProbeFinder at www.universalprobelybrary.com.

For the RT-PCR reaction, RNA was diluted in RNase free water and 2 µl of the dilution were mixed with 8 µl of the master mix, which was prepared according to the instruction provided in the LightCycler TaqMan Master kit. Later the mix was transferred to capillaries or wells, and samples were run under the following conditions:

Step	Temperature (ºC)	Time (sec)	Cycles
Initial denaturation	95	600	1
Denaturation	95	10	55
Annealing	56	30	
Amplification	72	1	
Cooling	40	30	1

3.2.17 Protein extraction and sample preparation

After cell culture, 2 x 10^6 cells were transferred to 1.5 ml centrifuge tubes, washed twice with 1 ml of PBS and then the supernatant was totally removed. Cells were lysed by adding 40 to 60 µl of 1% N-Octyl-β-D-thioglucopyranoside (ODGP) lysis buffer, and vortexed. After 20 min of incubation on ice, samples were centrifuged at 4ºC and 12000 *g* for 10 min. The resultant supernatants were transferred to a fresh centrifuge tube and then stored at -20ºC until Western blotting or immunoprecipitation was performed.

3.2.18 SDS-polyacrylamide-gel electrophoresis (SDS-PAGE)

SDS-PAGE allows separation of proteins with respect to their mobility, which is a function of the polypeptide length and charge. For this objective the Mini-Protean Tetra Electrophoresis System® from BIO-RAD was used.

Discontinuous polyacrylamide gels consist of a 6% stacking gel in which the samples are loaded and a 12% resolving gel in which the protein separation takes place. These gels were prepared as follows:

Reagent	6% stacking gel (ml)	12% resolving gel (ml)
H_20	3.075	10.2
Stacking/Resolving buffer	1.25	7.5
20% SDS	0.025	0.15
Acrylamide/Bis	0.67	12
10% APS	0.025	0.15
TEMED	0.005	0.02

The unpolymerized resolving gel mixture was transferred into a glass cassette of 1.5 mm space, fixed in a casting stand and then after the mixture was layered with water in order to keep flat the upper edges for the ulterior assembly of the stacking gel. Polymerization occurred after 1 hr and then the water content was removed from the cassette and replaced with the stacking gel mixture. A 15 well comb was carefully inserted into the cassette to create the sample slots, which were ready after 45 min of polymerization.

Prepared gels or ready to use precast gels were transferred and fixed to the electrode stand, which was assembled into the electrophoresis chamber. The chamber and the space between the gels in the electrode stand were filled with running buffer. Then equal

amounts of protein (20-40 µg) in a 10 µl volume were mixed with 10 µl of Laemmli sample buffer and then heated at 95ºC for 5 min. Samples were cooled down on ice and 15 µl of each sample and 5 µl of the protein marker were loaded into the wells. Electrophoresis was completed after a run of 60 min and 150 V.

3.2.19 Western Blotting

After electrophoresis was finalized, gels were removed from the glass cassettes and then resolving gels were parted from the stacking gels. Proteins were transferred to nitrocellulose membranes using the wet transfer system XCell II Blot Module, NuPAGE® from Life Technologies. Prior the transfer the gel, filter papers and fiber pads were equilibrated in transfer buffer. The gel bound to the membrane was sandwiched between two filter papers and two fiber pads (pad, pad, paper, paper, gel, membrane, paper, paper, pad, pad) in the blot module and then held tightly after confirming that no air bubbles were present between the gel and the membrane. The blot module was transferred and fixed into the blotting chamber and filled fully with transfer buffer. The outer chamber was filled with Millipore water in order to dissipate the heat produced during the run. Protein transfer was performed for 1 hr at 30 V.

3.2.20 Immunodetection of proteins

After protein transfer, membranes were allowed to dry and then incubated at room temperature with blocking solution for 1 hr. Primary Abs were diluted in blocking buffer plus 0.1% Tween 20 and used for labeling of membranes overnight at 4ºC on a rotary shaker at 100 r.p.m. Next day, membranes were washed 3 times (5 min/time) with abundant washing buffer and then incubated for 1 hr at room temperature with an infrared fluorochrome conjugated monoclonal antibody diluted in blocking buffer plus 0.1% tween 20. After removal of the secondary antibody, the membranes were washed as described above and kept in washing buffer at 4ºC until they were scanned by the Odyssey Infrared Imaging System (LI-COR).

As a loading control procedure, the blots were labeled with β-actin antibody and its secondary antibody. For this, the blots were treated previously with stripping solution during 15 min at room temperature and constant agitation in order to remove previous Abs.

Next, the blots were washed and treated as described above. The following table indicates the combination of primary and secondary Abs used for protein immunodetection.

	Primary Antibody	Secondary Antibody
β-actin	Mouse anti-mouse β-actin	IRDye 800CW goat anti mouse IgG (H+L)
RTP4	Rat anti-mouse RTP4	IRDye 800CW goat anti-Rat IgG (H+L)
TIM23	Mouse anti-mouse TIM23	IRDye 800CW goat anti mouse IgG (H+L)
GAPDH	Mouse anti-mouse GAPDH	IRDye 800CW goat anti mouse IgG (H+L)

3.2.21 Fractionation

In order to identify the possible cellular localization of RTP4, the cell proteome was separated according to its solubility using the ProteoExtract® Subcellular Proteome Extraction Kit (Calbiochem). After culture and proper stimulation, 5×10^6 BMMC were collected from cell culture plates and washed twice with the washing buffer provided in the kit. Then, cells were exposed to different extraction buffers containing a proteases inhibitor cocktail. The separation process resulted in 4 protein fractions belonging to cytosol, cell membranes (plasmatic and organelle derived), nuclear and cytoskeleton. The subcellular fractions were stored at -80ºC and later used for SDS-PAGE and Western blot analysis, as described in section 1.2.21. To control the purity of the fractionation procedure, cytosol and membrane proteomes were labeled with the specific compartment markers anti-GAPDH and anti-TIM23 Abs, respectively. Secondary infrared Abs were used for the detection of the primary Abs according to their Fc and then detected by the LI-COR imaging system.

3.2.22 Molecular cloning of RTP4

Gene cloning involves the isolation of a particular gene DNA, its insertion in an expression vector and the transformation and/or transfection of host cells.

rtp4 was amplified through PCR using as a template cDNA from BMMC stimulated for 8 hr with NDV. Proofreading DNA polymerase (iProof High-Fidelity DNA Polymerase, BioRad) was used together with primers for amplifying RTP4 cDNA. Both primers were designed for inserting restriction sites at the 5' and 3' ends of the amplicon.

Three vectors called "pMAST" were created as part of my work as a way to improve the expression of inserts in mast cells. For this, the vector p-max (Lonza Group Ltd), which

shows high transfection rates and a small size compared with other vectors, was used. The vector was linearized using restriction enzymes and 3 different inserts were ligated to the backbone of the vector. The inserts were amplified using proofreading polymerase and specific primers for the polylinker and tag region from the destination vectors pcDNA-DEST 14 (no tag), pcDNA-DEST 40 (V5 tag) and pcDNA-DEST 47 (GFP tag) of the Gateway® cloning system (Life Technologies Inc). The vectors received the name p-MAST-ATT, p-MAST-GFP and pMAST-V5. They can be used for the expression of proteins with the above mentioned tags, through direct ligation of the insert or by recombination between entry and destination vectors of the Gateway system.

The vector pMAST-ATT, which expresses the inserted sequence without any tag was linearized with the restriction enzymes for further ligation with the *rtp4* fragment. Ligation was performed in a ratio 3:1 insert : vector, using 5 U of T4 ligase and followed by an incubation at 18ºC overnight.

The construct was then used for transforming *Escherichia coli* DH5α competent bacteria. For this, competent bacteria were thawed on ice for receiving 3 µl of the construct and then incubated for 30 min on ice. Next, bacteria were heat shocked for 30 sec at 42ºC and brought back to ice for at least 2 minutes. Bacteria were incubated with 200 µl of S.O.C medium for 1 hr, at 37ºC and shaken at 200 r.p.m. 30 to 60 µl of bacterial inoculum were seeded on LB agar plates overnight in order to allow the formation of clonal colonies. Clones were then amplified in 4 ml of LB medium. Plasmid DNA was isolated using the NucleoSpin Plasmid kit® (Machery Nagel GmbH.) and sent for sequencing to the facilities of AGOBA GmbH, to verify the correct orientation (5' to 3') of the fragment and to identify mistakes during the amplification steps. After confirming the construct integrity, bacteria were again amplified in 100 ml of LB medium for plasmid extraction and glycerol stocks preparation. Plasmid DNA concentration was determined by spectrophotometric measurement at 260 nmλ and then stored at -20ºC.

3.2.23 Cell transfection for expression of RTP4

Human embryonic kidney 293 cells (HEK293T) are widely used as expression system for gene products. Transfection of these cells with RTP4 was performed for ulterior experiments for the identification of RTP4 interaction partners.

The day before transfection, 5 x 10^5 HEK293T cells were seeded in 6 well plates to obtain approximately 60 to 70% of cellular confluence. During the procedure, cells were always cultured with MEM medium without antibiotics. In a microcentrifuge tube, 5 µg of DNA was mixed with DMEM medium, which corresponds to the constructs pMAST RTP4 or pDREAM 2.1 RTP4-FLAG. In a second tube, 10 µl of the transfection reagent Lipofectamine 2000 were mixed with 250 µl of DMEM medium. After 5 min of incubation at RT, the content of both tubes was joined together, mixed and left for additional 20 min for promoting the formation of liposomes containing DNA. In the meantime, cultured cells were washed twice and then left with 500 µl of medium. Finally 500 µl of the mixture (DNA+Lipofectamine) was split into wells and then incubated during 4 hr at 37ºC and 5% CO_2. Wells were then supplemented with 1 ml of complete DMEM medium without antibiotics and cells were collected for total protein extraction after 48 hr of incubation.

3.2.24 Immunoprecipitation

Immunoprecipitation (IP) experiments were performed in order to identify possible RTP4 interaction partners. For this, 5 x 10^6 wild-type BMMC were stimulated with NDV or left untreated. Alternatively, 3 x 10^6 RTP4 and RTP4-FLAG transfected HEK293 cells were used. After 24 or 48 hr, cells were recovered, centrifuged at 390 *g* and then washed twice with cold PBS. Cell pellets were resuspended in 100 µl of ODGP lysis buffer for total protein isolation. Total protein was first subjected to a precleaning step, where products or proteins that bind unspecifically to the beads were removed. For this, 50 µl of G-protein coated magnetic beads (Dynabeads®, Life Technologies) were prepared by collecting them into microcentrifuge tubes. Next, tubes were placed in proximity to the Dynal® magnet, which concentrates and immobilizes the beads at the bottom of the tube, allowing the removal of the liquid phase. Using the same procedure, magnetic beads were washed 3 times with ODGP lysis buffer and finally mixed with 250 µg of total protein in a total volume of 300 µl, during 1 hr at 4ºC and on a rotary mixer. Then, magnetic beads were removed from the tubes and the precleaned protein was incubated with 5 µg of anti-FLAG antibody at 4ºC on a rotary mixer. After 18 hr of incubation, antibody-treated protein was mixed with freshly prepared beads for 1 hr at 4ºC on a rotary mixer. Afterwards, tubes were placed on the Dynal® magnet and magnetic beads with bound protein were retained, washed 3 times with lysis buffer and resuspended with 15 µl of ODGP lysis buffer and

15 µl of Laemmli buffer. Finally, protein elution from the beads was performed by boiling the samples at 95ºC for 5 min. SDS-PAGE and Western blot for detection of RTP4 was performed.

Additionally, protein gels were stained with Coomassie's blue dye for identification *in-situ* of protein complexes. For this, gels were washed 3 times with filtered water during 10 min and exposed overnight to the dye at RT on a rotary shaker.

3.2.25 Induction and isolation of lipid bodies

Immortalized macrophages (IM) were kindly provided by Dr. Golenbock, from the Medical School at the University of Massachusetts. These cells are bone morrow derived macrophages that had been transduced with the murine retrovirus J2 which contains the oncogenes v-raf and v-myc, resulting in an unlimited proliferation phenotype. IM were split every two days in DMEM complete medium until having a number of 6 to 7 x 10^8 cells. Cells were transferred in 6 bottles of 175 cm^2 culture flasks. 24 hr before the experiment the medium was changed and then 3 flasks were treated with 2.4 HAU/ml of NDV or left untreated. Additionally all the flasks were treated with 200 µM of oleic acid overnight. Next day, cells were harvested by centrifugation at 390 *g* and washed twice with PBS. At this point 2 x 10^6 cells were collected for total protein isolation. The rest of the cells were resuspended with HLM buffer (5 times the volume of the pellet size). The protease inhibitor cocktail Mini EDTA free was added according to the final volume. Next, cells were homogenized passing the cell solution through syringes mounted with 21, 25 and 27 gauge needles. The whole cell lysate was centrifuged at 1000 *g* for 10 min and 4ºC. Supernatant was recovered and then transferred to 15 ml tubes, where it was mixed with a volume of 60% sucrose HLM buffer to reach a final concentration of 20% sucrose. The mixture was transferred to ultracentrifuge tubes, then layered with 5 ml of 5% sucrose HLM buffer and finally with 6 ml of buffer. The tubes were ultracentrifuged at 14000 *g* for 30 min and 4ºC. The resultant upper top layer (LB fraction) was collected and used for SDS-PAGE analysis and for detection of RTP4 and ADRP by Western blot.

3.2.26 Statistical analysis and data management

3.2.26.1 General data processing

Data from experiments were registered in Excel (Microsoft office) data sheets and then figures and tables were elaborated.

For statistical analysis, data were exported to SPSS, where the type of distribution was established using the Shapiro-Wilk normality test. Descriptive analyses of the variables were performed and statistics for central tendency (mean) and dispersion (standard deviation and standard error) were calculated.

For determining differences between means the independent sample Student's T and Mann-Withney's U tests were performed, according to their parametric and non-parametric distribution, respectively. All tests were done considering a confidence interval of 95%.

3.2.26.2 Quantification of the gene expression for qRT-PCR

The method used to determine the changes in the mRNA levels was through the calculation of the relative expression. This method compares the expression of the target gene related to the expression of a reference gene, also called housekeeping gene. Reference genes are constitutively expressed independently of experimental conditions. In this work the hypoxanthine-guanine phosphoribosyltransferase (*hprt*) was used as a housekeeping gene (Pfaffl, 2001). Calculations were performed using the RealQuant and LightCycler 480 software from Roche Diagnostics.

3.2.26.3 Calculation of relative density for Western blot bands

For densitometric band quantification the software ImageJ was used. This software calculates the pixels constituting a specific band depending on the blot background (threshold). Relative density was then calculated by dividing the values of density of the target protein and density of the housekeeping gene (Gassmann *et al.*, 2009).

3.2.26.4 Analysis of microarray data

The data images from the chips were transformed by the Affymetrix Facility Core into values of fluorescence intensity after previous background subtraction. The obtained data was then converted to base 2 logarithms and the fold increase ratio of 2 samples was calculated. The fold increase value is one of the most common methods used to analyze microarray data due to its simple interpretation and results from the difference between the logarithmic means of the samples. Genes with a logarithmic fold change equal or higher than 2 (fold change of 4 in linear scale) were considered as genes with a relevant change (Babu, 2004; Whitworth, 2010). Upregulated genes were screened using the online tools from the DAVID bioinformatic resources (National institute of Allergy and Infectious Diseases), which group genes according to their function and pathway involvement (Huang *et al.*, 2008; Huang *et al.*, 2009).

Additionally, statistical tests were also performed and consisted in the calculation of significant differences between the means of the experimental replicates by two-tailed Student's T test. It is important to note that the two methods of analysis were interpreted independently.

4. Results

4.1 Mast cells display an antiviral program.

MC play an essential role in pathologies such as asthma and immune responses against parasites. However new evidence suggests that MC may contribute in controlling anti-viral immune responses (Dawicki *et al.*, 2007). It has been reported that MC are activated by the virus mimetic pIC, which is synthetic doubled-stranded RNA, via binding and signaling through TLR3 (Kulka *et al.*, 2004; Orinska *et al.*, 2005). Thus eliciting a type I interferon response after infection with vesicular stomatitis virus, dengue virus and hantavirus, among others (Dietrich *et al.*, 2010; Guhl *et al.*, 2010; St John *et al.*, 2011). Chickens maintained under pathogen free conditions (SPF) and infected with bursal disease virus, showed activation of MC, their migration to infected organs and the release of MC mediators such as tryptase (Wang *et al.*, 2008). Moreover, Stelekati (2008) reported that MC upon direct contact with $CD8^+$ T cells in the absence of Ag, up-regulated genes coding for proteins involved in the cascade of type I interferon-mediated immune responses.

A first strategy to investigate the role of MC in anti-viral immunity was to define a gene expression profile in MC which is induced upon viral infection via the use of gene array analysis. To this purpose, BMMC obtained from three WT mice were infected with 2.4 HAU/ml NDV for 8 hr. Uninfected cells were used as control. Total RNA was isolated and sent to the Expression Core Facility at the Technische Universität München for performing the gene array analysis. NDV is an avian paramyxovirus that has been widely used for studying anti-viral immune responses in both human and murine immune cells, due to its ability to induce type I interferons and related genes (Guha-Thakurta *et al.*, 1997; Wilden *et al.*, 2009).

The comparison of the gene expression between uninfected and NDV-infected BMMC showed that 110 genes exhibit a fold-increase higher than the cutoff value of 2. These

genes were entered in the bioinformatic tool DAVID, which validated 101 genes to be used in clustering analysis based on functionality. Table 4-1, lists the genes grouped in 7 functional categories. The first group corresponds to 23 upregulated genes having roles in "**antiviral defense**". This category embrace genes coding for proteins involved in antiviral immune responses at different levels, like viral recognition (*ddx60*, *dhx58*, *ifih1 zbp1* and *ddx58*), effector mechanisms, which include cytokines and mediators that amplify the responses (*irf7*, *ifna2*, *stat1*, *ifna1*, *ifna7*, *ifna6*, *stat2*, *ifna5*, *ifna4* and *irf9*) and final products that participate in the control of viral replication (*ifit1*, *rsad2*, *ifit2*, *isg15*, *ifit3*, *mx1*and *ifitm3*). The second group "**cytokines**", include genes that are upregulated as a consequence of the activation of PRRs, like *ccl5*, *cxcl0*, *tnfsf10*, *tnfsf8* and members of the type I interferon that were also included in the antiviral defense group. The third group, "**innate immunity**" collects genes whose coded proteins participate in general immune processes such Ag processing/presentation and inflammation (*irgm1*, *nlrc5*, *samhad1* and *tap1*). The fourth group, "**nucleotide binding**" comprise 24 genes that code for proteins with the property of binding nucleotide-based molecules such as, RNA, DNA, ATP and GTP. Some of these coded proteins can interact directly with viral nucleic acids inhibiting their replication (*isg20*, *oasl2*, *gbp3*, *oas3*, *gbp2*). The "**nuclear**" group is the fifth category of upregulated genes, whose proteins localize mainly in the cell nucleus and participate in a variety of cell processes. The sixth group "**ubiquitination**", includes genes that translate for proteins involved in protein regulation/degradation mediated by the axis proteasome-ubiquitin. The last group of "**unclassified**" genes is composed by 28 genes, whose functions remain unknown.

These results showed that mast cells upon viral infection are able to upregulate a great variety of genes that not only belong to the anti-viral program but that also mediate other effector and regulatory functions.

Table 4-1: Viral infection induces a selective gene expression profile in mast cells.
BMMC generated from wild-type mice were stimulated with 2.4 HAU/ml of NDV. After 8 hr of incubation, RNA was isolated and microarray analysis was performed by using the GeneChip Mouse Genome 430 2.0. Fold changes were calculated as the logarithmic difference (log base 2) of the means from untreated (unt) and NDV treated cells. The table lists genes that displayed a fold change ≥ 2 and that were group in different categories based on their functional features, according to the bioinformatic tool DAVID. *n*=3.

Gene	Gene Description	Mean expression		Fold change	Position
		unt	NDV		
Antiviral defense					
ifit1	Interferon-induced protein with tetratricopeptide repeats 1	2.3	9.5	7.2	1
rsad2	radical S-adenosyl methionine domain containing 2	3.3	9.9	6.5	3
irf7	Interferon regulatory factor 7	3.8	9.5	5.6	6
ddx60	DEAD (Asp-Glu-Ala-Asp) box polypeptide 60	2.7	7.5	4.8	14
dhx58	DEXH (Asp-Glu-X-His) box polypeptide 58 (LGP2)	3.3	8.0	4.7	16
ifih1	Interferon induced with helicase C domain 1 (MDA5)	3.3	8.1	4.7	17
ifit2	Interferon-induced protein with tetratricopeptide repeats 2	2.6	7.4	4.7	18
ifna2	Interferon alpha 2	2.7	7.2	4.4	20
stat1	Signal transducer and activator of transcription 1	5.2	9.5	4.3	24
isg15	ISG15 ubiquitin-like modifier	2.7	6.9	4.2	25
ifit3	Interferon-induced protein with tetratricopeptide repeats 3	2.7	6.9	4.1	28
ifna1	Interferon alpha 1	3.5	7.1	3.5	38
ifna7	Interferon alpha 7	3.3	6.9	3.5	39
mx1	Myxovirus (influenza virus) resistance 1	2.4	5.9	3.5	42
ifna6	Interferon alpha 6	2.4	5.9	3.4	45
zbp1	Z-DNA binding protein 1	3.3	6.7	3.4	47
eif2ak2	Eukaryotic translation initiation factor 2-alpha kinase 2	4.5	7.7	3.1	56
stat2	Signal transducer and activator of transcription 2	5.1	8.3	3.1	57
ddx58	DEAD (Asp-Glu-Ala-Asp) box polypeptide 58 (RIG-I)	6.0	9.1	3.1	58
ifna5	Interferon alpha 5	4.7	7.5	2.8	69
ifitm3	Interferon induced transmembrane protein 3	8.8	11.3	2.4	86
ifna4	Interferon alpha 4	2.4	4.8	2.4	87

irf9	Interferon regulatory factor 9	5.3	7.6	2.3	92
Cytokines					
cxcl10	Chemokine (C-X-C motif) ligand 10	2.8	7.7	4.9	12
ccl5	Chemokine (C-C motif) ligand 5	3.6	8.1	4.5	19
tnfsf10	Tumor necrosis factor (ligand) superfamily, member 10	4.3	7.6	3.3	49
tnfsf8	Tumor necrosis factor (ligand) superfamily, member 8	4.3	6.8	2.5	81
Innate immunity responses					
irgm2	Immunity-relatedGTPase family M member 2	4.5	8.5	4.0	27
nlrc5	NLR family, CARD domain containing 5	2.7	5.4	2.7	65
samhd1	SAM domain and HD domain, 1	7.2	10.0	2.8	71
tap1	Transporter 1, ATP-binding cassette, sub-family B (TAP)	6.4	8.6	2.1	96
Nucleotide binding					
cmpk2	Cytidine monophosphate (UMP-CMP) kinase 2, mitochondrial	2.6	8.5	5.9	4
isg20	Interferon-stimulated protein	3.6	9.4	5.8	5
oasl2	2'-5' oligoadenylate synthetase-like 2	3.4	8.9	5.4	8
gbp3	Guanylate binding protein 3	3.2	8.4	5.1	10
tgtp1	T-cell specific GTPase 2; T-cell specific GTPase	4.6	9.6	5.0	11
oas3	2'-5' oligoadenylate synthetase 3	3.0	7.8	4.8	15
gvin1	GTPase, very large interferon inducible 1	4.0	8.4	4.4	23
gbp2	Guanylate binding protein 2	6.0	9.6	3.6	36
tor3a	Torsin family 3, member A	5.6	9.2	3.6	37
oas1a	2'-5' oligoadenylate synthetase 1A	4.2	7.7	3.6	40
oasl1	2'-5' oligoadenylate synthetase-like 1	4.7	8.2	3.5	44
oas1g	2'-5' oligoadenylate synthetase 1G	4.9	8.3	3.4	46
gbp6	Guanylate binding protein 6	6.1	9.5	3.4	48
iigp1	Interferon inducible GTPase 1	2.2	5.4	3.2	51
ifi47	Interferon gamma inducible protein 47	3.6	6.8	3.2	55
gbp9	Guanylate-binding protein 9	3.1	6.1	3.0	60
ehd4	EH-domain containing 4	3.7	6.7	3.0	61
trim21	Tripartite motif-containing 21	5.8	8.6	2.8	68

gbp5	Guanylate binding protein 5	2.9	5.6	2.6	76
mov10	Moloney leukemia virus 10; predicted gene 7357	4.6	7.1	2.5	80
gbp4	Guanylate binding protein 4	4.5	6.8	2.4	88
map3k8	Mitogen-activated protein kinase kinase kinase 8	3.1	5.4	2.3	90
adar	Adenosine deaminase, RNA-specific	4.7	7.0	2.3	91
pnpt1	Polyribonucleotide nucleotidyltransferase 1	4.7	6.9	2.3	94
Nuclear regulation					
parp14	Poly (ADP-ribose) polymerase family, member 14	4.3	8.2	3.9	30
xaf1	XIAP associated factor 1	3.8	7.6	3.8	31
parp12	Poly (ADP-ribose) polymerase family, member 12	4.7	8.4	3.7	33
setdb2	SET domain, bifurcated 2	2.9	6.4	3.5	43
trim30	Tripartite motif-containing 30	7.2	10.5	3.3	50
parp9	Poly (ADP-ribose) polymerase family, member 9	5.4	8.4	2.9	66
ifi35	Interferon-induced protein 35	5.1	8.0	2.9	67
sp100	Nuclear antigen Sp100	5.8	8.5	2.7	74
ifi203	Interferon activated gene 203; interferon activated gene 203	3.0	5.7	2.7	75
psmb10	Proteasome (prosome, macropain) subunit, beta type 10	5.6	8.2	2.6	79
clic4	Chloride intracellular channel 4 (mitochondrial)	5.6	7.9	2.3	93
Ubiquitination					
usp18	Ubiquitin specific peptidase 18;	5.2	10.1	4.9	13
ube2l6	Ubiquitin-conjugating enzyme E2L 6	4.2	8.7	4.4	22
herc5	Hect domain and RLD 5	5.3	9.1	3.8	32
dtx3l	Deltex 3-like (Drosophila)	4.9	8.1	3.2	52
trim25	Tripartite motif-containing 25	4.7	7.7	3.0	63
Unclassified					
rtp4	Receptor transporter protein 4	2.6	9.4	6.8	2
gm12250	Predicted gene 12250	2.9	8.4	5.5	7
slfn5	Schlafen 5	3.1	8.5	5.3	9
aI451617	Expressed sequence AI451617	3.2	7.7	4.4	21
gm12597	Predicted gene 12597; interferon, alpha 14	3.2	7.4	4.3	26

irgm2	Immunity-related GTPase family M member 2	4.6	8.6	4.0	29
h2-gs10	MHC class I like protein GS10	4.0	7.6	3.6	34
bst2	Bone marrow stromal cell antigen 2	6.2	9.8	3.6	35
ifi44	Interferon-induced protein 44	2.8	6.3	3.5	41
slfn8	Schlafen 8	4.8	8.0	3.2	53
mpa2l	Macrophage activation 2 like	5.1	8.3	3.2	54
lgals3bp	Lectin, galactoside-binding, soluble, 3 binding protein	7.4	10.5	3.1	59
slfn9	Schlafen 9	4.0	7.0	3.0	62
ifi27l2a	Interferon, alpha-inducible protein 27 like 2A	3.9	6.9	3.0	64
tdrd7	Tudor domain containing 7	4.1	6.8	2.8	70
epsti1	Epithelial stromal interaction 1 (breast)	2.6	5.4	2.8	72
cd69	CD69 antigen	5.6	8.2	2.6	77
h2-t24	Histocompatibility 2, T region locus 24	5.3	7.9	2.6	78
samd9l	Sterile alpha motif domain containing 9-like	6.0	8.6	2.5	82
bc006779	cDNA sequence BC006779	3.5	5.9	2.5	83
trafd1	TRAF type zinc finger domain containing 1	6.4	8.9	2.5	84
9930111 J21Rik2	RIKEN gene; interferon-inducible GTPase family member	2.9	5.4	2.5	85
i830012 O16Rik	RIKEN cDNA I830012O16 gene	2.2	4.4	2.2	95
apobec1	Apolipoprotein B mRNA editing enzyme, catalytic polypeptide 1	3.8	5.9	2.1	97
mitd1	MIT, microtubule interacting and transport, domain containing 1	4.7	6.8	2.0	98
mlkl	Mixed lineage kinase domain-like	5.3	7.3	2.0	99
sp110	Predicted gene 15753; Sp110 nuclear body protein	6.2	8.3	2.0	100
zufsp	Zinc finger with UFM1-specific peptidase domain	4.3	6.3	2.0	101

4.2 The unclassified gene *rtp4* and the antiviral gene *rsad2* are highly up-regulated in mast cells upon infection with NDV

In the work of Stelekati, (2008) focused to identify changes in the gene expression profile of BMMC after co-cultured with $CD8^+$ T cells, it was found that *rtp4* and *rsad2* were the 1^{st} and 4^{th} most up-regulated genes, respectively. Furthermore, other studies focused on

characterizing IFN responses, using different cell types (PBMC, macrophages, NK cells) and stimuli (NDV, IFNβ), report *rtp4* and *rsad2* genes as prominent up-regulated genes (Tracey *et al.*, 2004; Venter *et al.*, 2005; Sanda *et al.*, 2006; Reder *et al.*, 2008). Interestingly in this work, the same genes *rtp4* and *rsad2* were in the 2nd and 3rd position of the most expressed genes, with fold changes of 6.8 and 6.5 times, respectively when BMMC were treated with NDV (Table 4-1).

In order to quantify the expression of *rtp4* and *rsad2* mRNA in mast cells upon NDV infection and to verify the findings obtained from the microarray analysis, qRT-PCR was performed. To this end, wild-type BMMC were infected with 2.4 HAU/ml of NDV for 8 hr and untreated BMMC were used as negative control. The relative expression of *rtp4* and *rsad2* mRNA was normalized to the expression of the house keeping gene hypoxanthine phosphoribosyltransferase (*hprt*).

As shown in figure 4-1, treatment of BMMC with NDV leads to a statistically significant increase of *rtp4* and *rsad2* mRNA expression (1600 and 4700-fold, respectively) in comparison to the negative control. Hence, the results of qRT-PCR confirm the findings obtained from the microarray analysis.

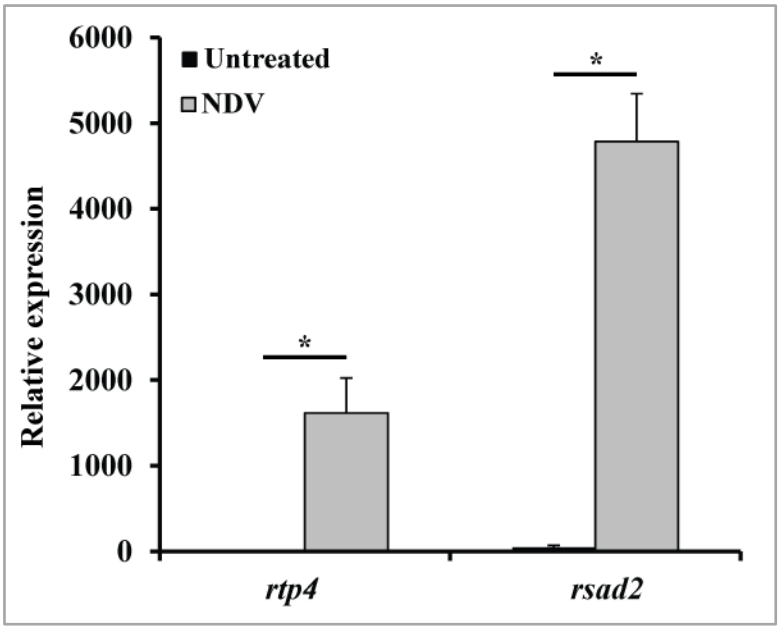

Figure 4-1: Expression of *rtp4* and *rsad2* in mast cells after stimulation with NDV.

BMMC from wild-type mice were stimulated with NDV (2.4 HAU/ml) or left untreated. After 8 hr of incubation, RNA was isolated and then cDNA was synthetized. The figure shows, qRT-PCR analysis for the mean ± SEM expression of *rtp4* and *rsad2* normalized to the house-keeping gene *hprt*. * $p \leq 0.05$. $n=4$, (Independent samples Mann-Whitney U test).

The gene radical S-adenosyl methionine domain containing 2 (*rsad2*), also known as VIPERIN has been described to be induced in fibroblasts upon infection with cytomegalovirus and in response to IFNs production (Chin *et al.*, 2001). Furthermore, VIPERIN has been described to be expressed in dendritic cells, macrophages, neutrophils and induced by other viruses such as HCV, human immunodeficiency, influenza A, yellow fever and murine lymphocytic choriomeningitis (Helbig *et al.*, 2005; Khaiboullina *et al.*, 2005; Hinson *et al.*, 2009; Hinson *et al.*, 2010; Nasr *et al.*, 2012). VIPERIN is as an antiviral protein, which inhibits the formation of new viral particles by disrupting the lipid rafts present on the cell membrane and used for viral budding (Wang *et al.*, 2007).

Little is known about the functions of RTP4. It has been proposed that it serves as a chaperone-like protein, facilitating odorant, taste and opioid receptors to be loaded into the cell membrane. Nevertheless its role in the immune response remains unclear (Behrens *et al.*, 2006; Decaillot *et al.*, 2008).

4.3 RTP4 is a prominent antiviral gene expressed in BMMC

Influenza A virus belongs to the family of ortomyxovirus and is the causative agent of severe respiratory disease in humans and poultry. The mouse has been shown to be a useful model to study different aspects of IAV such as virulence, pathogenicity and host defense since it reproduces the features of the infection (Lu *et al.*, 1999). As well as NDV, IAV is a single strand RNA virus that triggers immune responses dependent on the synthesis of interferons (Opitz *et al.*, 2007).

In order to understand whether the upregulation of *rtp4* expression is not specific for NDV but is a general response to virus infection, wild-type BMMC were infected with 20.4 HAU/ml of IAV and 2.4 HAU/ml of NDV for 8 hr. NDV infected cells and untreated cells were used as positive and negative controls, respectively. Relative expression of *rtp4* mRNA was quantified by qRT-PCR and values were normalized to the expression of the house keeping gene *hprt*.

Results in figure 4-2, show that induction of *rtp4* mRNA in BMMC upon infection with IAV was 1000 times higher in comparison to the negative control (untreated cells).

Likewise, the expression levels of *rtp4* mRNA upon infection with IAV are comparable to the expression of the positive control (cells infected with NDV).

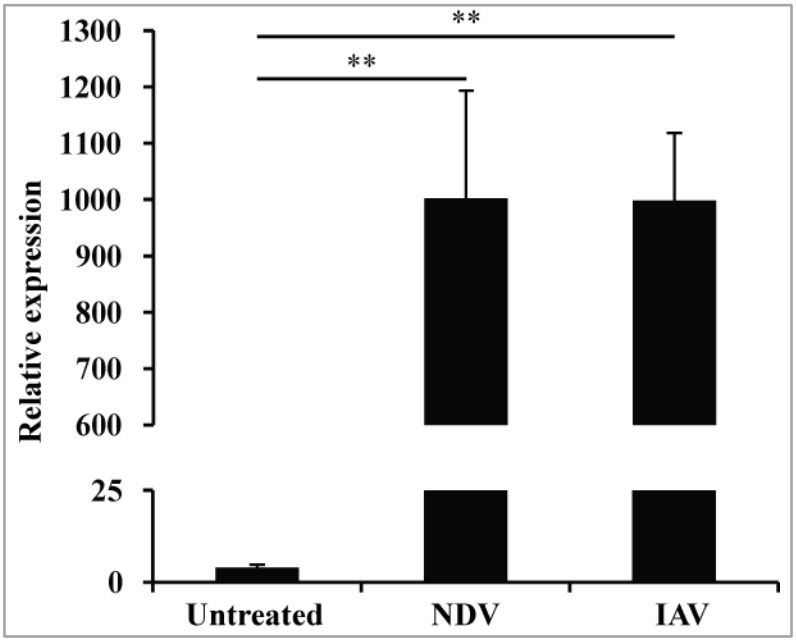

Figure 4-2: *rtp4* mRNA is up-regulated in BMMC after viral stimulation.
BMMC from wild-type mice were stimulated with 2.4 HAU/ml of Newcastle disease virus (NDV), 20.4 HAU/ml of influenza A virus (IAV) or left untreated. After 8 hr of incubation, mRNA was isolated and first strand cDNA was synthesized. The figure shows, qRT-PCR analysis for the mean ± SEM expression of *rtp4* normalized to the house-keeping gen *hprt*. ** $p \leq 0.01$. untreated $n=7$, NDV $n=7$ and IAV $n=4$, (Independent samples Student's T-test).

This comparable expression of *rtp4* mRNA upon the infection of BMMC with IAV and NDV demonstrates that the upregulation of RTP4 transcripts in mast cells is induced by different RNA viruses.

4.4 Regulation of RTP4 through toll like receptors

Toll like receptors play an important role in the recognition of microbial structural components, TLR3, TLR7, TLR8 and TLR9. Their activation upon ligand binding triggers different signaling pathways, which results in specific responses focused on eliminating invading microbes from the host via the release of cytokines and chemokines and anti-viral proteins (Kawai *et al.*, 2008).

In order to verify whether TLRs engagement is required in the upregulation of RTP4 expression, BMMC were treated with TLRs agonists and the expression of RTP4 transcripts and protein was evaluated. For this wild-type BMMC where stimulated with 1 μg/ml of pIC, 100 ng/ml of LPS and 3 μM of CpG which are agonist of TLR3, TLR4 and TLR9, respectively. BMMC were also infected with 2.4 HAU/ml of NDV or left untreated, here used as positive and negative controls. RNA and protein were isolated after 8 and 24 hr, respectively for qRT-PCR and SDS-PAGE/WB analysis.

Figure 4-3, A, shows that BMMC cultured with TLRs ligands exhibit an increased expression of *rtp4* mRNA. Treatment of BMMC with the ligands pIC and LPS leads to a significant increase in *rtp4* RNA of 5 and 7 times in comparison to the negative control (untreated cells). CpG also induces expression of RTP4 but the increase is not statistically significant. Although an increase in *rtp4* mRNA expression was detectable upon TLR-agonist stimulation, the levels of induction were much lower to the ones detected in the positive control (BMMC infected with NDV).

Western blot analyses were performed using specific Abs against RTP4 and β-actin, this last one served to determine the protein loading. A control was used to determine the molecular weight of RTP4 (28 kDa), for this, lysates form HEK 293T cells transfected with RTP4 were used. Quantification of the results was done by the calculation of the bands relative density (Figure 4-3, B).

Hence, the results show that RTP4 is detectable only when BMMC were treated with NDV reflecting the sevenfold increase of relative density of the RTP4 band. Moreover the RTP4 protein detected in lysates from BMMC lysates upon NDV treatment presents the same molecular weight as the control cells transfected with RTP4 (positive control), confirming the specificity of the antibody and the detected product. These results confirm that RTP4 is induced by TLRs ligands.

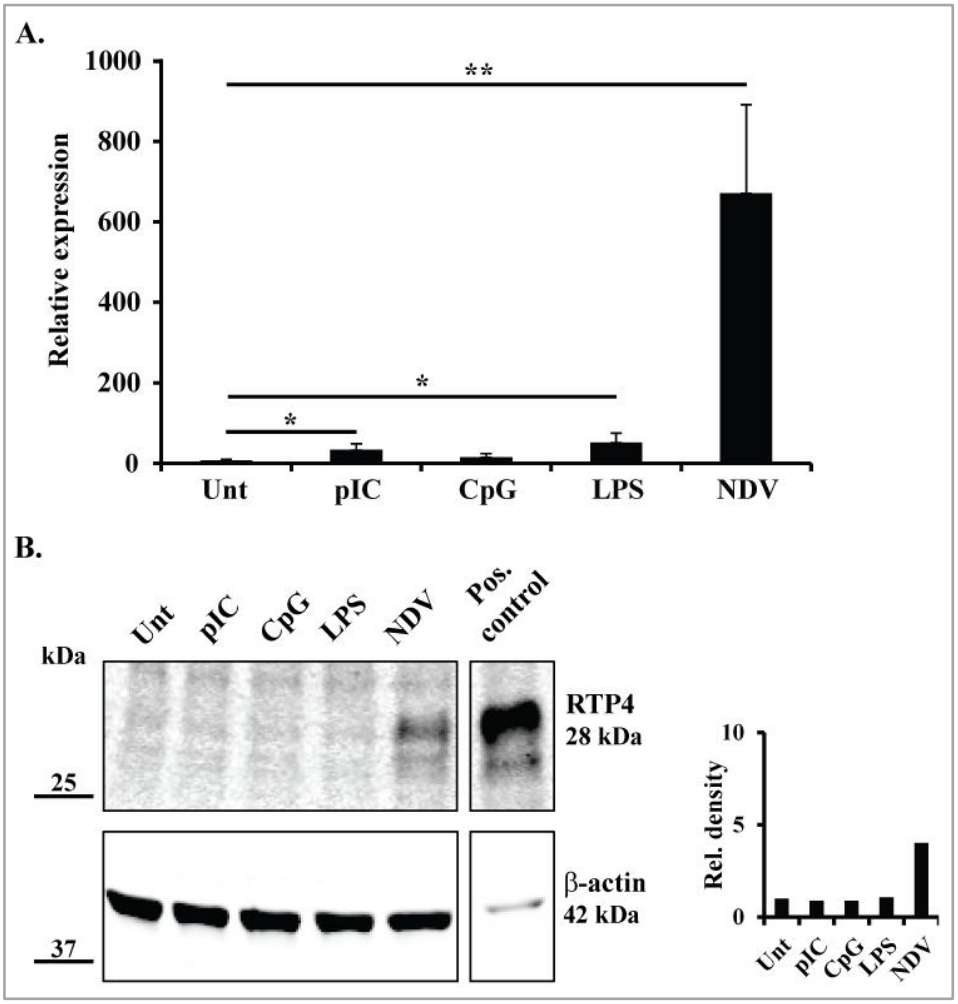

Figure 4-3: Expression of *rtp4* mRNA and protein in mast cells after stimulation with toll like receptor ligands.
BMMC from wild-type mice were stimulated with pIC (1 µg/ml), CpG 1826 (3 µM), LPS (100 ng/ml), NDV (2.4 HAU/ml) or left untreated (Unt). (**A.**)After 8 hr, RNA was isolated and then cDNA was synthetized, the figure shows, qRT-PCR analysis for the mean ± SEM expression of *rtp4* normalized to the house-keeping gene *hprt*. * $p \leq 0.05$, ** $p \leq 0.01$. n=4-6. (Independent samples Mann-Whitney's U test). (**B.**) After 24 hr total protein was extracted and separated through SDS-PAGE for Western blotting analysis of RTP4 and β-actin as loading control. The histogram chart shows the relative density of the bands normalized to β-actin. Positive control is the lysate of RTP4 transfected HEK293 cells. Data is representative of three independent experiments.

4.5 RTP4 is expressed in other cells of the immune system

Results from the previous section showed that murine BMMC up-regulate RTP4 upon viral stimulation. However, innate and adaptive immunity engage a number of different cell types involved in anti-viral immune responses. In order to investigate whether RTP4 is expressed in other immune cells, qRT-PCR was performed. To this end, bone marrow progenitor were isolated and cultured for 7 days with GM-CSF or M-CSF for

differentiation into dendritic cells or macrophages; spleen and lymph nodes were dissected from WT mice, homogenized and used for magnetic cell sorting of B cells and $CD4^+$ and $CD8^+$ T cells, respectively. BMDC, BMM and B cells were treated with the TLRs ligands pIC (1μg/ml), CpG (3 μM) and LPS (100 ng/ml) for 8 hr. Cells were also infected with NDV (2.4 HAU/ml) or left untreated for setting up positive and negative controls. $CD4^+$ and $CD8^+$ T-cells were treated for 8 hr with 3μg/ml of concanavalin A. which is a lectin able to activate T cells. Isolation of RNA and synthesis of cDNA were performed and then *rtp4* mRNA expression was measured by qRT-PCR.

Results indicate that treatment of BMDC with pIC and CpG significantly increases the expression of *rtp4* mRNA 2600 and 1800 times, respectively, higher than the negative control (untreated cells). In contrast, treatment of BMDC with LPS does not induce changes in *rtp4* mRNA expression, and values are comparable to the negative control (Figure 4-4, A).

BMM up-regulated *rtp4* mRNA expression when treated with pIC and LPS 1600 and 3300 times higher. Such increase was statistically significant. *rtp4* mRNA expression levels in cell treated with CpG were comparable to the negative control (Figure 4-4, B).

Treatment of both, BMDC and BMM with NDV (positive control) led to a significant increase of *rtp4* mRNA expression

On the other hand, B cells constitutively express high levels of *rtp4* mRNA in comparison to the other cell types. Treatment of this subset with pIC, LPS and NDV did not increase *rtp4* mRNA expression significantly. Surprisingly, B cells upon treatment with CpG significantly reduced *rtp4* mRNA expression 18 times (Figure 4-4, C).

$CD4^+$ and $CD8^+$ T cells activated with ConA did not exhibit changes in *rtp4* mRNA expression and the levels were comparable to the negative control (Figure 4-4, D).

Taken together these results indicate that induction of RTP4 upon virus stimulation is also extended to other cells of the immune system such as BMDC and BMM. Although B cells did not significantly up-regulate *rtp4* mRNA, their high constitutive expression suggests an important role in this cell type.

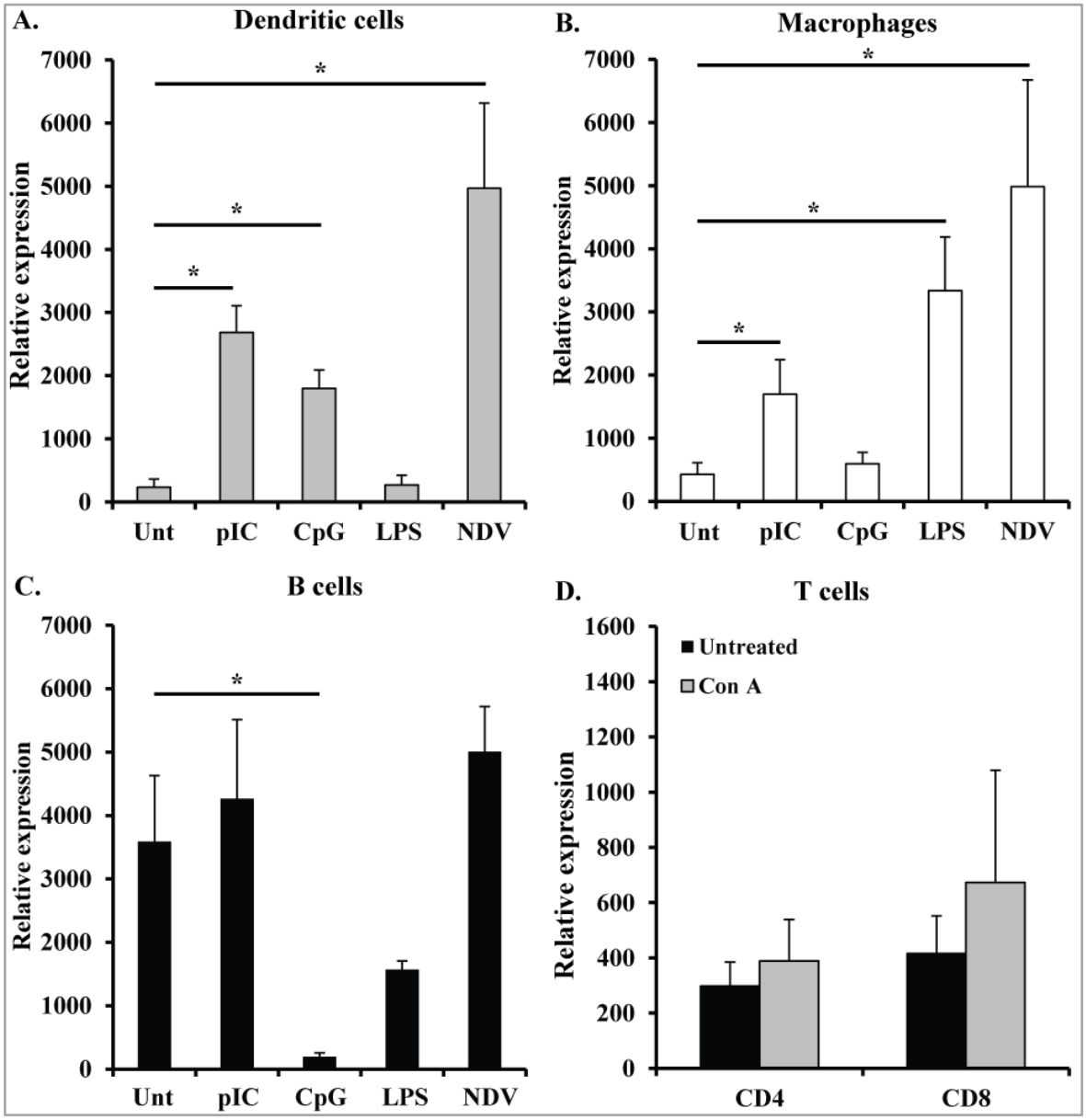

Figure 4-4: Expression of *rtp4* mRNA in different cell types after stimulation with toll like receptor ligands.
B cells, (**A.**) Dendritic cells (**B.**) and Macrophages (**C.**) from wild-type mice were stimulated with pIC (1 µg/ml), CpG 1826 (3 µM), LPS (100 ng/ml), NDV (2.4 HAU/ml) or left untreated (Unt). After 8 hr of incubation, RNA was isolated and then cDNA was synthetized. The figure shows, qRT-PCR analysis for the mean ± SEM expression of *rtp4* normalized to the house-keeping gene *hprt*. * $p \leq 0.05$. $n=4$ (Independent samples Mann-Whitney's U test).

4.6 TLRs are partially responsible for the up-regulation of RTP4 in mast cells

The cascade of events after the engagement of TLRs, involves the recruitment and binding of adaptor proteins to the TIR domain of the receptors. In this regard almost all TLRs recruit the adaptor protein MyD88, with the exception of TLR3 that binds exclusively

TRIF. Adaptor proteins work as inducers and amplifiers of the signaling cascade, through the activation of different sets of kinases. Activation and translocation to the nucleus of the transcription factors NF-κB, IRF3 and IRF7 is the final consequence of TLRs activation which ends in the production of pro-inflammatory cytokines and interferons (Blasius *et al.*, 2010; Kawai *et al.*, 2011)

In order to confirm the findings from the previous section (4.4) that showed that induction of RTP4 is mediated by TLRs and to investigate which signaling pathways are required for RTP4 expression, BMMC simultaneously lacking TLR2, TLR3, TLR4, TLR7 and TLR9 and BMMC lacking the adaptor proteins MyD88 and TRIF were used for assessing the expression of *rtp4* mRNA and protein. For this, BMMC from the deficient mice *tlr23479*$^{-/-}$, *myd88*$^{-/-}$ and *trif*$^{-/-}$ were stimulated for 8 and 24 hr with the TLR ligands pIC (1µg/ml), CpG (3 µM) and LPS (100 ng/ml). Additionally, BMMC were also infected with 2.4 HAU/ml of NDV or left untreated for setting positive and negative controls. After isolation of RNA and total protein, qRT-PCR and WB analysis were performed.

qRT-PCR analysis showed that the expression of *rtp4* mRNA in BMMC from *tlr23479*$^{-/-}$ mice treated with TLR ligands, pIC, CpG and LPS, was not induced. *rtp4* mRNA levels were comparable to the negative control (untreated cells). Only the positive control, cells infected with NDV, exhibited a significant increase of 400 times more *rtp4* mRNA. Likewise, WB analysis showed that BMMC stimulated with TLR ligands did not express RTP4. RTP4 was only detected in BMMC from the positive control and according to the calculation of relative density its expression was seven times higher in comparison to the negative control (Figure 4-5, A).

Stimulation of *myd88*$^{-/-}$ BMMC with TLR ligands led to an increase in the expression of *rtp4* mRNA when values were compared to the negative control, however such increase was not statistically significant. On the other hand, results from *trif*$^{-/-}$ deficient cells showed that *rtp4* mRNA expression was not induced. For both *trif*$^{-/-}$ and *myd88*$^{-/-}$ BMMC infected with NDV (positive control), the expression of *rtp4* mRNA levels was 900 and 400 times significantly higher than the negative control. In WB analysis, detection of RTP4 was not achieved in *trif*$^{-/-}$ and *myd88*$^{-/-}$ BMMC after treatment with TLR ligands. Only BMMC from the positive control show five times more RTP4 protein according to the band's relative density analysis (Figure 4-5, B and C).

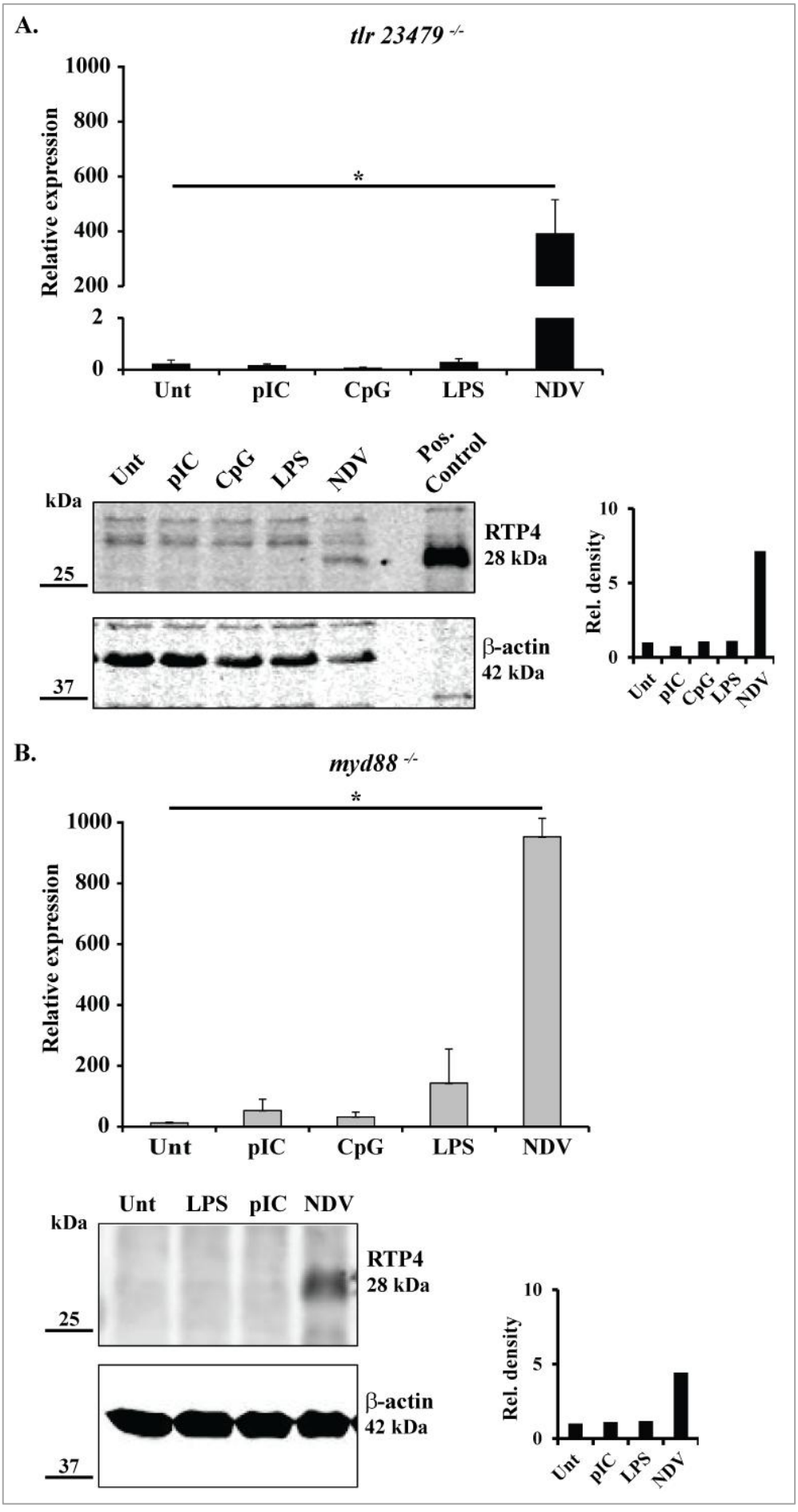
A.
tlr 23479 -/-
Relative expression
1000
800
600
400
200
2
0
*
Unt
pIC
CpG
LPS
NDV
Unt
pIC
CpG
LPS
NDV
Pos. Control
kDa
25
RTP4
28 kDa
37
β-actin
42 kDa
Rel. density
10
5
0
Unt
pIC
CpG
LPS
NDV
B.
myd88 -/-
*
Relative expression
1000
800
600
400
200
0
Unt
pIC
CpG
LPS
NDV
Unt
LPS
pIC
NDV
kDa
25
RTP4
28 kDa
37
β-actin
42 kDa
Rel. density
10
5
0
Unt
pIC
LPS
NDV

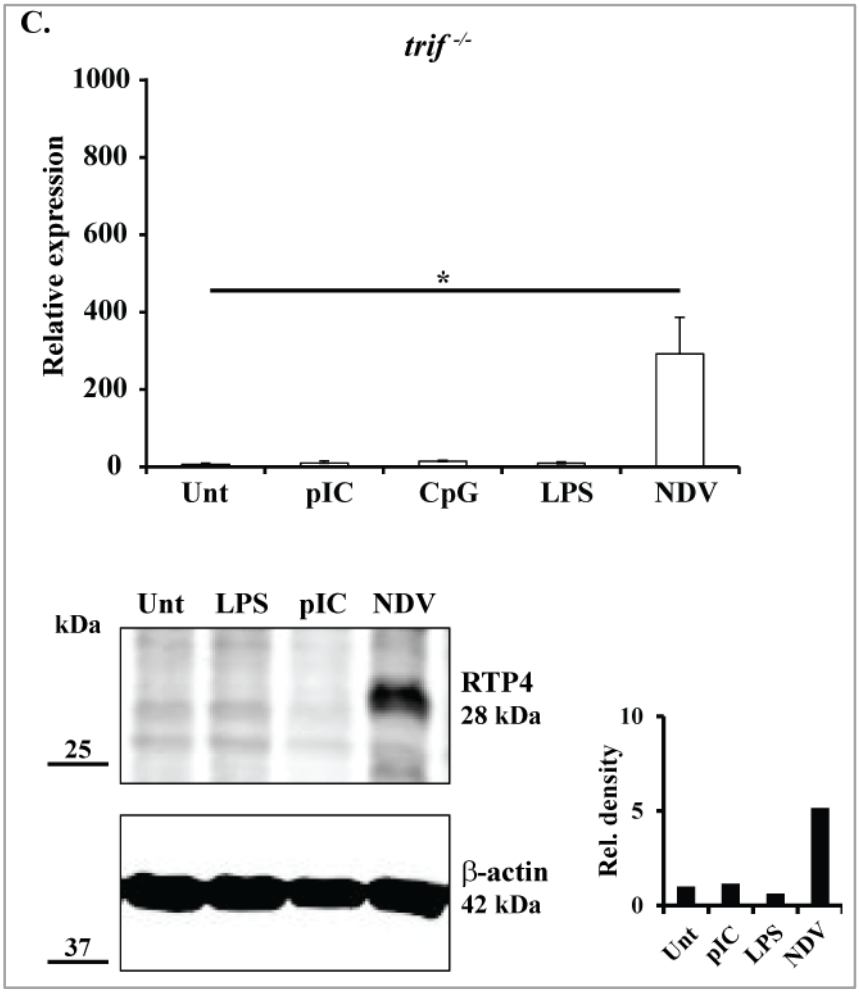

Figure 4-5: Expression of *rtp4* mRNA and protein in mast cells from the deficient mice for *tlr23479*$^{-/-}$, *myd88*$^{-/-}$, *trif*$^{-/-}$ after stimulation with toll like receptor ligands.
BMMC from the multi-deficient *tlr23479*$^{-/-}$, *myd88*$^{-/-}$ and *trif*$^{-/-}$ mice were stimulated with pIC (1 µg/ml), CpG 1826 (3 µM), LPS (100 ng/ml), NDV (2.4 HAU/ml) or left untreated (Unt). After 8 hr of incubation, RNA was isolated and then first strand cDNA was synthetized, the figure shows, qRT-PCR analysis for the mean ± SEM expression of *rtp4* normalized to the house-keeping gene *hprt*. * $p \leq 0.05$. $n=3$. (Independent samples Mann-Whitney's U test). After 24 hr total protein was extracted and separated through SDS-PAGE for Western blotting analysis of RTP4 and β-actin as loading control. The histogram chart shows the relative density of the bands normalized to β-actin. Positive control is the lysate of RTP4 transfected HEK293 cells. Data is representative of three independent experiments.

These results demonstrate that TLRs as well as the adaptor proteins are contributing to the induction of RTP4. But, since deletion of these genes did not result in a total abrogation of RTP4 expression, this is not totally dependent on the TLRs investigated. Therefore, other signaling pathways should be involved in the regulation of RTP4 expression.

4.7 Expression of RTP4 depends on type I interferons activities

Viral particles are sensed by surface and endosomal TLRs or by cytosolic receptors such as RIG-I and MDA5, which belong to the family of RNA helicases. Induction of cytokines such as IL-6, TNFα, IL-12 is commonly triggered, however the real hallmark of the antiviral response is the production of type I interferons. Type I interferons binds to their receptor IFNAR, which is responsible for the induction of a large number of genes through the recruitment of the transcription activators (IRF and STAT) that finally lead to the production of interferon stimulated genes (Thompson *et al.*, 2011).

In order to assess the involvement of type I interferons in the regulation of RTP4 expression, BMMC from mice lacking the alpha sub-unit of the interferon α/β receptor (*ifnar1*$^{-/-}$) were treated with TLR ligands and assessed for the expression of *rtp4* mRNA and protein. For this, *ifnar1*$^{-/-}$ BMMC were treated with the TLR ligands pIC, CpG and LPS using the doses previously described. BMMC were also infected with 2.4 HAU/ml of NDV or left untreated for setting up positive and negative controls, respectively. Total RNA and protein were isolated after 8 and 24 hr of culture and qRT-PCR and WB analysis were performed.

Interestingly, treatment of *ifnar1*$^{-/-}$ BMMC with TLR ligands did not induce expression of RTP4. *rtp4* mRNA levels were comparable to the negative control (untreated cells). Likewise, induction of RTP4 mRNA in BMMC infected with NDV (positive control) was abolished. In accordance to the result of RNA expression, WB analysis showed that RTP4 protein could not be detected in BMMC treated with TLR ligands even in cells infected with NDV, that were considered as positive control (Figure 4-6).

These results strongly demonstrate that induction of RTP4 expression is dependent on interferons and the signaling pathways triggered by activation of IFNAR.

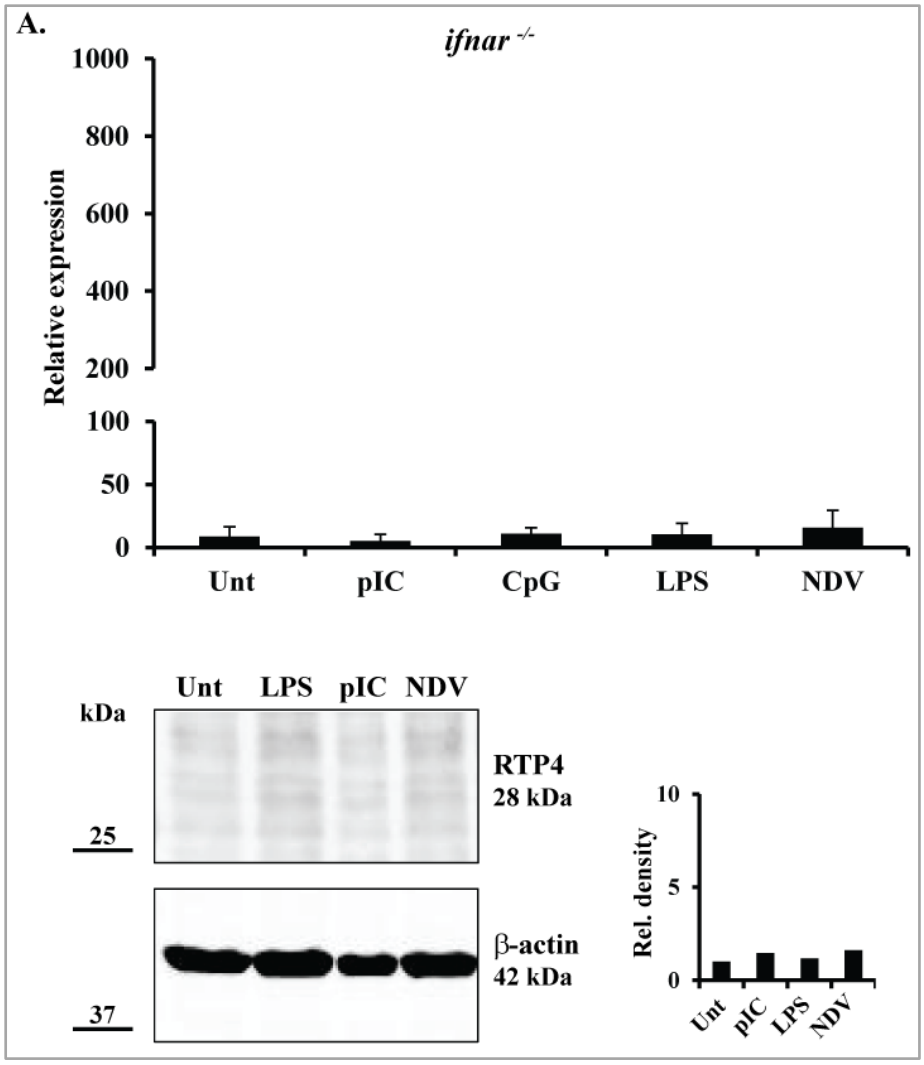

Figure 4-6: *rtp4* expression is abrogated in BMMC from the *ifnar1*$^{-/-}$ mice.
BMMC from *ifnar1*$^{-/-}$mice were stimulated with pIC (1 µg/ml), CpG 1826 (3 µM), LPS (100 ng/ml), NDV (2.4 HAU/ml) or left untreated (Unt). After 8 hr, RNA was isolated and then cDNA was synthetized, the figure shows, qRT-PCR analysis for the mean ± SEM expression of *rtp4* normalized to the house-keeping gene *hprt*. *n*=3. After 24 hr total protein was extracted and separated through SDS-PAGE for Western blotting analysis of RTP4 and β-actin as loading control. The histogram chart shows the relative density of the bands normalized to β-actin.

To test the hypothesis that viruses induce RTP4 expression via type I interferons, wild type BMMC were treated with 1000 and 5000 IU of recombinant murine-IFNβ for 8 hr. RNA was isolated and transcribed into first strand cDNA for assessment of RTP4 expression by qRT-PCR. As is seen in figure 4-7, BMMC treated with 1000 and 5000 IU of IFNβ significantly expressed 6000 and 8000 times more *rtp4* mRNA than the negative control

(untreated cells). This experiment confirms that *rtp4* mRNA expression is induced by type I interferon and that such expression is dose dependent.

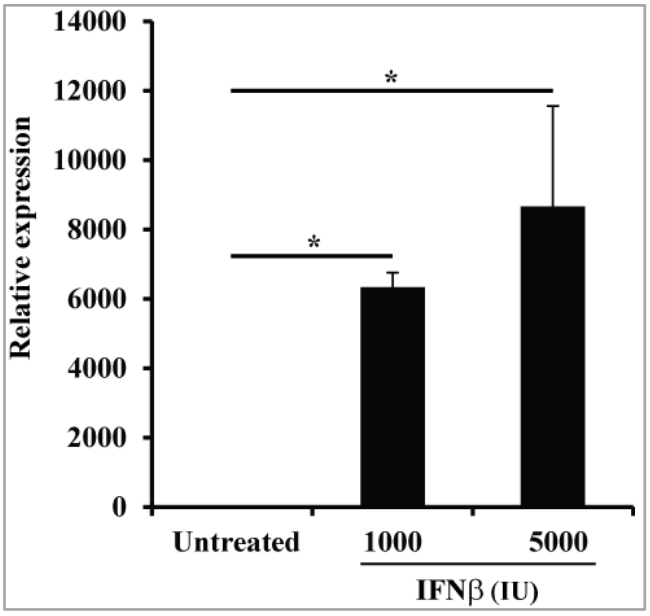

Figure 4-7: Expression of *rtp4* mRNA in mast cells after stimulation with mouse recombinant interferon β.
BMMC from wild-type mice were stimulated with 1000 and 5000 IU of mouse recombinant interferon β (IFNβ). After 8 hr of incubation, RNA was isolated and then first strand cDNA was synthetized. The figure shows, qRT-PCR analysis for the mean ± SEM expression of *rtp4* normalized to the house-keeping gene *hprt*. * $p \leq 0.05$. $n=3$. (Independent samples Mann-Whitney's U test).

4.8 Subcellular proteome isolation

The investigation of protein localization and compartmentalization is crucial to understand the conditions in which proteins work, their interaction with other proteins, their role in the general metabolism of the cells and ultimately their function. In order to gain insights into the subcellular localization of RTP4, proteome fractionation and WB analysis were performed. For this, 5 x 10^6 BMMC were stimulated with 2.4 HAU/ml of NDV, which had been shown to induce RTP4 protein expression. Untreated cells were also cultured and used as negative control. After 24 hr, cells were collected and washed with PBS for performing the extraction of the subcellular proteome. The resulting protein fractions corresponding to cytosol (cyt), cell membranes (mem) (including organelle membranes), nucleus (nuc) and cytoskeleton (Cytk) were subjected to SDS-PAGE. Western blot analysis included the Abs used for the detection of murine RTP4 and compartment markers

like TIM23 (membranes) and GAPDH (cytosol), used for controlling the purity of the fractions.

Western blot analysis showed that RTP4 was detected only in the membrane fraction from cells infected with NDV and not in the negative control (untreated cells). Additionally, the marker TIM23 was present only in the fraction corresponding to membranes and the marker GAPDH was detected in the cytosolic fraction. These findings were observed for both, cells infected with NDV and in the negative control and confirmed the purity of the fractions. This result concluded that RTP4 associates to cellular membranes upon stimulation with NDV (Figure 4-8).

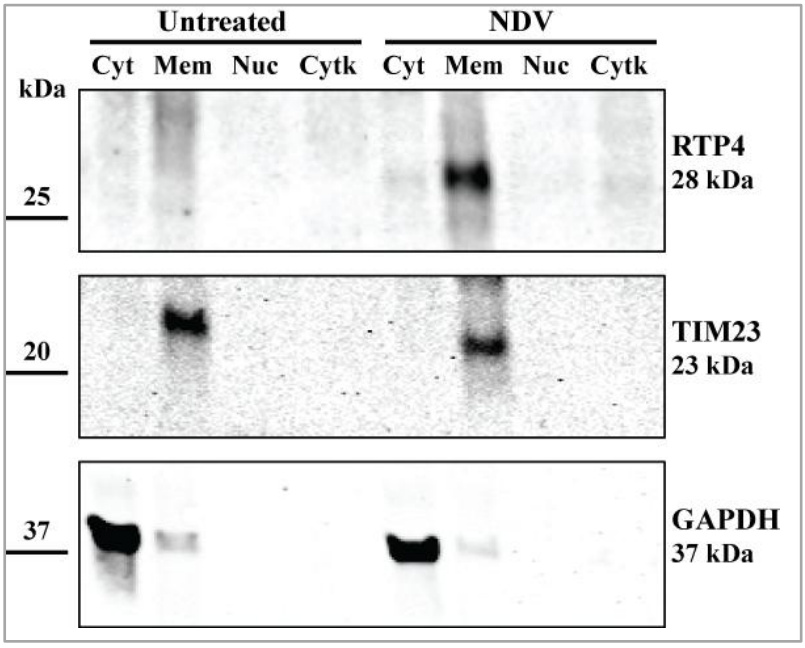

Figure 4-8: Western blots of BMMC subcellular fractions for detection of RTP4.
Wild-type BMMC were stimulated with NDV (2.4 HAU/ml) for 24 hr or left untreated. Cells were used for subcellular protein fractionation and protein was separated by SDS-PAGE. The resulting protein extracts from cytosol (cyt), membranes (mem), nucleus (nuc) and cytoskeleton (cytk) were analyzed by Western blotting for detection of RTP4, TIM23 and GAPDH. One of three representative experiments is shown.

4.9 Evaluation of expression dynamic and subcellular localization of RTP4

Translated proteins are transported through a series of membrane organelles, whose functions are to modify, target and pack proteins for being later delivered to specific cellular compartments or secreted to places where they carry out their final functions.

Confocal microscopy is an imaging tool that allows the evaluation of proteins and their relationships with other cell components via optics and electronics. Cells are treated with fluorochrome-labeled Abs that simultaneously detect two or more Ags. The overlapping signals coming from different fluorochrome-labeled Abs at the same section of the cell, (image pixel) is known as colocalization (Zinchuk *et al.*, 2007).

With the purpose of evaluating the dynamic of expression of RTP4 after viral encounter, cellular localization of RTP4 was evaluated at different time points by confocal microscopy. For this, BMMC were stimulated with 2.4 HAU/ml of NDV or left untreated and used as negative control. 1 x 10^5 cells where adhered to coverslips after 0.5, 6, 12, 18, 24 and 48 hr of virus infection and then fixed, permeabilized and labeled with the antibody rat anti-mouse RTP4 and the secondary antibody, fluorochrome- labeled anti-rat IgG. Fixed cells were also incubated with DAPI, which was used as a marker for the cell nucleus. An intra-assay control was included in experiments, consisting of the incubation of cells only with the secondary antibody. Additionally, BMMC were infected with NDV and collected at the time points previously described for SDS-PAGE and WB for RTP4 detection, as a way to confirm the results obtained from confocal microscopy experiments.

The results acquired by confocal microscopy (Figure 4-9, A) showed that RTP4 appeared to be spread out throughout the cytosol. The intensity of the staining indicating the different expression of the RTP4 protein varied at different time points after infection. Cluster of RTP4 proteins could be seen in the cytosol, in uninfected mast cells, as well as in the time points 0.5 and 6 hr. At 12 and 18 hr upon infection, RTP4 clusters appeared to be smaller and diffused. At time points 18 and 24 hr RTP4 expression was reacquired in the cytosol of the cells. The control cells treated only with the secondary antibody showed that BMMC lacked of fluorescence signals, confirming the specificity of the primary Abs and excluded the possibility of false positives.

The dynamic of expression of RTP4 was evaluated by WB. RTP4 was detected from 6 to 48 hr upon virus infection (Figure 4-9, B). At the time point 24 hr, RTP4 reached its highest peak of expression. Relative density analysis also showed the same pattern for the dynamic of RTP4 expression. These findings were replicated in 3 experiments.

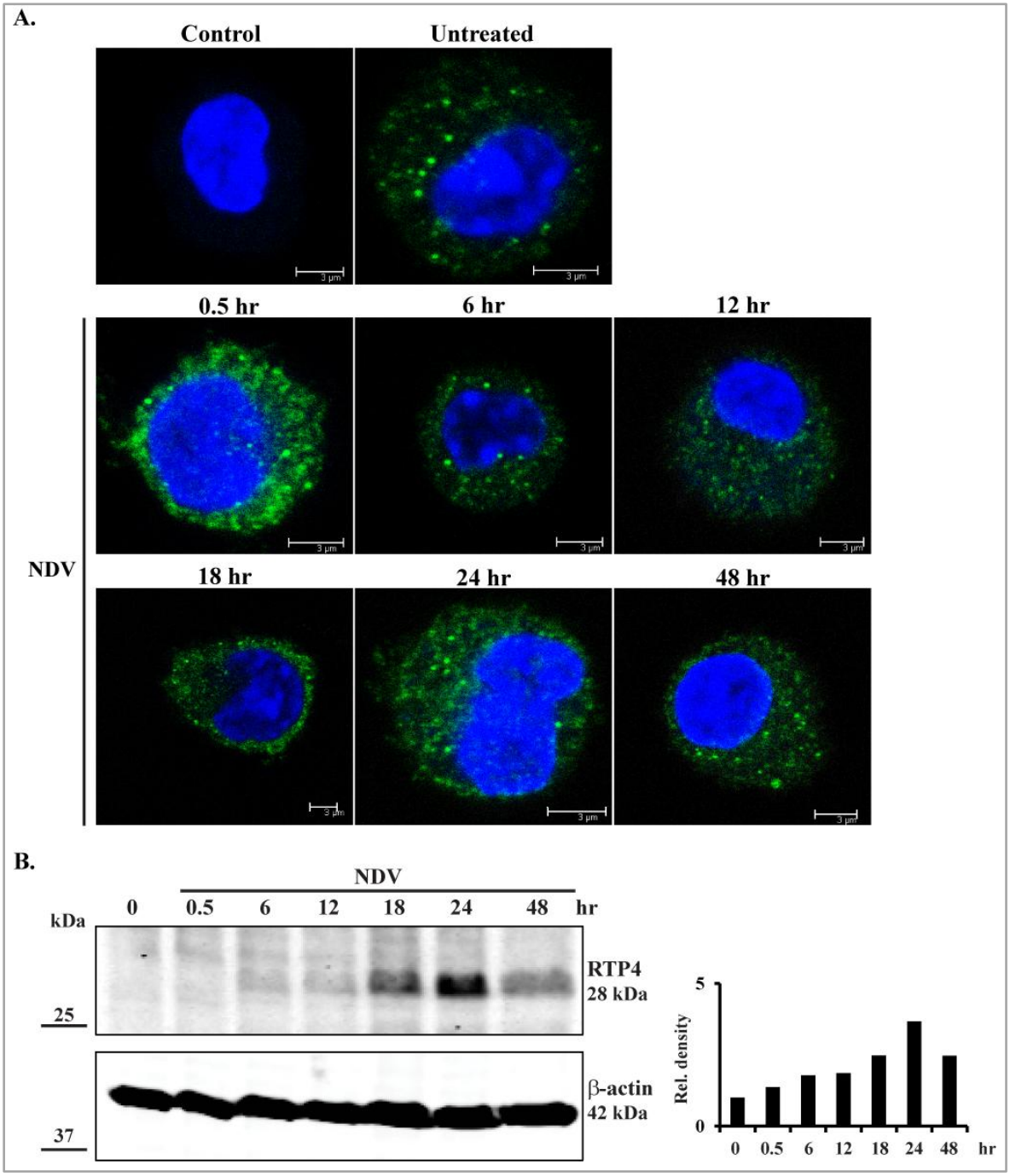

Figure 4-9: Kinetic of expression of RTP4 in BMMC.
Wild-type BMMC were stimulated for 24 hr with 2.4 HAU/ml of NDV during different time points. **(A.)** BMMC where adhered to coverslips, fixed, permeabilized and stained with anti-RTP4 and the secondary antibody Alexa 488 ant-rat IgG. Control cells were stained only with the secondary antibody. Cells were then analyzed using the confocal microscope LEICA SP5. (**B.**). Total protein was extracted and separated through SDS-PAGE. The figure shows Western blot analysis for detection of RTP4 with specific antibodies. β-actin was used as a protein loading control. The histogram shows the relative density of the RTP4 bands normalized to β-actin. The figure is shown as representative data of three independent experiments.

The experiments on subcellular fractionation showed that RTP4 is located in the membrane fraction. However, this approach did not allow to distinguish which membrane-organelles RTP4 was associated to. In order to determine co-localization of RTP4 with membrane-organelles, BMMC were infected with NDV and stained with organelle markers and analyzed by confocal microscopy. To this aim, wild-type BMMC were infected with 2.4 HAU/ml of NDV for 24 hr or left untreated and used as negative control for further comparison. Cells were adhered to coverslips, fixed, permeabilized and labeled with anti-RTP4 and the cellular markers for endoplasmic reticulum (PDI), early endosomes (EEA1), cell membrane (WGA) and lipid bodies (ADRP). Fluorochrome-labeled Abs anti IgG were used as secondary Abs and DAPI as nuclear marker.

Confocal experiments demonstrated that RTP4 co-localizes partially with markers for the endoplasmic reticulum and early endosomes (Figure 4-10, A). This feature is observed as dots of yellow color resulting from the convergence of the images obtained separately from RTP4 (red color) and the marker (green color). Co-localization of RTP4 with markers in BMMC was found to be independent of infection with NDV.

Membrane staining with WGA (Figure 4-10, B), which is a lectin that strongly binds to sugar moieties present in the cell glycocalyx, showed that RTP4 does not associate to the plasma membrane in resting states or after infection with NDV. Membrane glycocalyx was observed as a green ring that entirely surrounds the cell contour.

Lipid bodies were observed as a green circular-like shape that corresponds to the phospholipid membrane that delimits the LB's core and the cytosol. The LB staining showed that RTP4 is present in two forms: one co-localizing with its marker, ADRP (yellow color) and second, being part of the phospholipid membrane and not associating with ADRP (red dots). This finding was reproduced in the 3 experiments replicates.

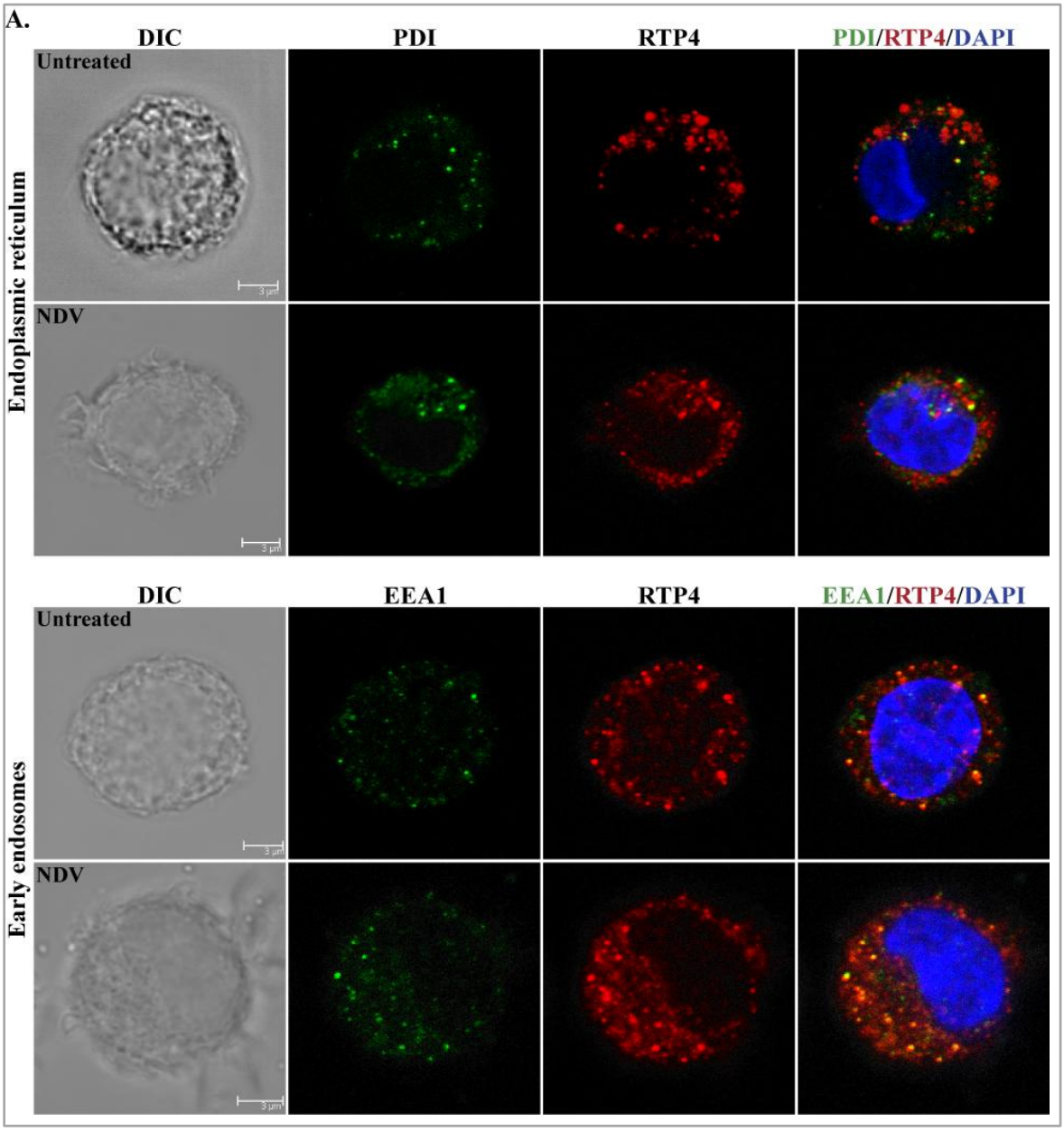
A.
DIC
PDI
RTP4
PDI/RTP4/DAPI
Untreated
NDV
Endoplasmic reticulum
DIC
EEA1
RTP4
EEA1/RTP4/DAPI
Untreated
NDV
Early endosomes

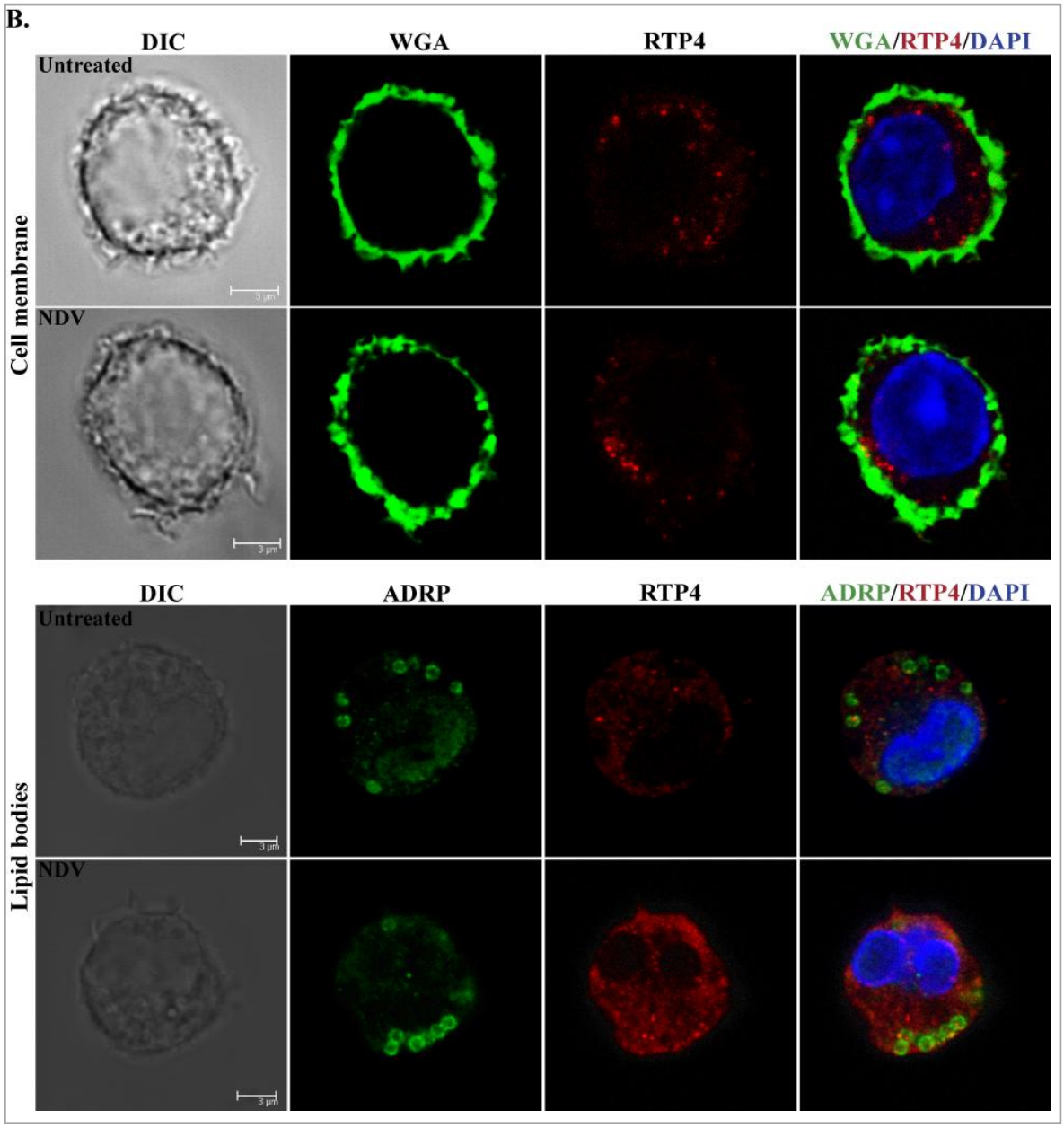

Figure 4-10: Co-localization of RTP4 with cell organelles.
Wild-type BMMC were stimulated for 24 hr with 2.4 HAU/ml of NDV or left untreated. 1 x 10^5 cells where adhered to coverslips, fixed with paraformaldehyde, permeabilized with a solution containing triton X-100 and labeled with the primary antibodies for the detection of (**A.**) RTP4, endoplasmic reticulum (PDI), early endosomes (EEA1) and (**B.**) lipid bodies (ADRP); wheat germ agglutinin (WGA) was used for membrane labeling. After incubation and washing steps, cells were again labeled with fluorochrome conjugated antibodies against the IgG Fc of primary antibodies. The dye DAPI was used as a marker for nucleus. Finally, cells were analyzed using the confocal microscope LEICA SP5. DIC=Differential interference contrast

Taken together, these results show that in BMMC, RTP4 is detectable after 6 hr of infection with NDV. RTP4 is present in the cytoplasm of the cell, but associated to

membrane organelles such as ER, EE and LB. This finding also confirms the result obtained from subcellular fractionation experiments, which shows the presence of RTP4 in the membrane fraction.

4.10 Interaction of lipids bodies and RTP4

Lipid bodies are cellular organelles lately rediscovered with a function in immune responses. It has been shown that in mast cells, lipid bodies are responsible for protein synthesis and for the storage and metabolism of arachidonic acid and its pro-inflammatory lipid mediators (Dvorak, 2005; Fujimoto *et al.*, 2008). Moreover, the protein VIPERIN that has shortly been explored in this work, was found to specifically associate to LB, where it is involved in the recruitment of the adaptor protein TRAF6 and the kinase IRAK1 which participate in the activation of the transcription factor IRF7 (Hinson *et al.*, 2009).

In order to confirm the findings obtained by confocal microscopy that showed that RTP4 co-localizes with lipid bodies, lipid bodies were purified and used for SDS-PAGE and WB analysis. BMMC have been the matter of research of this work, however these cells have limitations. Since they are derived from bone marrow, only small numbers of their progenitors are available to differentiate into MC, with a proliferation rate much lower than the one of cell lines As a consequence immortalized macrophages were used, since it was shown in section 3.5 that macrophages express high levels of RTP4 upon NDV infection.

For performing this experiment, immortalized macrophages were cultured in at least 6 culture flasks with 100 ml of medium until having approximately 7 x 10^8 cells. At this point cells were divided into two groups. Both groups were treated over night with 200 µM of oleic acid in order to induce formation of lipid bodies. Additionally, one group was treated with 2.4 HAU/ml of NDV. The second group was kept uninfected and was used as control. After 24 hr of incubation, cells were collected, washed with PBS and homogenized for the extraction of lipid bodies by sucrose gradient. Total protein and LB fractions were separated by SDS-PAGE and WB analysis for immune-detection of RTP4 and ADRP (lipid bodies marker) was performed.

Western blot analysis (Figure 4-11) showed that in cell lysates (total protein), RTP4 was expressed only upon NDV, stimulation. Sucrose gradient centrifugation raised two fractions: the first fraction or soluble, contained membrane-organelles, membranes and free lipids and the second fraction on the top of the tube, corresponded only to LB. ADRP bands were detected by WB in total protein and only in the lipid bodies fraction. The lack of ADRP in the soluble fraction reflected the specific isolation of LB. In the other hand, RTP4 was detected only in the soluble and not in the LB fraction.

These results exclude a localization of RTP4 in lipid bodies of immortalized macrophages.

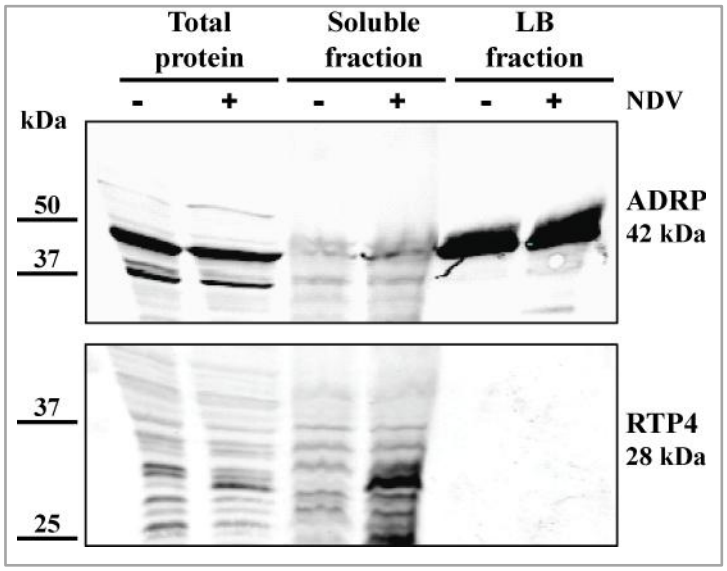

Figure 4-11: Isolation of lipid bodies and detection of RTP4 in immortalized macrophages.
Two groups of 350 x 10^6 immortalized macrophages were treated overnight with 200 µM of oleic acid. Additionally, one group of cells received 2.4 HAU/ml of NDV for 24 hr. Next, cells were collected, centrifuged and washed with PBS. 2 x 10^6 cells were taken for total protein extraction and the rest was resuspended in HLM buffer for cell homogenization. Cell lysates were centrifuged and the supernatants (soluble fraction) were transferred to a ultracentrifuge tube together with sucrose layers. After centrifugation at 20.000 g for 30 min, the LB fraction was recovered for later analysis by SDS-PAGE and for detection of ADRP and RTP4 by WB. The figure shows one representative experiment out of three.

4.11 Interaction partners for RTP4

Cellular and biochemical processes are performed and regulated by large groups of proteins that not exert their function alone, instead proteins must interact with other protein partners in order to lead and regulate their ultimate function. According to this, identification of interaction partners is an indirect approach to establish protein functions.

In order to identify RTP4 interaction partners and hence elucidate its function, immunoprecipitation analysis were performed.

Immunoprecipitation is commonly used for determining protein-protein interactions, this method is based on the expression of the protein of interest in an expression system and the protein precipitation (single or in complexes) from the cell lysate by the use of specific Abs. For this, 5×10^5 HEK293T cells were liposome-mediated transient transfected with DNA constructs expressing murine RTP4 or RTP4 tagged with FLAG. FLAG tag is a polypeptide of eight amino acids fused to the C-terminus of RTP4 that enables protein precipitation by monoclonal Abs. Total protein from RTP4-FLAG, RTP4 transfected and untransfected cells was isolated after 48 hr and then incubated overnight with 5 μg of the antibody anti-FLAG. Untransfected and RTP4 transfected cells were used as controls for comparing the band profile of the RTP4-FLAG transfected cells. After washing steps, lysates were incubated for 1 hr with protein G coated magnetic beads, which bound to the Fc region of Abs. Supernatant and magnetic beads were collected and used for protein separation by SDS-PAGE. Acryladmide gels were blotted to nitrocellulose membranes or stained with Coomassie´s blue for immune-detection of RTP4 or identification of differential bands, respectively. An additional control was set for the gel staining experiments and consisted in the analysis of the anti-FLAG antibody by SDS-PAGE in order to compare it band profile with the other samples and to establish specific bands for RTP4 IP.

Left panel (input) in figure 4-12 showed WB analysis confirming the expression of RTP4 in HEK293T cells transfected with the constructs for RTP4 or RTP4-FLAG expression. RTP4 is identified as a band of 28 kDa. RTP4-FLAG presented slower gel mobility and hence a higher molecular weight, since the FLAG polypeptide increased its weight in one kDa. These results also showed that lysates from transfected cells could be used for immunoprecipitation experiments.

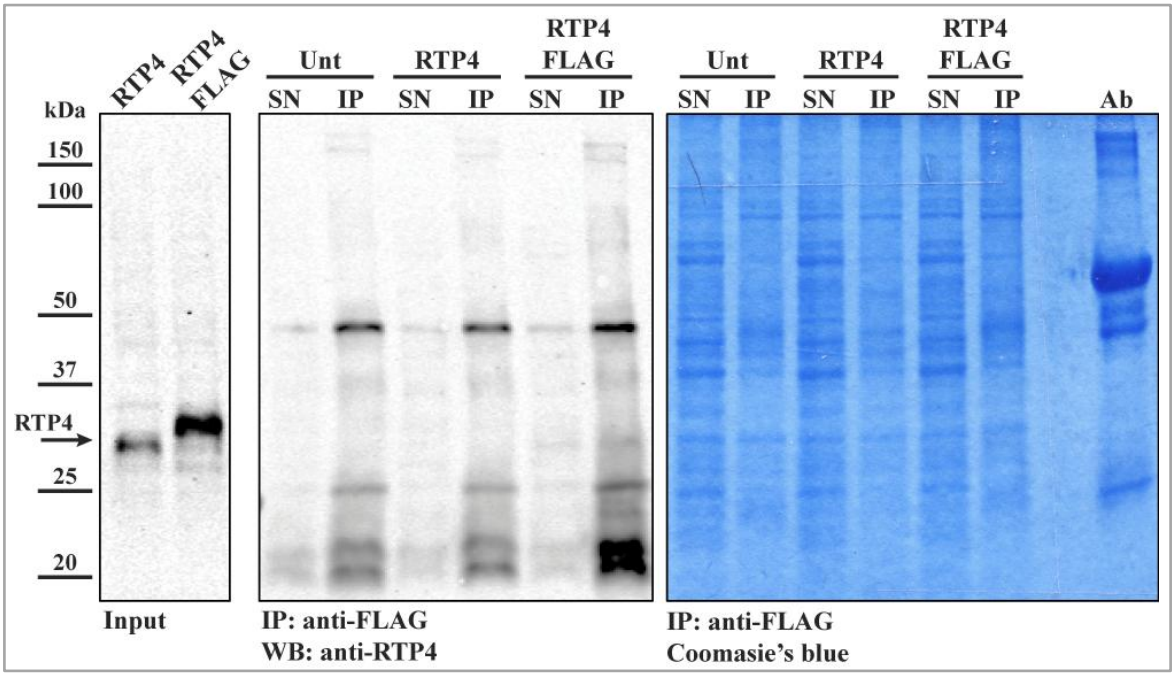

Figure 4-12: Immunoprecipitation of RTP4 or RTP4-protein complexes.
HEK293T cells were transient transfected with 5 µg of DNA of the constructs for the expression of RTP4, and RTP4-FLAG. Lysates from untransfected cell (Unt) were used as negative control. 250 µg of total protein from samples were incubated overnight with 5 µg of anti-FLAG antibody. G-protein-coated magnetic beads were used for binding protein-antibody complexes, supernatants and beads were separated and stored. Beads resuspended in Laemmli buffers were boiled at 95ºC for 5 min for eluting protein-antibody complexes. Protein from supernatants (SN) and eluted-beads (immunoprecipitation (IP)) were separated by SDS-PAGE. Acrylamide gels were stained with Coomassie's blue or blotted with antibodies for detection of RTP4. Figure shows one representative experiment out of three. After 48 hr of cell culture, total protein was extracted and used for confirming the expression of RTP4 or RTP4-FLAG by WB and for IP experiments.

Center panel shows WB analysis for detection of RTP4 protein from supernatants and immunoprecipitated products obtained from cells lysates treated with anti-FLAG Abs. RTP4 or RTP4-protein complexes were not detected, since specific bands were not observed in the IP product from RTP4-FLAG lysates. Likewise, the band profile for cells transfected with RTP4-FLAG was similar to the negative controls, untransfected and RTP4 transfected cells. Unspecific bands with molecular weights of 25 and 50 kDa were observed and they correspond to the heavy and light chain of Ab.

Coomassie's blue stained gel (left panel), confirmed the data obtained from WB analysis, in which RTP4 or RTP4-protein complexes were not detected since the band profile from RTP4-FLAG lysates was similar to the profile of the controls, RTP4 transfected and untransfected cell lysates.

The obtained results showed that interaction partners for RTP4 could not be identified.

4.12 Use of *rtp4*$^{-/-}$ mice as a tool/strategy to define the RTP4 function

4.12.1 Analysis of the immune phenotype of *rtp4*$^{-/-}$ mice

Deletion of a specific gene in an *in vivo* mouse model is performed in order to identify the functions of gene products. However, gene targeting may result in unexpected or not apparent mice phenotype. In order to evaluate the effect of gene targeting in *rtp4*$^{-/-}$ mice and to analyze whether the gene deletion affects the homeostasis of immune cell subsets, immune organs from WT and *rtp4*$^{-/-}$ mice were dissected and their cell subsets were analyzed by flow cytometry. To this end, WT and *rtp4*$^{-/-}$ mice were euthanized and peritoneal liquid, spleen, thymus and draining lymph nodes (superficial cervical, axillar, brachial, mesenteric, and inguinal) were isolated. Organ's stroma was disrupted to obtain a homogenous cell suspension. 5 x 10^5 cells were stained with fluorochrome-conjugated Abs against specific receptors of immune cell lineages and then analyzed by FCM.

So far, *rtp4* gene deletion did not result in fetal lethality, stillbirth, or off-spring death. Likewise, *rtp4*$^{-/-}$ mice were healthy and macroscopical examination did not reveal obvious physical alterations. The tables below list the different cells subsets grouped by organs, their percentages and the markers used in the analysis. In the thymus, the subsets of thymocytes were comparable between WT and *rtp4*$^{-/-}$ mice (Table 4-2, A). In secondary lymphoid organs, such as spleen and lymph nodes there were no significant differences in the percentages from WT and *rtp4*$^{-/-}$ mice for $CD4^+$ and $CD8^+$ T cells (activated and memory T cells), B cells (mature and immature B cells), dendritic cells, natural killer cells, macrophages and granulocytes (Table 4-2, B and C). Similar results were found in the peritoneal lavage where cell's percentages were comparable between the analyzed genotypes for neutrophils, eosinophils, mast cells, macrophages and B cells (Table 4.2, D).

Table 4-2: Analysis of cell lineages in immune related compartments.
WT and *rtp4*$^{-/-}$ mice were euthanized with an overdose of inhaled CO_2. Eight ml of 0.9% saline solution were injected into the peritoneal cavity for being later collected. After mouse dissection the spleen, lymph nodes and thymus were isolated and later processed for stroma cell obtention. 2.5 x 10^5 cells were resuspended in 100 µl of FCM buffer and incubated for 30 min with 0.4 µg/ml of fluorochrome-conjugated antibodies, depending on the cell population. After washing steps, cells were resuspended and analyzed by the FACSCalibur flow cytometer. Results are showed as the mean of the *n* percentages ± SEM for each cell population analyzed in thymus (**A.**), lymph nodes (**B.**), spleen (**C.**) and peritoneal lavage (**D.**).

A. Thymus

Cell Type	Surface Marker	Percentage	
		WT	*rtp4*$^{-/-}$
Triple-positive thymocytes	$CD3^+$ $CD4^+$ $CD8^+$	92.3 ± 13.8	95.8 ± 1.9
$CD4^+$ thymocytes	$CD3^+$ $CD4^+$ $CD8^-$	17.4 ± 15.4	19.4 ± 20.1
$CD8^+$ thymocytes	$CD3^+$ $CD8^+$ $CD4^-$	7.1 ± 8.9	8.3 ± 7.7
Triple-negative thymocytes	$CD3^-$ $CD4^-$ $CD8^-$	6.9 ± 14.1	3.0 ± 0.7

WT and *rtp4*$^{-/-}$ *n*=18

B. Lymph nodes

Cell Type	Surface Marker	Percentage	
		WT	*rtp4*$^{-/-}$
$CD4^+$ T cells	$CD3^+$ $CD4^+$	40.1 ± 6.6	38.3 ± 7.1
Activated $CD4^+$ T cells	$CD4^+$ $CD69^+$	5.0 ± 3.1	5.1 ± 3.3
$CD8^+$ T cells	$CD3^+$ $CD8^+$	24.8 ± 3.9	23.7 ± 4.9
Activated $CD8^+$ T cells	$CD8^+$ $CD69^+$	7.1 ± 7.9	7.1 ± 8.0
B cells	$B220^+$	30.9 ± 11.5	32.1 ± 16.2
Immature B cells	$B220^+$ IgM^+	19.1 ± 13.2	16.8 ± 14.4
Granulocytes	$Gr1^{high}$ $CD11b^+$	0.8 ± 0.5	0.8 ± 0.5
NK cells	NK1.1	3.1 ± 1.9	3.6 ± 2.4
DC cells	$CD11c^+$	2.3 ± 1.9	3.1 ± 2.7
Macrophages	$Gr1^{low}$ $CD11b^+$	7.7 ± 15.9	10.6 ± 18.2

WT and *rtp4*$^{-/-}$ *n*=15

C. Spleen

Cell Type	Surface Marker	Percentage	
		WT	*rtp4*$^{-/-}$
CD4$^+$ T cells	CD3$^+$ CD4$^+$	21.2 ± 4.7	21.2 ± 5.8
Activated	CD4$^+$ CD69$^+$	2.8 ± 1.4	2.8 ± 1.4
Effector memory CD4$^+$ T cells	CD4$^+$ CD44$^+$	16.4 ± 4.8	15.2 ± 4.6
Memory CD4+ T cells	CD4$^+$ CD62L$^+$	17.7 ± 4.3	15.3 ± 5.4
CD8$^+$ T cells	CD3+ CD8$^+$	10.4 ± 4.3	9.6 ± 3.7
Activated CD8$^+$ T cells	CD8$^+$ CD69$^+$	5.5 ± 4.0	5.0 ± 4.0
Effector memory CD8$^+$ T cells	CD8$^+$ CD44$^+$	6.1 ± 2.5	6.5 ± 2.2
Memory CD8+ T cells	CD8$^+$ CD62L$^+$	10.3 ± 4.5	10.1 ± 4.4
B cells	B220$^+$	41.6 ± 14.9	42.7 ± 13.4
Immature B cells	B220$^+$ IgM$^+$	36.1 ± 13.2	36.2 ± 11.9
Mature B cells	B220$^+$ IgD$^+$	35.1 ± 13.8	36.6 ± 13.5
Granulocytes	Gr1^{high} CD11b$^+$	5.1 ± 10.8	7.3 ± 14.1
NK cells	CD3$^-$ NK1.1$^+$	4.1 ± 1.8	4.6 ± 1.66
DC cells	CD11c$^+$	4.4 ± 2.6	4.6 ± 2.7
Macrophages	Gr1^{low} CD11b$^+$	4.2 ± 1.4	4.7 ± 2.3

WT *n*=19 and *rtp4*$^{-/-}$ *n*=18

D. Peritoneal lavage

Cell Type	Surface Marker	Percentage	
		WT	*rtp4*$^{-/-}$
B cells	B220$^+$	24.6 ± 15.4	24.9 ± 15.5
Immature B cells	B220$^+$ IgM$^+$	14.5 ± 16.3	14.5 ± 16.9
Mast cells	CD117$^+$ ST2$^+$	1.6 ± 0.8	1.4 ± 0.8
Eosinophils	CD11b$^-$ F4/80$^+$	3.2 ± 4.2	3.3 ± 5.2
Neutrophils	Gr1^{high} CD117$^-$	3.1 ± 2.3	2.5 ±1.7
Macrophages	CD11b$^+$ F4/80$^+$	34.7 ± 14.8	40. 0± 16.4

WT and *rtp4*$^{-/-}$ *n*=17

These results demonstrate that *rtp4* deletion does not induce changes in the development of immunocytes, since the percentages of the different subsets were found comparable between the WT and *rtp4*$^{-/-}$ mice. Thus one can conclude that either RTP4 is not a protein

whose expression is essential for immune cells development or that RTP4 is contributed to the differentiation process however its function *in vivo*, an RTP4 absence, can be complemented by others.

4.12.2 Characterization of *rtp4*$^{-/-}$ BMMC

To study the functional characteristics of *rtp4*$^{-/-}$ mast cells, it was firstly important to determine whether differentiation and maturation of bone marrow progenitors into MC from *rtp4*$^{-/-}$ mice were normal. For this purpose, BMMC derived from *rtp4*$^{-/-}$ mice were examined to assess the expression of differentiation and maturation markers by flow cytometry. 2.5 x 10^5 BMMC from *rtp4*$^{-/-}$ and WT mice used as controls, cultured for 5 weeks were labeled for 30 min with fluorochrome-conjugated Abs against the mast cells receptors CD117, ST2 and FcεR1 and then analyzed by flow cytometry.

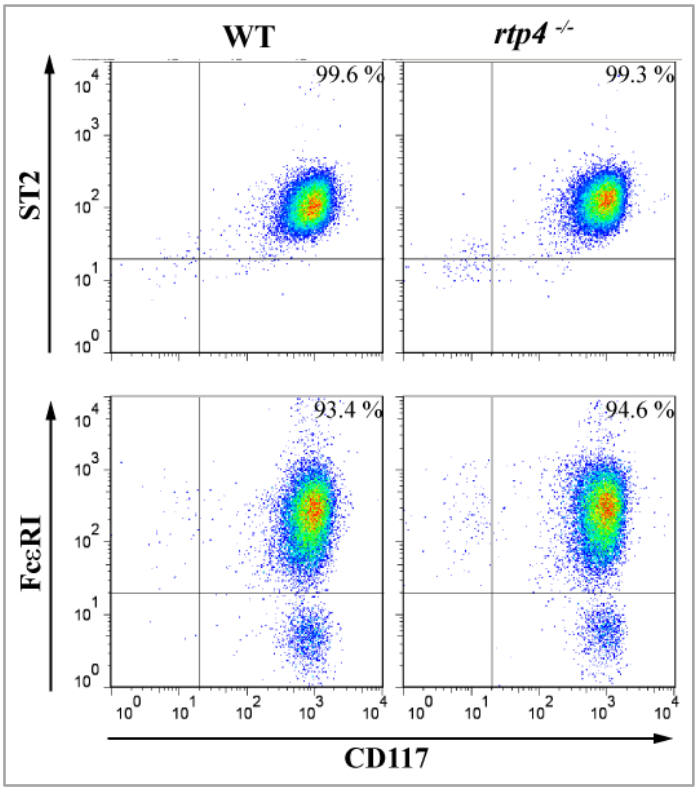

Figure 4-13: Differentiation and maturation of WT and *rtp4*$^{-/-}$ BMMC.
WT and *rtp4*$^{-/-}$ BMMC were used after 5 weeks of culture with IL-3 (5 ng/ml) and SCF (10 ng/ml). 3 x 10^5 cells were collected, washed with PBS and resuspended in 100 µl of FCM buffer. Then, cells were incubated for 30 min at 4ºC with 0.4 µg/ml of fluorochrome-conjugated antibodies against murine CD117, ST2 and FcεR1. 20.000 cells were acquired using the FACSCalibur flow cytometer and then the data was analyzed with the software FlowJo. Percentages were defined

according to the frequency of expression of the population markers. The figure is shown as representative data of three experiments with a total of $n = 9$.

Figure 4-13 shows one representative experiment in which after 5 weeks of culture, BMMC populations from r*tp4*$^{-/-}$ and WT mice were comparable. The mean percentage obtained from three independent experiments for the population of mature BMMC defined as CD117^{+} ST2^{+} were 99.7 ± 0.13 and 99.8 ± 0.16 for WT and *rtp4*$^{-/-}$, respectively. Similar results were obtained for the population CD117^{+} FcεR1^{+} where the percentages for WT and *rtp4*$^{-/-}$ BMMC were 96.5 ± 1.7 and 97.1 ± 1.1.

To verify whether *rtp4* was successfully targeted, *rtp4* mRNA and protein expression were examined in WT and *rtp4*$^{-/-}$ BMMC by qRT-PCR and WB analysis. For this purpose 2 x 10^{6} cells from WT and *rtp4*$^{-/-}$ mice were infected for 8 and 24 hr with NDV and IAV at doses of 2.4 and 20.4 HAU/ml, respectively. Untreated cells were used as negative control. RNA and protein were isolated and used for qRT-PCR and WB analysis; *rtp4* mRNA levels were expressed in function of the house keeping gene *hprt* and β-actin was used as loading control in WB analysis.

Results show that after infection with IAV and NDV, *rtp4* mRNA was neither detected in *rtp4*$^{-/-}$ BMMC nor in the negative control (untreated cells). In contrast, WT BMMC, which served as positive control, expressed 1400 and 1000 times more *rtp4* mRNA upon infection with NDV and IAV (Figure 4-14, A). WB experiments confirmed the data of the qRT-PCR since RTP4 protein was only detectable in WT BMMC infected with NDV and IAV. In BMMC from *rtp4*$^{-/-}$ mice protein expression was completely abrogated. Analysis of band relative density showed that RTP4 was expressed 4 times more in WT BMMC upon virus infection and that the values for *rtp4*$^{-/-}$ BMMC were even lower than the negative control of uninfected WT cells (Figure 4-14, B).

In summary, these results indicate that BMMC from *rtp4*$^{-/-}$ mice differentiate and mature in a similar manner like WT and demonstrate a successful targeting of *rtp4* in deficient mice.

Therefore, *rtp4*$^{-/-}$ BMMC are a suitable for further studies intended to define the gene functionality.

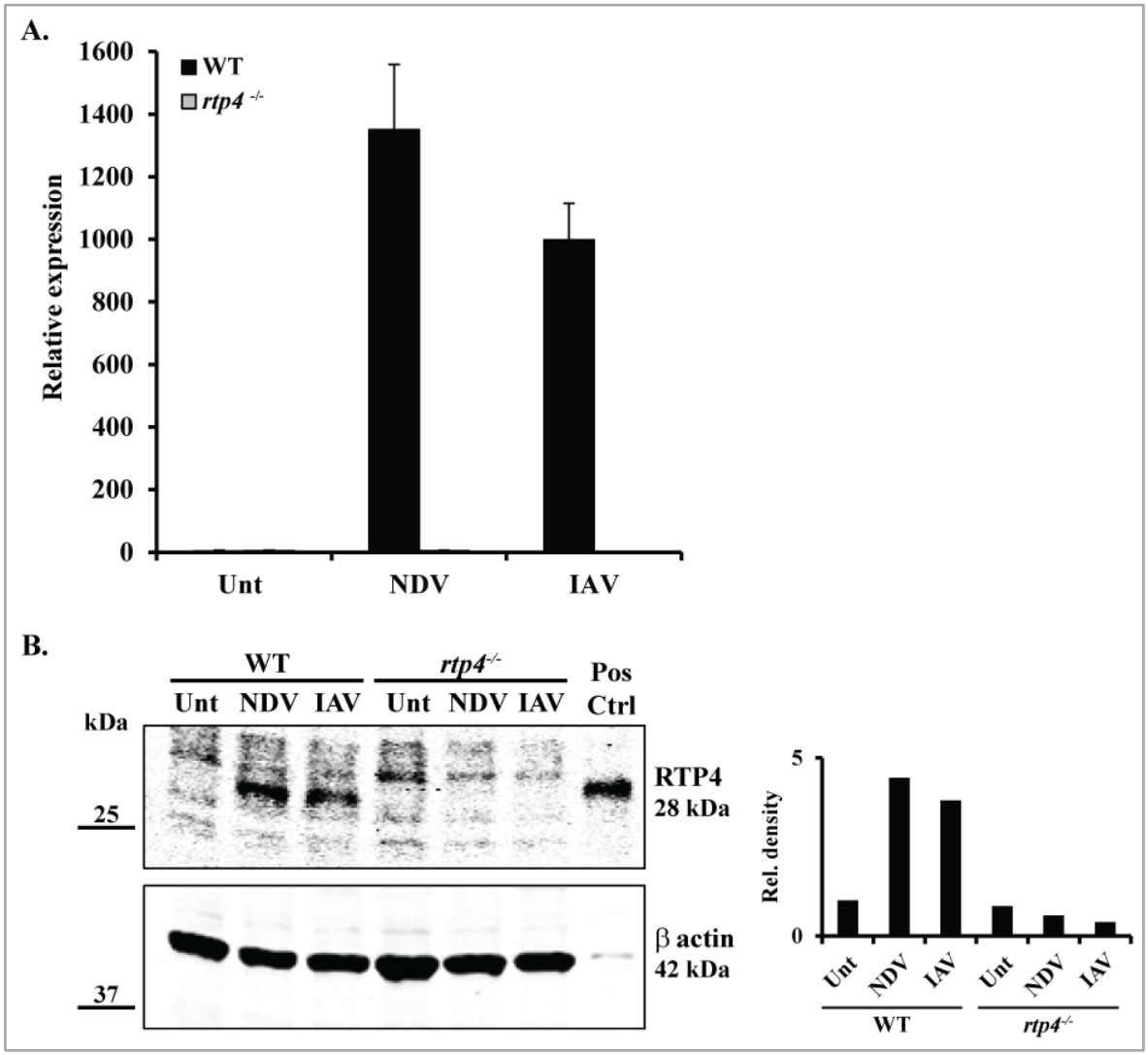

Figure 4-14: Verification of *rtp4* gene targeting by qRT-PCR and western blot.
BMMC from WT and *rtp4*$^{-/-}$ mice were incubated with 2.4 HAU/ml of NDV and 20.4 HAU/ml of IAV or left untreated (Unt). (**A.**)After 8 hr of incubation, RNA was isolated and then cDNA was synthetized, figure shows, qRT-PCR analysis for the mean ± SEM expression of *rtp4* normalized to the house-keeping gene *hprt*. (**B.**) After 24 hr total protein was extracted and separated through SDS-PAGE for western blot analysis of RTP4 and β-actin as loading control. The histogram chart shows the relative density of the bands normalized to β-actin. Positive control is the lysate of RTP4 transfected HEK293 cells. Data is representative of three independent experiments.

4.12.3 *rtp4* deletion does not change the gene expression profile of BMMC

Gene deletion may lead to changes in the expression of co-regulated genes. In order to evaluate the consequences of *rtp4* targeting in the expression of RTP4-dependent genes, BMMC from WT and *rtp4*$^{-/-}$ mice were used for gene expression profiling by microarray analysis. To achieve this aim, 2 x 10^6 BMMC from WT and *rtp4*$^{-/-}$ mice were infected for 8 hr with 2.4 HAU/ml of NDV. Uninfected cells from both genotypes were used as negative controls. Total RNA was isolated and sent to the facilities of the Affymetrix Core at the Technische Universität München for gene expression microarray analysis. The profile of gene expression between WT and *rtp4*$^{-/-}$ BMMC as well as for NDV infected WT and *rtp4*$^{-/-}$ BMMC was analyzed. Only an expression fold change higher than 2 was considered significant.

Results obtained indicate that targeting of *rtp4*$^{-/-}$ did not induce significant changes in the gene expression profile of resting *rtp4*$^{-/-}$ BMMC when compared to the WT counterpart (Table 4-3, A). Only the gene *mela*, which codes for the melanoma antigen, exhibited an increase in the fold change of 2.8 times. Statistically significant differences between means of *rtp4*$^{-/-}$ and WT BMMC were observed for the up-regulated gene *il28a*, however its fold change was lower than 2 (cutoff value). The remaining genes were listed due to their link to the immune response, but they did not show significant variations neither in the fold change value nor in their means.

The comparison of gene expression between WT and *rtp4*$^{-/-}$ BMMC infected with NDV revealed changes only for the genes *mela* and *rtp4*$^{-/-}$ (Table 4-3, B). The gene *mela* was 2.6 times up-regulated, while *rtp4*, as expected, was the most down-regulated gene in 4.8 times. The genes *fzd9* and *ifi30* coding for the proteins frizzled homolog 9 and interferon gamma inducible protein 30, respectively, presented statistically significant differences in their means, however these genes presented a fold increase lower than the cut off value.

Table 4-3: Differential expression of genes in *rtp4*$^{-/-}$ BMMC.
BMMC derived from wild-type and *rtp4*$^{-/-}$ mice were infected with 2.4 HAU/ml of NDV or left untreated. After 8 hr of incubation, RNA was isolated and gene expression analysis were performed using the GeneChip Mouse Genome 430 2.0. The table lists the genes that were up or down-regulated in *rtp4*$^{-/-}$ mice (**A**) or upon stimulation with NDV (**B**). Just genes with a fold change ≥ 2 are considered as genes with significant change. Fold change values are the result of the logarithmic difference (log base 2) between the WT and *rtp4*$^{-/-}$ means. Additionally, independent-samples Student's *t*-test was calculated to evidence differences between the means of the cells treated or not with NDV. *n*=3.

A.

Gene	Gene Description	Mean		Fold change	*p* value	Position
		WT	*rtp4*$^{-/-}$			
Up-regulated genes						
mela	Melanoma antigen	2.6	5.4	2.8	0.235	1
il28a	Interleukin 28A	3.8	4.6	0.8	0.042	4
mmp12	Matrix metallopeptidase 12	4.0	4.8	0.7	0.669	5
ssp1	Secreted phosphoprotein 1 (osteopontin)	3.4	4.1	0.7	0.634	6
cd36a	CD36 antigen	2.3	3.0	0.7	0.434	8
Down-regulated genes						
tcrg-v3	T-cell receptor gamma, variable 3	4.5	3.6	- 0.8	0.365	1
lif	Leukemia inhibitory factor	4.4	3.8	- 0.6	0.064	4
xlr4c	X-linked lymphocyte regulated 4C	4.4	3.7	- 0.6	0.316	7
mcpt8	Mast cell protease 8	7.8	7.2	- 0.6	0.557	12
cd48	CD48 antigen	6.5	5.9	- 0.5	0.169	34

B.

Gene	Gene Description	Mean		Fold change	*p* value	Position
		WT NDV	*rtp4*$^{-/-}$ NDV			
Up-regulated genes						
mela	Melanoma antigen	2.6	5.3	2.6	0.208	1
mmp13	Matrix metallopeptidase 13 (collagenase 13)	2.8	3.8	1.1	0.432	2

mmp12	Matrix metallopeptidase 12	3.8	4.6	0.8	0.556	4
cybb	Cytochrome b-245, beta polypeptide	3.4	4.2	0.8	0.613	5
ifi205	Interferon activated gene 205	2.7	3.4	0.7	0.565	6
irg1	Immunoresponsive gene 1	3.4	4.1	0.7	0.655	8
ifi203	Interferon activated gene 203	5.6	6.2	0.5	0.544	19
ifi204	interferon activated gene 204	3.3	3.9	0.5	0.667	31
Down-regulated genes						
rtp4	Receptor transporter protein 4	9.3	4.5	- 4.8	0.131	1
ifna6	Interferon alpha 6	5.9	5.1	- 0.7	0.653	3
ifna5	Interferon alpha 5	7.5	6.8	- 0.6	0.693	6
ifnab	Interferon alpha B	3.7	3.1	- 0.5	0.554	12
fzd9	Frizzled homolog 9	3.5	2.9	- 0.5	0.025	18
ifnb1	Interferon beta 1, fibroblast	3.2	2.8	- 0.4	0.455	25
ifi30	Interferon gamma inducible protein 30	3.2	2.8	- 0.4	0.014	26
mcpt2	Mast cell protease 2	6.1	5.7	- 0.4	0.626	29

In summary, these results indicate that BMMC from *rtp4*$^{-/-}$ mice do not exhibit significant differences in the gene expression and that *rtp4* does not highly regulate the expression of the other genes analyzed in this study.

4.12.4 Assessment of degranulation in *rtp4*$^{-/-}$ BMMC

Degranulation is an important feature of mast cells by which mediators are secreted in response to allergens. Moreover, it has been demonstrated that mast cells upon contact with vaccinia and bovine respiratory syncytial virus are induced to degranulate, releasing antimicrobial peptides that can inhibit viral replication (Jolly *et al.*, 2004; Wang *et al.*, 2012). In order to evaluate whether *rtp4* deletion induces changes in the degranulation profile of BMMC, mast cells were analyzed by FCM for the expression of CD107a. For

this purpose 1 x 10^6 BMMC from WT and *rtp4*$^{-/-}$ mice were cultured overnight with 5 µg/ml of the recombinant DNP IgE. BMMC were then incubated for 30 min with 5, 10 and 20 ng/ml of DNP Ag. Untreated and IgE treated cells as well as cells incubated with PMA-IO were used as negative and positive control, respectively. Cells were treated for 30 min with 0.4 µg/ml of anti-CD107a antibody, which is expressed on the surface of mast cells as a consequence of degranulation.

Flow cytometry experiments indicated that treatment of WT and *rtp4*$^{-/-}$ BMMC with 5, 10 and 20 ng of DNP increased the degranulation percentages to 5, 14 and 19%, respectively, in comparison to the negative controls (untreated cells and IgE loaded cells). However, degranulation percentages were comparable between WT and *rtp4*$^{-/-}$ BMMC and significant differences were not detected. BMMC treated with PMA-IO (positive control) exhibited an increase in degranulation of 55 and 61% for WT and *rtp4*$^{-/-}$ BMMC, showing the ability of these to degranulate and the validity of the assay (Figure 4-15).

These results demonstrate that deletion of *rtp4* does not induce changes in the degranulation profile of BMMC.

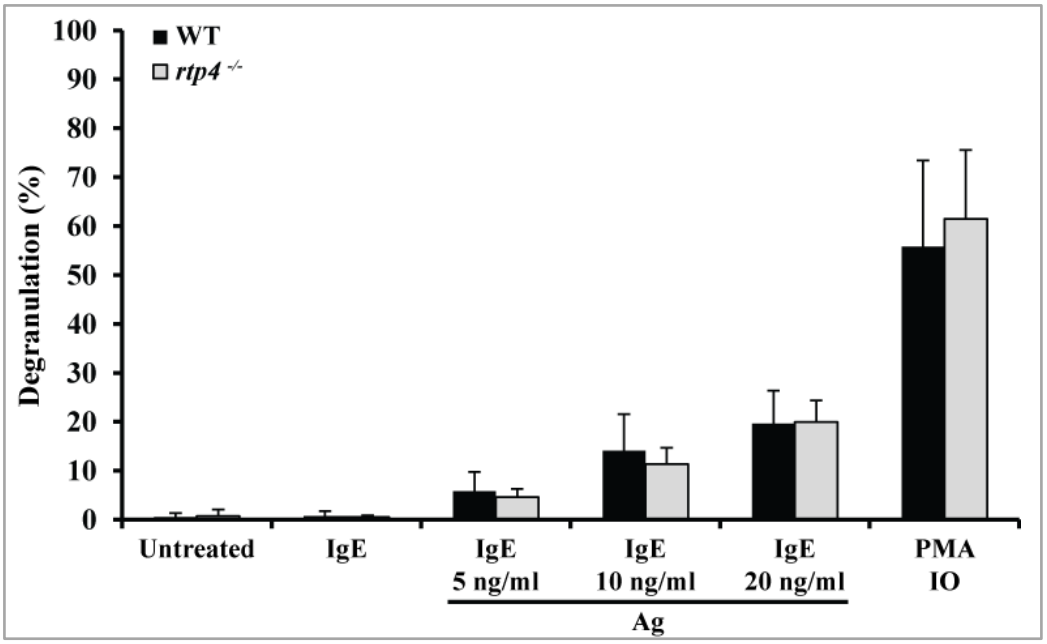

Figure 4-15: Comparison of degranulation between wild-type and *rtp4*$^{-/-}$ BMMC.
BMMC were sensitized overnight with anti-DNP IgE and then stimulated with 5, 10 and 20 ng of the antigen (Ag) DNP-HAS or the combination phorbol-myristate-acetate and ionomycin (PMA-IO) as positive control. Untreated cells and IgE loaded BMMC were used as negative controls. Degranulation was assessed by flow cytometry detecting the expression of LAMP on the plasma membrane. The figure shows the mean ± SEM of the degranulation percentage. *n*=12.

4.12.5 Cytokine production in *rtp4*$^{-/-}$ BMMC

Cytokines are mediators released by cells in order to drive and regulate immune responses. It is well known that MC release cytokines in response to challenge with IgE and specific Ags as wells as upon contact with microbial products. To determine whether *rtp4* contributes to the regulation of cytokine production in MC, IL-6, IP-10 and osteopontin secretion was measured by ELISA. For this 2 x 10^6 BMMC from *rtp4*$^{-/-}$ and WT mice were stimulated with 1000 IU of recombinant mouse IFN-β and infected with 2.4 and 20.4 HAU/ml of NDV and IAV, respectively. Untreated cells were used as negative controls. After 24 hr, supernatants were collected and used to quantify IL-6, IP-10 and osteopontin by performing indirect ELISA.

The results indicate that infection of WT and *rtp4*$^{-/-}$ BMMC with NDV and IAV increases the secretion of IL-6 from 250 to 300 pg/ml, in comparison to the negative control (untreated cells). Stimulation of BMMC with IFNβ also induced IL-6 secretion, increasing the levels from 70 to 100 pg/ml. Although IL-6 secretion was increased, significant differences between WT and *rtp4*$^{-/-}$ BMMC were not observed (Figure 4-16, A).

ELISA assays revealed an increase in the secretion of IP-10 in BMMC upon infection with NDV and IAV. In WT and *rtp4*$^{-/-}$ BMMC, NDV induced comparable IP-10 levels of 212 and 197 pg/ml, respectively. IAV induced IP-10 levels of 87 and 108 pg/ml for WT and *rtp4*$^{-/-}$ BMMC. IP-10 secretion was comparable in BMMC stimulated with IFNβ. Significant differences in the secretion levels of IP-10 in WT and *rtp4*$^{-/-}$ BMMC were not observed (Figure 4-16, B).

Infection of WT and *rtp4*$^{-/-}$ BMMC with NDV and IAV, as well as the stimulation with IFNβ did not induce osteopontin secretion, since the levels of this cytokine were comparable to the negative controls: untreated cells (Figure 4-16, C).

Since deletion of *rtp4*$^{-/-}$ did not induce changes in the secretion profile of IL-6, IP-10 and osteopontin, one can conclude that RTP4 expression is not essential for the secretion control of these cytokines.

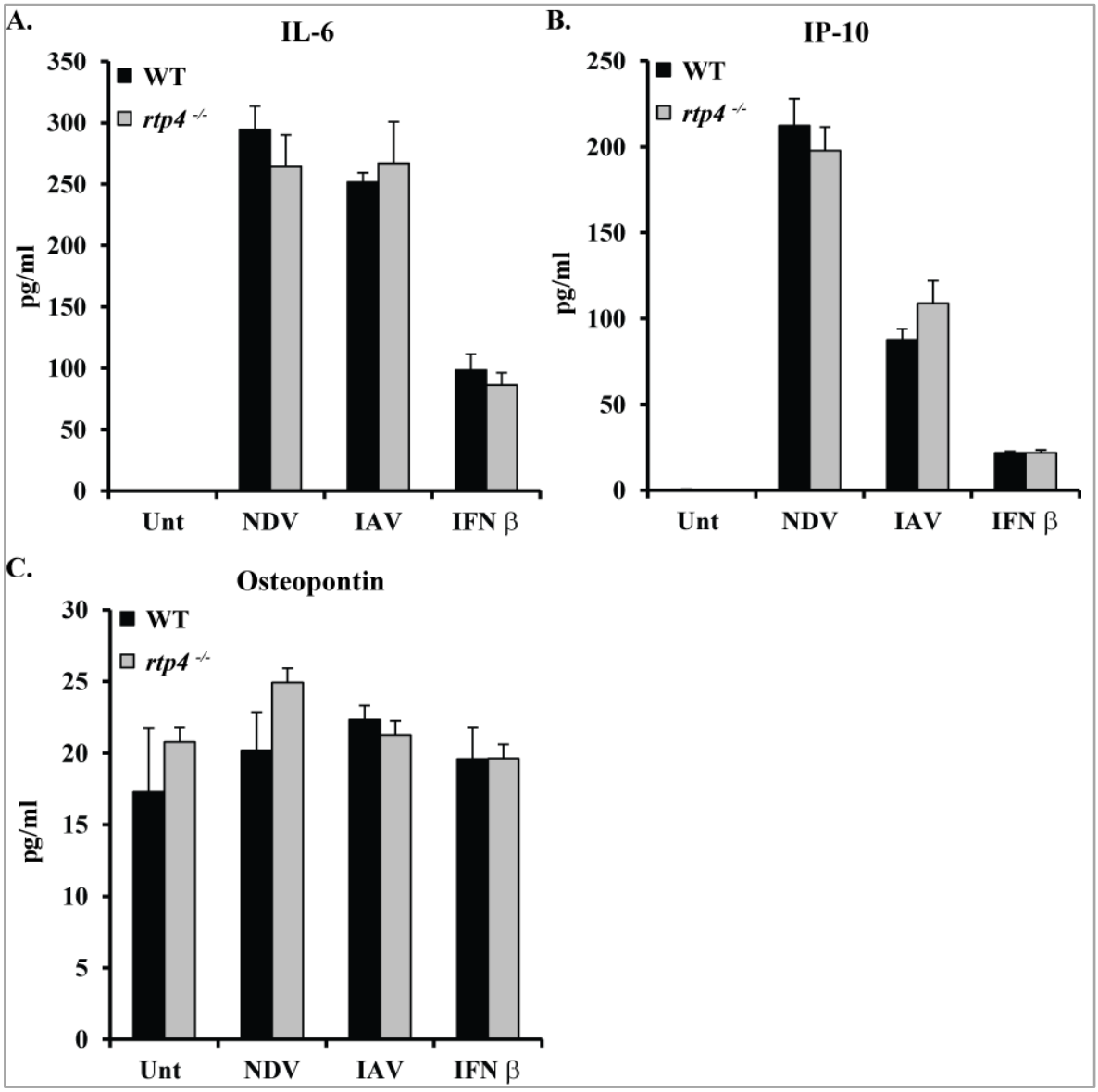

Figure 4-16: Quantification of cytokine release in wild-type and *rtp4*$^{-/-}$ BMMC.
BMMC were infected for 24 hr with 2.4 and 20.4 HAU/ml of NDV and IAV, respectively, and stimulated with 1000 IU of IFNβ. Untreated cells (Unt) were used as negative control. Culture supernatants were collected and used for quantification of IL-6, IP-10 and osteopontin by indirect ELISA. The figure shows the mean ± SEM of the cytokine secretion in pg/ml. *n*=3.

5. Discussion

Immune responses against viral pathogens involve the participation of a large variety of cells that range from basic epithelial and stroma cells to specialized immune cells that answer the call of infected cells, migrating to the sites of infection and eliminating viral particles. Although immune responses against virus have been largely studied, important aspects remain still undefined; new cytoplasmic PRRs for sensing viral nucleic acids, mechanisms for the recognition of self and non-self RNA and DNA, new members of the type III interferon family, immune evasion mechanism are just examples of recent discoveries that show the dynamic and the progress on the field (Onoguchi *et al.*, 2007; Bruns *et al.*, 2012).

MC, which have been considered mainly as "mono-tasking cells" for their role in type I hypersensitivity reactions, and hence in asthma and allergy, are have now been shown as versatile immune players bearing a multiplicity of functions. Interestingly, recent reports indicate that MC mediate immune responses against virus, either by activation of other immune cells (*vg*. NK or $CD8^+$ T cells) or by the release of their granular content (Galli *et al.*, 2010). Therefore the goal of the project was to provide a better understanding of the role played by MC in antiviral responses using differential analysis for gene expression and investigating the expression patterns and functions of RTP4.

Here I report that BMMC are activated by infection with NDV, and such activation triggers the expression of antiviral genes, inducing the production of effector cytokines like type I interferons and ISG. BMMC prominently upregulate the gene *rtp4* whose induction is partially mediated by TLRs and the adaptor proteins MyD88 and TRIF. Expression of *rtp4* was found to be abrogated in BMMC lacking IFNAR1, indicating the dependency of this gene on the signaling pathways induced by type I IFNs. Upregulation of *rtp4* was also triggered in other immune cells such as macrophages and DC upon viral infection. Experiments using confocal microscopy revealed that RTP4 is located in organelle membranes of ER, early endosomes and lipid bodies. Characterization of *rtp4*$^{-/-}$ mice

showed that the immune cell compartments were comparable to WT animals and that *rtp4*$^{-/-}$ BMMC did not exhibit differences in development or functionality, since gene expression analysis, degranulation and cytokine production were comparable to WT BMMC.

Thus, this study demonstrates that BMMC mount an antiviral immune response characterized by the upregulation of a wide variety of genes. Among them, interestingly appears as the second most upregulated gene in BMMC upon viral infection.

5.1 MC display an antiviral program

To understand the outcome in MC of viral infections, an *in vitro* model in which BMMC were infected with NDV was used. BMMC have been used extensively to investigate different aspects of MC biology (Galli *et al.*, 1982; Krishnaswamy *et al.*, 2006). On the other hand, NDV is considered as one of the most potent interferon inducers, and thus used to study PRRs signaling and interferon-derived responses in different cell types like macrophages, DC, MC and tumor cell lines (Brehm *et al.*, 1986; Zawatzky *et al.*, 1991; Orinska *et al.*, 2005; Matsui *et al.*, 2006; Wilden *et al.*, 2009). Although mice are not the natural host of NDV, murine infection with this virus was early established and since then widely used to understand viral pathogenesis, the functional role of interferons in viral infections and lately to investigate the oncolytic properties of NDV (Salerno *et al.*, 1975; Burks *et al.*, 1976; Elankumaran *et al.*, 2010; Zaslavsky *et al.*, 2010; Khattar *et al.*, 2011). For these reasons NDV was chosen to evaluate the antiviral responses of MC *in vitro*.

Gene expression analysis showed 101 genes that were upregulated in BMMC in response to NDV infection. These genes were classified in 7 groups according to their functional features by the bioinformatic tool DAVID, being the categories “antiviral defense”, “nucleotide binding” and “unclassified” the most prominent.

The “antiviral defense” gene group is subdivided in 3 phases according to the chain of events triggered after viral engagement (Figure 5-1): (1.) the “immediate” genes, induced after viral binding and responsible for initiating and amplifying signaling pathways which activate effector genes. For instance, it is well known that the upregulated genes *dhx58*

(LGP2), *ifih1* (MDA5), *ddx58* (RIG-I) *ddx60* and *zbp1* code for PRRs that activate signaling pathways; the genes *irf7*, *stat1*, *stat2* and *irf9*, represent transcription factor that are products of the activation of TLRs, RLRs and IFNAR. Translocation to the nucleus of IRF7 and IRF9 induces the expression of IFNα subtypes and to a lesser extent IFNβ and ISG, respectively. However, induction of *irf7* is also described not only as a result of the responses occurring after ligand binding but also as the consequence of signaling through IFNAR1, which is considered as a late event, and a result of PRRs activation. (2.) The "effector" genes that code for effector proteins that positively feedback the signaling loop. In this work, those genes are represented by members of the IFNα subtype like *ifna2*, *ifna1*, *ifna7*, *ifna6*, *ifna5* and *ifna4*. The positive feedback mediated by type I IFNs through IFNAR1, results in the phosphorylation of STAT1 and STAT2 that later bind to IRF9 to form the ISGF3 complex. In the nucleus, ISGF3 binds to ISRE sequences, promoting the induction of ISG. (3.) "ISG", whose regulation was described above and comprises a wide variety of genes that in some cases are completely unknown. For instance, the proteins coded by the genes *ifit1*, *ifit2* and *ifit3* have recently been described to form a complex able to bind viral 5'ppp RNA interfering with viral replication (Pichlmair *et al.*, 2011). Similar functions have been described for the protein coded by the gene *mx1*, which binds to viral nucleocapside proteins (Hefti *et al.*, 1999; Haller *et al.*, 2002), as well as for *rsad2* that inhibits viral budding (Wang *et al.*, 2007) and for *ifitm3* that is able to prevent viral fusion of IAV and limit the replication of the Dengue and West Nile virus (Feeley *et al.*, 2011; Everitt *et al.*, 2012). Additionally, the gene *isg15* leads the ISGylation, which is a ubiquitin-like process that protects type I IFN signaling mediators from degradation (Ritchie *et al.*, 2004).

Surprisingly, the genes expressed in the "nucleotide binding" group correspond mainly to genes upregulated by signaling through type I IFNs and considered as ISG. These genes are involved in the sequestering of different types of nucleic acids. For instance, the group of the genes *oasl2*, *oas3*, *oas1a*, *oasl1* and *oas1g* code for proteins belonging to the olygoadenylate synthetase family that after recognition of viral dsRNA activates RNase L. This enzyme mediates degradation of viral RNA and hence prevents viral replication (Lin *et al.*, 2009; Kristiansen *et al.*, 2011). The genes *gbp3*, *gbp2*, *gbp6*, *gbp9*, *gbp5* and *gbp4* translate for proteins members of the guanylate binding family of proteins which are induced by type I and II IFNs and have been shown to have antiviral and antibacterial properties, due to their ability to hydrolyze GTP (Carter *et al.*, 2005; Vestal *et al.*, 2011).

The gene *adar1* codes for a deaminase that replaces the adenosine bases from viral dsRNA with inosine, allowing recognition of RNA by the PRR ZBP1. The gene coding for ZBP1 is also listed as upregulated gene (Wang *et al.*, 2008; Li *et al.*, 2010). Genes with similar functions and dependent on type I IFNs signaling, but less studied are *cmpk2*, *isg20*, *tgtp1*, and *iigp1* (Carlow *et al.*, 1998; Uthaiah *et al.*, 2003; Espert *et al.*, 2005; Xu *et al.*, 2008).

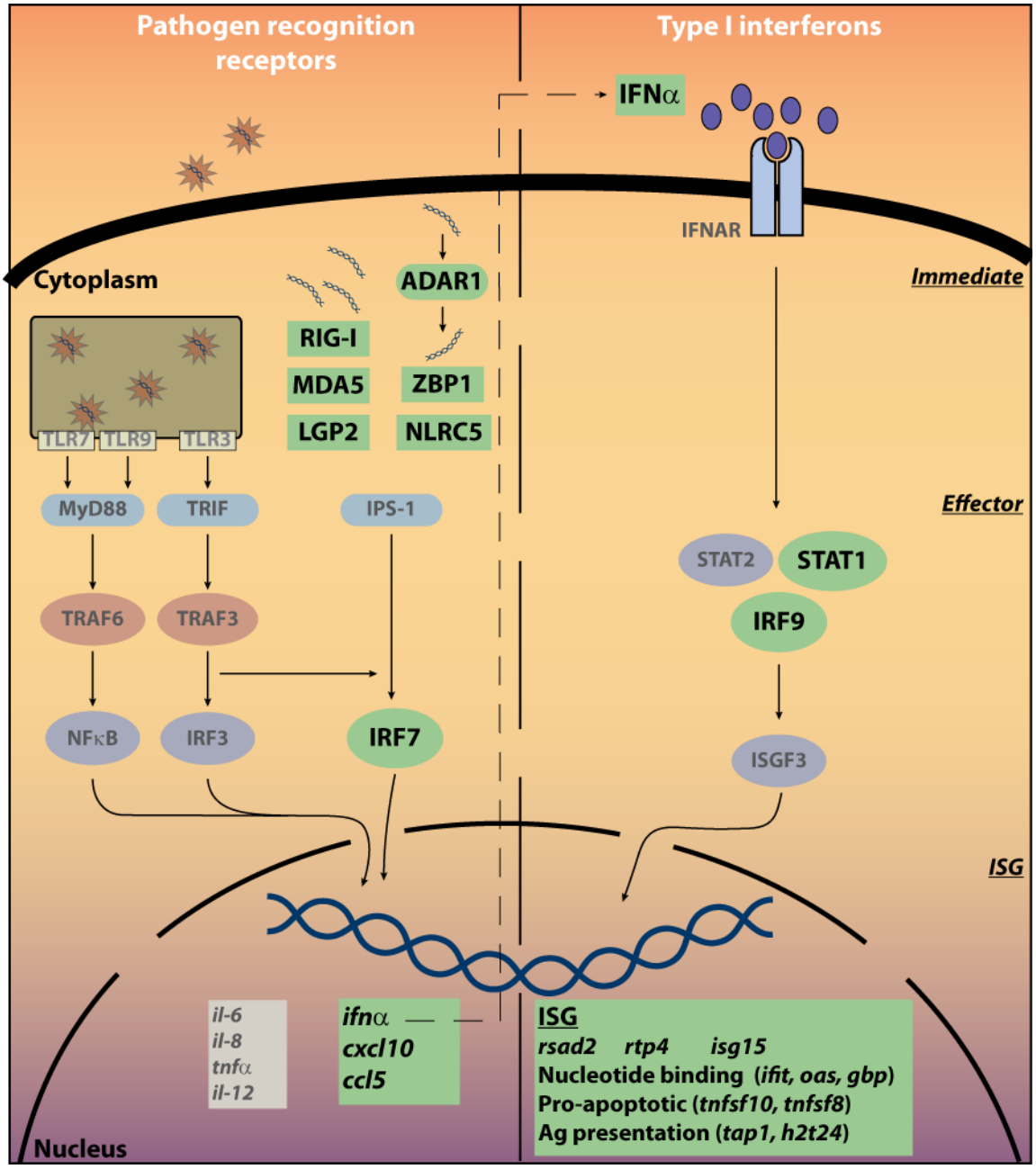

Figure 5-1: Mast cells display an antiviral program.
After viral infection BMMC upregulate genes that mediate antiviral response. Immediate genes coding for pathogen recognition receptors (PRR) such as *dhx58* (LGP2), *ifih1* (MDA5), *ddx58* (RIG-I) *ddx60*, *zbp1* and *nlrc5*, increase the ability of BMMC to sense viral particles and to initiate antiviral responses through the activation of signaling pathways. Effector genes that positively feedback antiviral responses, like the transcription factors *irf7*, *stat1* and *irf9* that mediate the

upregulation of antiviral genes. Additionally, type I IFNs are included in this category since they trigger the expression of interferon stimulated genes (ISG) through the activation of the IFNAR. ISG are expressed as a consequence of the activation of PRRs; most of these genes are able to interact directly with the virus to inhibit their replication. Green boxes represent genes that were found to be upregulated in BMMC infected with NDV. The figure depicts some of the mediators involved in the signaling pathways and to illustrate the context of the upregulated genes.

Furthermore, other genes considered as ISG were not included by the bioinformatic tool DAVID in the "antiviral defense" group but they play important roles in antiviral responses. This is the case with the genes *ccl5, cxcl10, nlrc5, usp18* and *ube2l6* that translate for the chemokines RANTES and IP-10 which have been well described for playing a role in the recruitment of immune cells to sites of infection (Miller *et al.*, 2004), the viral PRR NLRC5 known for viral recognition and inflammasome activation (Davis *et al.*, 2011) and the enzymes USP18 and UBE216, which mediate and regulate the ISGylation pathway (Chen *et al.*, 2011).

Here upregulated genes were also found to participate in other cell and immune processes. That is the case with the genes *tnfsf10, tnsf8* and *tap1* that translate for the proteins TRAIL, CD153 and TAP1. The first two proteins have been shown to mediate apoptosis, via caspase 8 of tumor cells and activated T cells (Wiley *et al.*, 1995; Cerutti *et al.*, 2000; Blazar *et al.*, 2004; Mihalich *et al.*, 2012). The protein TAP1 that constitutes the transporter TAP is known for its role in transporting cytosolic degraded peptides into the ER, where they bind to MHC I molecules for later expression on the cell surface (Suh *et al.*, 1994).

The gene expression pattern described above confirms that BMMC activate a complete antiviral program, comprising the induction of mechanisms to sense virus, engage signaling pathways intended to produce interferons and hence to induce all the set of ISG that confers to these cells the "antiviral state". Likewise, these findings suggest that MC might contribute to contain viral infections by different mechanism such as, the recruitment of immune cells (T cells, macrophages and DC) through chemokines upregulation; the activation of other cells via type I IFN genes expression; the inhibition of viral replication by the expression of a wide variety of nucleotide-binding proteins.

The antiviral gene pattern found in BMMC upon NDV infection is similarly induced in other cell types classically involved in antiviral immune responses. For example, human primary macrophages infected with IAV, showed a significant upregulation of ISG genes (*vg. ccl5, cxcl10, dhx58, gbp4, gbp5, herc5, ifih1, ifit1, ifit2,* ifit3*, ifna1, isg15, mx1,oasl rsad2, rtp4, tnfsf10* and *usp18*) that were also found to be upregulated in this work (Lee *et al.*, 2009). Interestingly, BMMC co-cultured with $CD8^+$ T cells also showed a strong upregulation of, *rtp4*, *rsad2* and *irf7* and the expression of these genes was reported to be in 1st, 4th and 5th place, respectively (Stelekati, 2007). Additionally, in other non-immune cells like conjunctival epithelium stimulated with pIC, genes here reported like *ccl5, cmpk2, cxcl10, mx1, ifi44, ifi203, rsad2* and *rtp4* were listed to be within the top 10 of the most up-regulated genes in conjunctival cells (Ueta *et al.*, 2011). Similar findings have been shown in the human liver carcinoma cell line HepG2 infected with dengue virus (Fink *et al.*, 2007), human airway epithelial cells infected with rhinovirus (Chen *et al.*, 2006) and in chronic HCV-infected human patients treated with IFN2αb (Sarasin-Filipowicz *et al.*, 2008).

Thus, this work provides new evidence on the participation of MC in antiviral immune responses.

This project focused on analyzing the gene expression profile induced in MC by NDV, which is an RNA virus and was used here as an experimental model. The results obtained raised the question, whether DNA virus infections would act similarly. Indeed DNA virus activate similarly pathways leading to the production of type I interferons, for instance through TLR9 (Luckhardt *et al.*, 2011). Moreover, it has been described that the receptors RIG-I and MDA5 are able to recognize cytosolic DNA through conversion to RNA by RNA polymerase III. Examples of this conversion comprise the synthetic B-form DNA, poly (dA:dT) (Ablasser *et al.*, 2009; Chiu *et al.*, 2009) and virus like herpes simplex (Melchjorsen *et al.*, 2010).

This mechanism might be present also in MC allowing these cells to sense DNA viruses and to induce antiviral responses via the production of type I IFNs.

5.2 RTP4 is a prominent viral-induced gene expressed in MC

It is important to note that the genes *ifit1, rtp4, rsad2, cmpk2* and *isg20* were the five most upregulated genes according to microarray expression analysis. The genes *ifit1*, *isg20* and *rsad2* code for antiviral proteins that directly inhibit viral replication and were discussed above. Unlike the other genes, *rtp4* was listed in the "unclassified" group and its functions in immunity are unknown.

Upregulation of *rtp4* was confirmed by qRT-PCR in BMMC infected with NDV and additionally with IAV, which has been shown to be an inducer of interferons through activation of RIG-I (Pichlmair *et al.*, 2006). This is in agreement with reports on human alveolar cell lines that showed that activation of RIG-I by IAV induce the expression of IFNβ and hence of ISG (Opitz *et al.*, 2007). The fact that *rtp4* is strongly induced in BMMC led me to address experiments to understand the nature of this gene in aspects such as regulation pathways, intracellular localization/distribution, interaction partners and functionality.

5.3 RTP4 and regulatory pathways

I could demonstrate that the expression of *rtp4* is induced after activation of TLR3, TLR4, and TLR9 by pIC, LPS and CpG, respectively. It is not surprising that *rtp4* expression is induced by the activation of TLR3 and TLR9, since engagement of these receptors upregulates the expression of type I IFNs and as mentioned above *rtp4* expression is dependent on type I IFNs expression.

The induction of *rtp4* by stimulation of TLR4 was unexpected. This, however, can be explained by the indirect TLR4-mediated induction of type I IFNs expression. Once LPS-engaged TLR4 is internalized and located in phagosomes, the adaptor protein TRIF is recruited and hence type I IFNs expression is induced (Fitzgerald *et al.*, 2003; Clark *et al.*, 2011). Moreover, mice stimulated with a sublethal dose of LPS and then infected with IAV exhibit a significant lower lethal dose 50 than the mice that just received IAV, demonstrating the protective effects of the LPS- TLR4 mediated by TRIF and by the induction of type I IFNs (Shinya *et al.*, 2011).

One has to underline that the increased expression of *rtp4* mRNA upon pIC, CpG and LPS treatment of BMMC never reached expression levels induced by NDV; furthermore RTP4 protein was detectable by WB only in viral infected BMMC. This difference in RTP4 levels of expression could be explain by the fact that NDV infection via a number of different mechanisms strongly and rapidly activates RIG-I and thereby inducing a higher expression of type I IFNs (Yoneyama *et al.*, 2004).

Simultaneous deletion of TLR2, TLR3, TLR4, TLR7 and TLR9 and the single deletions for the adaptor proteins MyD88 and TRIF showed that these receptor/mediators are dispensable for *rtp4* expression. In contrast, in *ifnar1*$^{-/-}$ BMMC no expression of *rtp4* was found. These findings indicate that induction of *rtp4* relies on the signaling pathways triggered by type I IFNs through its receptor, IFNAR1. This could also suggest that induction of type I IFNs is independent on TLR pathways, since deletion of TLR3, TLR4, TLR9, MyD88 and TRIF were not required for RTP4 expression. Similar findings were reported in macrophages derived from doubled KO mice for MyD88 and TRIF, where the production of IFNβ was not altered after stimulation with bacterial DNA (Charrel-Dennis *et al.*, 2008). Thus, suggesting that other mechanism like RLRs are responsible for the induction of type I IFNs. In fact, it was demonstrated that deletion of *ips* abrogate the expression of CXCL10 and IFNβ in embryonic fibroblast infected with IAV; opposite results were obtained with fibroblast from *mydd8*$^{-/-}$ and *trif*$^{-/-}$ mice, confirming the major role of RIG-I in inducing type I IFNs and ISG (Koyama *et al.*, 2007). Similarly, one can suggests that the upregeulation of *rtp4* in BMMC is also mediated by the activation of RIG-I, since here was shown that *myd88*$^{-/-}$, *trif*$^{-/-}$ and *tlr23479*$^{-/-}$ BMMC infected with NDV expressed significant levels of *rtp4*.

5.4 RTP4 is expressed in a variety of immune cells

Almost all mammalian cells are able to produce type I IFNs upon viral infection, however such production differs among cells types and hence also the expression of ISG (Liu, 2005). Accordingly, the expression of *rtp4* may differ among cells, this study reports that BMM, BMDC express higher levels of *rtp4* in comparison to CD3-activated T cells. In this study I could demonstrate that B cells show high constitutive levels of *rtp4* and downregulation occurs after stimulation with LPS and CpG. These discrepancies in

requirements for *rtp4* expression can be explained by the intrinsic differences in the regulatory pathways present in different immune cell subsets. For instance, TLRs are differentially expressed in leukocytes (Applequist *et al.*, 2002; Zarember *et al.*, 2002); $CD14^+$ cells express the widest variety of TLRs and these cells efficiently uptake Ag and microorganisms, via phagocytosis, favoring the activation of immune signaling. It has also been reported that DC and monocytes expressed high levels of TLR3 in contrast to B, which lack this receptor (Muzio *et al.*, 2000). RTP4 expression has not characterized in immune cells, however the database BioGPS (Wu *et al.*, 2009), which is a repository for data from gene expression arrays, reports RTP4 to be expressed in human $CD56^+$ NK cells, $CD14^+$ monocytes and B lymphoblasts, as well as in murine macrophages stimulated with LPS, osteoclasts and DC (BioGPS).

Finally, this section brings forth the question of which regulatory pathways govern the expression of *rtp4* in B cells? Perhaps RTP4 play major roles in B cells, making these cells attractive for further experiments intended to define RTP4 functionality.

5.5 RTP4 subcellular localization

This report located the expression of the RTP4 protein to the cellular membranes; through confocal microscopy RTP4 was identified to colocalize with ER, LB and EE but interestingly not with plasma membrane markers of BMMC. These results suggest that after mRNA translation, RTP4 is sorted to the ER by a mechanism which is still unclear. Analysis of the RTP4 sequence by bioinformatic tools show a lack of signal peptide, transit or anchor signals responsible for protein sorting to ER, mitochondria, membranes and nucleus. (Appendix A.). These findings could explain why RTP4 does not reach the plasma membrane of BMMC. In addition, if one postulates that RTP4 acts as chaperone and therefore intracellularly interacting with other proteins one should not exclude the possibility that the epitope for antibody recognition is hidden by the stable protein-protein interaction condition. This would results in the absence of fluorescence in the confocal experiments performed and shown.

It has been described that LB originate from the budding or “hatching” of ER membranes that contain high levels of lipid esters (Ploegh, 2007; Fujimoto *et al.*, 2008). In fact, other ER-membrane proteins like caveolin-1 and ADRP have been demonstrated to be also

present in LB (Robenek *et al.*, 2004; Robenek *et al.*, 2006). This origin of LB is consistent with the findings that RTP4 associates with both ER and LB.

Activated-GPCR desensitization involves the binding of β-arrestin to the receptor, preventing G protein signaling and promoting the internalization of the receptor via endocytosis. Early endosomes are intermediaries of the endocytic pathway that after maturation, either fuse with lysosomes for proteolytic degradation of the receptors or form recycling endosomes for rapid relocation in the membrane of the GPCR (Tan *et al.*, 2004; Hanyaloglu *et al.*, 2008). Furthermore, dileucine motifs (LL or LxL) mediate internalization of GPCR such as β2-adrenergic receptor, vasopressin V1a receptor (Gabilondo *et al.*, 1997; Preisser *et al.*, 1999; Hannan *et al.*, 2011). RTP4 sequence analysis revealed the presence of three of these motifs: one at the C-terminal and two at the N-terminal (Appendix B.). Therefore either RTP4 or the transported/partner GPCR should follow the endocytic pathway for downregulation. However mutagenesis experiments must be performed to confirm this hypothesis.

In this study, the discovered localization of RTP4 in LB is particularly intriguing. LB are abundantly present in MC and macrophages and have been described as organelles for lipids storage and as the major site for the metabolism of arachidonic acid-derived inflammatory mediators (Dvorak *et al.*, 1983; Dvorak, 2005). In addition, after their recent "rediscovery", LB have been linked to regulatory sites for immune responses. For instance DC lacking the proteins ADRP and IGTP showed defects in LB formation and hence severely impaired cross-presentation of ovoalbumin Ag to $CD8^+$ T cells (Bougneres *et al.*, 2009); the antiviral protein VIPERIN localizes in lipid bodies where it can inhibit the replication of HCV (Hinson *et al.*, 2009).

In order to confirm the localization of RTP4 in LB, a biochemical approach consisting of the identification of RTP4 in a purified-LB fraction was used. Initially, BMMC were used for this aim but due to the limited availability of these cells the extraction process for LB could not be performed. Therefore a murine mast cell line MC9 was used for this aim. However this cell line was found to express low levels of RTP4 protein (data not showed). To overcome this problem immortal macrophages were used because of the large amount of LB present in the cytosol and high expression levels of RTP4. Despite this alternative approach, RTP4 could not be detected biochemically in the purified LB fraction. However,

a recent studies on the proteome of LB from the enterocyte CACO2/TC7 and the chinese hamster ovary (CHO) cell lines revealed a number of 105 and 110 proteins, respectively, that were associated to LB. The identification of proteins by mass spectrometry showed that 36 proteins were involved in lipid metabolism, the rest of the identified proteins were associated to metabolism of carbohydrates, cytosolic chaperones or components of ER, mitochondria and cytoskeleton/cytosol (Hodges *et al.,* 2010; Bouchoux *et al.,* 2011). Surprisingly, proteins already reported for their localization in LB and for having roles in immunity like VIPERIN and IGTP were not identified. These findings may suggest that the association of proteins to LB depends on the intrinsic functions of each cell type. Perhaps the presence of RTP4 in LB is limited to a certain group of immune cells that excludes the cell line of immortal macrophages used in this work.

With the goal of determining the functionality of RTP4 a strategy consisting in the identification of interaction partners was started. IP experiments were performed using BMMC infected with NDV and different cell lines like MC9, RBL, COS7 and HEK293 (data not showed) transfected with constructs expressing RTP4; several experimental conditions, *vg*. different lysis buffers (NP40 and ODGP), Abs (anti-RTP4, two different clones of anti-FLAG) and capture beads (agarose and magnetic beads) were used in order to pursue this objective but without any success. This failure in the IP experiments could be explained by the limited efficiency of the Ab to bind to the native structure of RTP4. Contrary to SDS-PAGE and WB experiments where RPP4 was detected as a result of the Ab binding to RTP4 in primary conformation. To sort that limitation a polyclonal antibody was developed but the detection of RTP4 in SDS-PAGE and WB was limited to the recognition of the peptide used for the generation of the Ab and not to the protein present in cell lysates from NDV-infected BMMC. Thus, the use of the polyclonal antibody in IP experiments was discarded. An alternative explanation relies on works that showed that GPCR commonly exists as dimers or complex oligomers and that GPCR activation provokes changes in the structural conformation of the receptor (Angers *et al.,* 2002; Rosenbaum *et al.,* 2009; Katritch *et al.,* 2012; Unal *et al.,* 2012). These events could induce epitope masking thus inhibiting Ab binding.

The yeast two-hybrid system is a genetic tool that allows the identification of protein-protein interactions. The method is based on the expression of a reporter gene that

is activated when the protein of interest (in this case RTP4) interacts with other proteins that are coded from a gene library (Fields *et al.*, 1989; Serebriiskii *et al.*, 2000). This procedure was performed by hired services for RTP4 using a normalized mouse universal and a normalized mouse embryo library, containing 2.8×10^6 and 2×10^7 gene clones, respectively. The results of these tests did not reveal interactors for RTP4.

Although the experiments described above were inconclusive, this does not rule out the existence of RTP4 interactors and instead set out the need to use alternative approaches for defining RTP4 functions.

5.6 Use of *rtp4*$^{-/-}$ mice as a strategy to define the RTP4 function

To determine the function of RTP4 we have chosen to investigate the phenotype of immune cells in particular in *rtp4*$^{-/-}$ mice. Mice lacking *rtp4* showed comparable percentages of immune cell lineages from primary and secondary immune organs to WT animals; similarly differentiation and maturation of *rtp4*$^{-/-}$ BMMC was found normal. From these results I can conclude that naïve non-immunized *rtp4*$^{-/-}$ mice show no apparent phenotype or pathology. However, if the upregulation of the gene relies on diseases or adverse situations, then the phenotype in "resting" mice would not be apparent (Barbaric *et al.*, 2007). For instance, mice lacking the glutathione peroxidase gene (*gpx1*) were healthy, fertile and did not present histological changes, however exposition to paraquat (poisoning reactive oxygen species-inducer), led to the death of all KO mice, contrary to WT mice that did not exhibit any toxicity (de Haan *et al.*, 1998). Similarly has been reported for mice lacking the genes *il21* (interleukin 21), *il23a* (interleukin 23, alpha subunit p19) and *pmm1* (phosphomannomutase 1) (Cromphout *et al.*, 2006; Deltagen, 2012; Deltagen, 2012; Eppig *et al.*, 2012). Therefore further *in vivo* experiment such as the viral infection of *rtp4*$^{-/-}$ mice are essential for the identification of RTP4 functions.

The gene expression pattern of *rtp4*$^{-/-}$ BMMC was comparable to their counterpart WT, even after the infection of both cell types with NDV. These findings suggest that *rtp4*$^{-/-}$ targeting does not interfere with the expression of other genes, rising the hypothesis that RTP4 is located in downstream regulatory pathways.

Only the gene *mela* was upregulated in both, in *rtp4*$^{-/-}$ BMMC infected with NDV or left untreated. This gene codes for the protein melanoma antigen that has been described as the product of endogenous retroviral sequences derived from proviruses integrated into the mice genome. The expression of the protein is tissue-specific, thymocytes are the cell target for this expression (Levy *et al.*, 1985; Hayashi *et al.*, 1992). The underlying mechanisms explaining the upregulation of *mela* in *rtp4* deficient mice are not clear. However, it has been reported that the expression of endogenous provirus derived from the retrovirus mouse mammary tumor virus (MMTV) in Balb/c mice increase the susceptibility for bacterial and viral infections (Bhadra *et al.*, 2006). Thus, a similar phenomenon of increased susceptibility to infections could be manifested in *rtp4*$^{-/-}$ mice where the upregulation of the provirus *mela* was detected.

Since BMMC prominently express RTP4, functional aspects of *rtp4*$^{-/-}$ BMMC were assessed. Results showed that *rtp4*$^{-/-}$ BMMC degranulate similar to its counterpart WT. Although degranulation is a process commonly triggered by crosslinking of the FcεRI and rarely described in viral infections, this process was investigated since it is known that the GPCR, C3aR (complement component C3a receptor) and CXCR1 (IL-8 receptor) mediate degranulation events (Barlic *et al.*, 2000; Ahamed *et al.*, 2001; Kashem *et al.*, 2011). Whether RTP4 serves as chaperone for other GPCR, deletion of *rtp4* could affect this process.

In addition, it has been found here that cytokine production (IL-6, IP-10 and osteopontin) by BMMC from both WT and *rtp4*$^{-/-}$ were comparable. This observation newly confirms the fact that RTP4 does not regulate the pathways responsible for the regulation of the proinflammatory (IL-6 NF-κB mediated) and antiviral-associated (IP-10 and osteopontin) cytokines.

This study has demonstrated that BMMC are able to activate a complete antiviral program that includes the upregulation of genes that trigger, maintain and regulate responses that ultimately mediate viral elimination. Additionally, this work reported findings on the regulation, localization and functionality of RTP4, a protein that is strongly upregulated

upon virus infection not only in BMMC but also in different cell types and whose involvement in immunity was unknown.

Thus, this study provided an analysis of the changes in the gene expression of MC in response to viral infections, supporting the hypothesis that MC mediate immune responses for the elimination of viruses. This work establishes the need for the characterization of genes like *rtp4* that although being highly upregulated not only in MC but in other cell types their function remains unknown.

5.7 Conclusions and perspectives

In conclusion, here was demonstrated that the infection of BMMC with NDV virus induces a change in the gene pattern and more in particular the upregulation of like those coding for PRRs (RIG-I, MDA5, LGP2) that increase viral sensing and activate antiviral signaling pathways. NDV-infected BMMC also upregulate genes whose role is to maintain and amplify antiviral responses; for example, transcription factors STAT1, IRF7, and IRF9 and type I IFNs members. More importantly BMMC activation results in the upregulation of genes recognized to inhibit viral replication via nucleic acids sequestration and viral budding inhibition. The proteins members of the OAS and GBP families fall in this gene category.

In addition, the gene *rtp4* that codes for a member of the GPCR family of receptors was found to be the second most upregulated gene in BMMC infected with NDV and since little is known about its properties, this gene was matter of our study. Here was shown that *rtp4* expression is partially regulated by TLRs and their adaptor proteins and that in contrast, its expression depends on the signaling trigger by type I IFNs and the receptor IFNAR. *rtp4* is mainly expressed in cells participating in innate immune responses such as MC, BMMC and macrophages; RTP4 was found to be associated to membrane cell proteomes but not to the cytosol or the nucleus, consequently RTP4 localizes in the organelle membranes of ER, LB and EE.

rtp4 knockout were developed in order to investigate the functions of this gene/protein in vivo and its involvement in antiviral responses. Characterization of immune subsets in *rtp4*$^{-/-}$ mice did not reveal differences in the cell content of primary and secondary lymphoid organs in comparison to WT mice. BMMC from *rtp4*$^{-/-}$ mice exhibited normal levels for development and maturation markers. Additionally, by gene expression analysis it was determined that *rtp4*$^{-/-}$ together with WT BMMC express a comparable gene pattern in response to NDV infection. These findings suggest that RTP4 does not regulate the expression of other genes and that instead RTP4 is an end product signaling pathway. Furthermore, *rtp4*$^{-/-}$ BMMC degranulation and cytokine production (IL-6, IP-10 and osteopontin) were shown to be equal to the ones of WT BMMC.

In this work several experiments intended to answer to the question of what is the function of RTP4 in antiviral responses and particularly in BMMC have been reported. However this question could not be fully answered and further experiments using *rtp4*$^{-/-}$ mice/cells should be planned to reach this aim.

Since gene expression analysis did not reveal differences in the pattern of expression of *rtp4*$^{-/-}$ and WT BMMC and since RTP4 has been suggested to act as a chaperone, one should consider whether the differences between these cell strains reside in the protein intracellular localization and distribution. A feasible approach to investigate differences in protein expression and distribution should be based on differential proteome analysis. Two dimensions-differential gel electrophoresis (2D-DIGE) is a technique that allows the identification of differentially expressed proteins (Alban *et al.*, 2003; Lilley *et al.*, 2004; Penno *et al.*, 2012). In this case the proteome from WT and *rtp4*$^{-/-}$ BMMC infected with NDV are first stained with different fluorescent dyes (*vg.* Cy3 and Cy5). Then the samples are mixed and run in a 2D electrophoresis gel that allows the separation of proteins by their isoelectric point and weight. After gel scanning, proteins equally or differentially expressed show a merged color or a single color, respectively. The identification of differentially-expressed proteins could give insights about interaction partners or for proteins whose expression is regulated by RTP4.

Since it has been demonstrated that co-expression of opioid and taste receptors with RTP4 improves their localization on the cell membrane (Behrens *et al.*, 2006; Decaillot *et al.*, 2008), the expression of other GPCR involved in antiviral responses should be evaluated. For instance, in this work it was reported that BMMC infected with NDV upregulate the expression of the chemokines RANTES and IP-10; other reports have shown that MC express receptors for the chemokines RANTES, IP-10 and MCP-1 (Bannert *et al.*, 2001; Juremalm *et al.*, 2005; Collington *et al.*, 2010). Since chemokine receptors (CCR) belong to the family of GPCR, chemotaxis experiments using the chemokines above mentioned and *rtp4*$^{-/-}$ and WT BMMC could be used to investigate the role of RTP4 in the expression of these CCR.

So far *rtp4*$^{-/-}$ mice and their BMMC have not exhibited an apparent phenotype that could explain the functions of the deleted gene. Accordingly, systemic infection of *rtp4*$^{-/-}$ mice with viruses could alter the homeostatic balance of these mice revealing a phenotype. To this *rtp4*$^{-/-}$ mice should be infected with vaccinia virus. This dsDNA virus has been used in mouse models for studying skin infections (Lee *et al.*, 1992; Oyoshi *et al.*, 2009). In addition, VV has been reported to induce type I IFNs in BMDC (Waibler *et al.*, 2007). It has recently been shown that MC deficient mice (*Kit*$^{wsh-/-}$) infected with VV exhibited larger lesion sizes and higher viral load in the skin than in WT mice (Wang *et al.*, 2012). This model allows the evaluation of skin-resident MC and their interaction with the virus. Evaluation of the lesion size, viral load, infiltrating cell types and the local production of cytokines could help to determine the role of RTP4 in immunity.

Thus, this study has revealed the consequences of viral infection in MC and has set the basis for investigating the role of highly induced genes, such as *rtp4* and its role in antiviral immune responses trigger in MC.

6. Zusammenfassung

Bislang wurden Mastzellen (MC) auf Grund ihrer der Allergie zugeschriebenen Rolle als "monotasking" Zellen betrachtet. Allerdings wurde in den letzten Jahren vermehrt gezeigt, dass MC in einer Vielfalt von verschiedenen Immunantworten eine Rolle spielen. MC modulieren die Rekrutierung von Immunzellen zum Entzündungsherd und kontrollieren Immunantworten durch die Ausschüttung vielfältiger Mediatoren. Während neue Hinweise die Rolle von MC bei der Kontrolle von bakteriellen Infektionen unterstützen, ist die Beteiligung dieser Zellen bei antiviralen Immunantworten immernoch geringfügig untersucht.

Ziel dieser Arbeit war es, die Reaktion von MC auf virale Infektionen zu untersuchen. Dabei wurde das Newcastle disease virus (NDV) als Modell für virale Infektionen verwendet und das durch NDV indizierte Genexpressionsprofil der MC analysiert. Die Genexpressionsanalysen hatten gezeigt, dass das Gen *rtp4*, welches für das Rezeptor Transporter Protein 4 (RTP4) kodiert, am zweithöchsten hochreguliert war. Aus diesem Grund umfasste ein weiterer Teil dieser Arbeit die Regulation und zelluläre Lokalisation von RTP4 sowie dessen funktionale Rolle in antiviralen Immunantworten zu untersuchen.

Genexpressionsanalysen zeigten, dass MC eine große Vielfalt antiviraler Gene hochregulieren, als Konsequenz der Bindung von NDV an "pattern recognition receptors" (PRRs), welche wie folgt klassifiziert werden können: (1.) direkte Gene, die MC befähigen virale Partikel wahrzunehmen und Signalwege zu aktivieren; (2.) Effektor-Gene, die die Antwort regulieren und verstärken und verantwortlich für die Induktion von Typ I IFN sind; (3.) Interferon-stimulierte Gene (ISG), die für Proteine kodieren, welche direkt die virale Replikation kontrollieren, was zur Auflösung der Infektion führt.

Die Expression von *rtp4* wurde als teilweise abhängig von TLR2, TLR3, TLR4, TLR7 und TLR9 sowie den Adaptorproteinen MyD88 und TRIF beschrieben. Typ I IFN-Rezeptor-Defizienz korreliert mit der fehlenden Expression von *rtp4*, was darauf hindeutet, dass Typ I Interferone verantwortlich für dessen Induktion sind. Zudem wurde gezeigt, dass die

Induktion von RTP4 in MC durch NDV und Influenza A virus (IAV) reguliert wird. Fraktionierungen und konfokalmikroskopische Analysen lokalisierten RTP4 in der Plasmamembran und dem endoplasmatischen Retikulum beziehungsweise in frühen Endosomen und Lipidkörpern. Um die Funktion von RTP4 zu untersuchen wurden "knock-out" Mäuse generiert. *rtp4*$^{-/-}$ Mäuse zeigten keine offensichtlichen phenotypischen Abnomalien. Zusätzlich zeigten Genexpressionsanalysen, dass *rtp4*$^{-/-}$ Mastzellen aus dem Knochenmark (BMMC) als Antwort auf eine NDV Infektion ein vergleichbares Genmuster exprimieren wie wildtypische (WT) BMMC. Die funktionalen Eigenschaften der *rtp4*$^{-/-}$ BMMC, wie Degranulation und Zytokinproduktion, waren ähnlich denen ihrem Gegenstück WT BMMC. Demzufolge verbleibt ungeklärt in welchem Schritt der antiviralen Immunkaskade RTP4 involviert ist. Diese Arbeit zeigt, dass viral infizierte MC ein antivirals Programm entwickeln zu dem das Membran-assoziierte und IFN-induzierte RTP4 Protein gehört.

7. Abstract

So far mast cells (MC) for their role in allergy have been considered “monotasking cells”. However, in the last years increasing evidence points out at the MC to participate in a variety of different immune responses. MC modulate the recruitment of immune cells to inflammation sites and control immune responses by the release of a wide variety of mediators. While new evidence supports the role of MC in the control of bacterial infections, the involvement of these cells in antiviral immune responses is still poorly investigated.

Goal of this project was to investigate the response of mast cells to viral infection by analyzing the gene expression profile induced in these cells upon Newcastle disease virus (NDV), used here as a model for viral infection. Additionally, gene expression analysis showed that the gene *rtp4*, which codes for the protein receptor transporter protein 4, was the second most upregulated gene. Therefore the second aim of this work was to study the regulation and cellular localization of RTP4 as well as its functional contribution in antiviral immune responses.

Gene expression analysis revealed that BMMC upregulate a wide variety of antiviral genes, as a consequence of the engagement of NDV to PRRs which can be classified as follow: (1.) immediate genes that enable MC to sense viral particles and to activate signaling pathways; (2.) effector genes that regulate and amplify the response and are responsible for the induction of type I interferons (IFN); and (3.) interferon stimulated genes that code for proteins that directly control viral replication, leading to the resolution of the infection.

Expression of *rtp4* was shown to be partially dependent on TLR2, TLR3, TLR4, TLR7 and TLR9 as well as the adaptor proteins MyD88 and TRIF. However, type I IFN receptor deficiency, correlates with the lack of *rtp4* expression, indicating that type I interferons are responsible for its induction. Additionally, induction of *rtp4* in BMMC was triggered by

NDV and influenza A virus (IAV) infection. Fractionation and confocal experiments localized RTP4 in the plasma membranes and in endoplasmic reticulum, early endosomes and lipid bodies, respectively. To investigate the functions of RTP4, knock-out mice were generated. *rtp4*$^{-/-}$ mice showed no obvious phenotypic abnormalities. Furthermore, gene expression analysis showed that *rtp4*$^{-/-}$ bone marrow derived MC (BMMC) express a comparable gene pattern to WT BMMC in response to NDV infection. Additionally, functional features of BMMC such as degranulation and cytokine production were similar to their counterpart WT BMMC. This work shows that virally infected MC develop an antiviral program to which the membrane-associated and IFN-induced RTP4 protein belongs.

8. References

Abbas, A. K., A. H. Lichtman and S. Pillai. Cellular and molecular immunology. 2007. Saunders Elsevier.

Ablasser, A., F. Bauernfeind, G. Hartmann, E. Latz, K. A. Fitzgerald and V. Hornung. RIG-I-dependent sensing of poly(dA:dT) through the induction of an RNA polymerase III-transcribed RNA intermediate. *Nat Immunol.* 2009; 10(10): 1065-1072.

Abraham, S. N. and A. L. St John. Mast cell-orchestrated immunity to pathogens. *Nat Rev Immunol.* 2010; 10(6): 440-452.

Ahamed, J., B. Haribabu and H. Ali. Cutting edge: Differential regulation of chemoattractant receptor-induced degranulation and chemokine production by receptor phosphorylation. *J Immunol.* 2001; 167(7): 3559-3563.

Akira, S., S. Uematsu and O. Takeuchi. Pathogen recognition and innate immunity. *Cell.* 2006; 124(4): 783-801.

Alban, A., S. O. David, L. Bjorkesten, C. Andersson, E. Sloge, S. Lewis and I. Currie. A novel experimental design for comparative two-dimensional gel analysis: two-dimensional difference gel electrophoresis incorporating a pooled internal standard. *Proteomics.* 2003; 3(1): 36-44.

Amin, K. The role of mast cells in allergic inflammation. *Respir Med.* 2012; 106(1): 9-14.

Andrejeva, J., K. S. Childs, D. F. Young, T. S. Carlos, N. Stock, S. Goodbourn and R. E. Randall. The V proteins of paramyxoviruses bind the IFN-inducible RNA helicase, mda-5, and inhibit its activation of the IFN-beta promoter. *Proc Natl Acad Sci U S A.* 2004; 101(49): 17264-17269.

Angers, S., A. Salahpour and M. Bouvier. Dimerization: an emerging concept for G protein-coupled receptor ontogeny and function. *Annu Rev Pharmacol Toxicol.* 2002; 42: 409-435.

Applequist, S. E., R. P. Wallin and H. G. Ljunggren. Variable expression of Toll-like receptor in murine innate and adaptive immune cell lines. *Int Immunol.* 2002; 14(9): 1065-1074.

Babu, M. M. An Introduction to Microarray Data Analysis. Computational Genomics: Theory and Application. R. P. Grant. Cambridge, UK, Horizon Bioscience 2004. 306.

Bannert, N., M. Farzan, D. S. Friend, H. Ochi, K. S. Price, J. Sodroski and J. A. Boyce. Human Mast cell progenitors can be infected by macrophagetropic human immunodeficiency virus type 1 and retain virus with maturation in vitro. *J Virol.* 2001; 75(22): 10808-10814.

Barbaric, I., G. Miller and T. N. Dear. Appearances can be deceiving: phenotypes of knockout mice. *Briefings in Functional Genomics & Proteomics.* 2007; 6(2): 91-103.

Barber, G. N. Innate immune DNA sensing pathways: STING, AIMII and the regulation of interferon production and inflammatory responses. *Curr Opin Immunol.* 2011; 23(1): 10-20.

Barlic, J., J. D. Andrews, A. A. Kelvin, S. E. Bosinger, M. E. DeVries, L. Xu, T. Dobransky, R. D. Feldman, S. S. Ferguson and D. J. Kelvin. Regulation of tyrosine kinase activation and granule release through beta-arrestin by CXCRI. *Nat Immunol.* 2000; 1(3): 227-233.

Barral, P. M., D. Sarkar, Z. Z. Su, G. N. Barber, R. DeSalle, V. R. Racaniello and P. B. Fisher. Functions of the cytoplasmic RNA sensors RIG-I and MDA-5: key regulators of innate immunity. *Pharmacol Ther.* 2009; 124(2): 219-234.

Behrens, M., J. Bartelt, C. Reichling, M. Winnig, C. Kuhn and W. Meyerhof. Members of RTP and REEP gene families influence functional bitter taste receptor expression. *J Biol Chem.* 2006; 281(29): 20650-20659.

Bhadra, S., M. M. Lozano, S. M. Payne and J. P. Dudley. Endogenous MMTV proviruses induce susceptibility to both viral and bacterial pathogens. *PLoS Pathog.* 2006; 2(12): e128.

Bischoff, S. C. Role of mast cells in allergic and non-allergic immune responses: comparison of human and murine data. *Nat Rev Immunol.* 2007; 7(2): 93-104.

Blasius, A. L. and B. Beutler. Intracellular toll-like receptors. *Immunity.* 2010; 32(3): 305-315.

Blazar, B. R., R. B. Levy, T. W. Mak, A. Panoskaltsis-Mortari, H. Muta, M. Jones, M. Roskos, J. S. Serody, H. Yagita, E. R. Podack and P. A. Taylor. CD30/CD30 Ligand (CD153) Interaction Regulates CD4+ T Cell-Mediated Graft-versus-Host Disease. *The Journal of Immunology.* 2004; 173(5): 2933-2941.

Bonjardim, C. A. Interferons (IFNs) are key cytokines in both innate and adaptive antiviral immune responses--and viruses counteract IFN action. *Microbes Infect.* 2005; 7(3): 569-578.

Bouchoux, J., F. Beilstein, T. Pauquai, I. C. Guerrera, D. Chateau, N. Ly, M. Alqub, C. Klein, J. Chambaz, M. Rousset, J. M. Lacorte, E. Morel and S. Demignot. The

proteome of cytosolic lipid droplets isolated from differentiated Caco-2/TC7 enterocytes reveals cell-specific characteristics. *Biol Cell.* 2011; 103(11): 499-517.

Bougneres, L., J. Helft, S. Tiwari, P. Vargas, B. H. Chang, L. Chan, L. Campisi, G. Lauvau, S. Hugues, P. Kumar, A. O. Kamphorst, A. M. Dumenil, M. Nussenzweig, J. D. MacMicking, S. Amigorena and P. Guermonprez. A role for lipid bodies in the cross-presentation of phagocytosed antigens by MHC class I in dendritic cells. *Immunity.* 2009; 31(2): 232-244.

Bowie, A. and L. A. O'Neill. The interleukin-1 receptor/Toll-like receptor superfamily: signal generators for pro-inflammatory interleukins and microbial products. *J Leukoc Biol.* 2000; 67(4): 508-514.

Brehm, G. and H. Kirchner. Analysis of the interferons induced in mice in vivo and in macrophages in vitro by Newcastle disease virus and by polyinosinic-polycytidylic acid. *J Interferon Res.* 1986; 6(1): 21-28.

Brown, M. G., S. M. McAlpine, Y. Y. Huang, I. D. Haidl, A. Al-Afif, J. S. Marshall and R. Anderson. RNA Sensors Enable Human Mast Cell Anti-Viral Chemokine Production and IFN-Mediated Protection in Response to Antibody-Enhanced Dengue Virus Infection. *PLoS One.* 2012; 7(3): e34055.

Bruns, A. M. and C. M. Horvath. Activation of RIG-I-like receptor signal transduction. *Crit Rev Biochem Mol Biol.* 2012; 47(2): 194-206.

Burke, S. M., T. B. Issekutz, K. Mohan, P. W. Lee, M. Shmulevitz and J. S. Marshall. Human mast cell activation with virus-associated stimuli leads to the selective chemotaxis of natural killer cells by a CXCL8-dependent mechanism. *Blood.* 2008; 111(12): 5467-5476.

Burks, J. S., O. Narayan, H. F. McFarland and R. T. Johnson. Acute encephalopathy caused by defective virus infection. I. Studies of Newcastle disease virus infections in newborn and adult mice. *Neurology.* 1976; 26(6 PT 1): 584-588.

Carlow, D. A., S. J. Teh and H. S. Teh. Specific antiviral activity demonstrated by TGTP, a member of a new family of interferon-induced GTPases. *J Immunol.* 1998; 161(5): 2348-2355.

Carter, C. C., V. Y. Gorbacheva and D. J. Vestal. Inhibition of VSV and EMCV replication by the interferon-induced GTPase, mGBP-2: differential requirement for wild-type GTP binding domain. *Archives of Virology.* 2005; 150(6): 1213-1220.

Castleman, W. L., R. L. Sorkness, R. F. Lemanske, Jr. and P. K. McAllister. Viral bronchiolitis during early life induces increased numbers of bronchiolar mast cells and airway hyperresponsiveness. *Am J Pathol.* 1990; 137(4): 821-831.

Cerutti, A., A. Schaffer, R. G. Goodwin, S. Shah, H. Zan, S. Ely and P. Casali. Engagement of CD153 (CD30 ligand) by CD30+ T cells inhibits class switch DNA recombination and antibody production in human IgD+ IgM+ B cells. *J Immunol.* 2000; 165(2): 786-794.

Charrel-Dennis, M., E. Latz, K. A. Halmen, P. Trieu-Cuot, K. A. Fitzgerald, D. L. Kasper and D. T. Golenbock. TLR-independent type I interferon induction in response to an extracellular bacterial pathogen via intracellular recognition of its DNA. *Cell Host Microbe.* 2008; 4(6): 543-554.

Chen, L., S. Li and I. McGilvray. The ISG15/USP18 ubiquitin-like pathway (ISGylation system) in hepatitis C virus infection and resistance to interferon therapy. *Int J Biochem Cell Biol.* 2011; 43(10): 1427-1431.

Chen, Y., E. Hamati, P. K. Lee, W. M. Lee, S. Wachi, D. Schnurr, S. Yagi, G. Dolganov, H. Boushey, P. Avila and R. Wu. Rhinovirus induces airway epithelial gene expression through double-stranded RNA and IFN-dependent pathways. *Am J Respir Cell Mol Biol.* 2006; 34(2): 192-203.

Chin, K. C. and P. Cresswell. Viperin (cig5), an IFN-inducible antiviral protein directly induced by human cytomegalovirus. *Proc Natl Acad Sci U S A.* 2001; 98(26): 15125-15130.

Chiu, Y. H., J. B. Macmillan and Z. J. Chen. RNA polymerase III detects cytosolic DNA and induces type I interferons through the RIG-I pathway. *Cell.* 2009; 138(3): 576-591.

Choe, J., M. S. Kelker and I. A. Wilson. Crystal structure of human toll-like receptor 3 (TLR3) ectodomain. *Science.* 2005; 309(5734): 581-585.

Clark, K., O. Takeuchi, S. Akira and P. Cohen. The TRAF-associated protein TANK facilitates cross-talk within the IkappaB kinase family during Toll-like receptor signaling. *Proc Natl Acad Sci U S A.* 2011; 108(41): 17093-17098.

Collington, S. J., J. Hallgren, J. E. Pease, T. G. Jones, B. J. Rollins, J. Westwick, K. F. Austen, T. J. Williams, M. F. Gurish and C. L. Weller. The role of the CCL2/CCR2 axis in mouse mast cell migration in vitro and in vivo. *J Immunol.* 2010; 184(11): 6114-6123.

Cromphout, K., W. Vleugels, L. Heykants, E. Schollen, L. Keldermans, R. Sciot, R. D'Hooge, P. P. De Deyn, K. von Figura, D. Hartmann, C. Korner and G. Matthijs. The normal phenotype of Pmm1-deficient mice suggests that Pmm1 is not essential for normal mouse development. *Mol Cell Biol.* 2006; 26(15): 5621-5635.

Davis, B. K., R. A. Roberts, M. T. Huang, S. B. Willingham, B. J. Conti, W. J. Brickey, B. R. Barker, M. Kwan, D. J. Taxman, M. A. Accavitti-Loper, J. A. Duncan and J. P. Ting. Cutting edge: NLRC5-dependent activation of the inflammasome. *J Immunol.* 2011; 186(3): 1333-1337.

Dawicki, W. and J. S. Marshall. New and emerging roles for mast cells in host defence. *Curr Opin Immunol.* 2007; 19(1): 31-38.

de Haan, J. B., C. Bladier, P. Griffiths, M. Kelner, R. D. O'Shea, N. S. Cheung, R. T. Bronson, M. J. Silvestro, S. Wild, S. S. Zheng, P. M. Beart, P. J. Hertzog and I. Kola. Mice with a homozygous null mutation for the most abundant glutathione peroxidase, Gpx1, show increased susceptibility to the oxidative stress-inducing agents paraquat and hydrogen peroxide. *J Biol Chem.* 1998; 273(35): 22528-22536.

Decaillot, F. M., R. Rozenfeld, A. Gupta and L. A. Devi. Cell surface targeting of mu-delta opioid receptor heterodimers by RTP4. *Proc Natl Acad Sci U S A.* 2008; 105(41): 16045-16050.

Deltagen, a. L. K. M. M. G. I. (2012). "il21 phenotypic analysis." Retrieved 30.07, 2012, from http://www.informatics.jax.org/external/ko/lexicon/341.html.

Deltagen, a. L. K. M. M. G. I. (2012). "il23a phenotypic analysis " Retrieved 30.07, 2012, from http://www.informatics.jax.org/external/ko/lexicon/7329.html.

Di Nardo, A., A. Vitiello and R. L. Gallo. Cutting edge: mast cell antimicrobial activity is mediated by expression of cathelicidin antimicrobial peptide. *J Immunol.* 2003; 170(5): 2274-2278.

Dietrich, N., M. Rohde, R. Geffers, A. Kroger, H. Hauser, S. Weiss and N. O. Gekara. Mast cells elicit proinflammatory but not type I interferon responses upon activation of TLRs by bacteria. *Proc Natl Acad Sci U S A.* 2010; 107(19): 8748-8753.

Donald, H. B. and A. Isaacs. Counts of influenza virus particles. *J Gen Microbiol.* 1954; 10(3): 457-464.

Dvorak, A. M. Mast cell secretory granules and lipid bodies contain the necessary machinery important for the in situ synthesis of proteins. *Chem Immunol Allergy.* 2005; 85: 252-315.

Dvorak, A. M., H. F. Dvorak, S. P. Peters, E. S. Shulman, D. W. MacGlashan, Jr., K. Pyne, V. S. Harvey, S. J. Galli and L. M. Lichtenstein. Lipid bodies: cytoplasmic organelles important to arachidonate metabolism in macrophages and mast cells. *J Immunol.* 1983; 131(6): 2965-2976.

Elankumaran, S., V. Chavan, D. Qiao, R. Shobana, G. Moorkanat, M. Biswas and S. K. Samal. Type I interferon-sensitive recombinant newcastle disease virus for oncolytic virotherapy. *J Virol.* 2010; 84(8): 3835-3844.

Eppig, J. T., J. A. Blake, C. J. Bult, J. A. Kadin and J. E. Richardson. The Mouse Genome Database (MGD): comprehensive resource for genetics and genomics of the laboratory mouse. *Nucleic Acids Res.* 2012; 40(Database issue): D881-886.

Espert, L., G. Degols, Y. L. Lin, T. Vincent, M. Benkirane and N. Mechti. Interferon-induced exonuclease ISG20 exhibits an antiviral activity against human immunodeficiency virus type 1. *J Gen Virol.* 2005; 86(Pt 8): 2221-2229.

Everitt, A. R., S. Clare, T. Pertel, S. P. John, R. S. Wash, S. E. Smith, C. R. Chin, E. M. Feeley, J. S. Sims, D. J. Adams, H. M. Wise, L. Kane, D. Goulding, P. Digard, V. Anttila, J. K. Baillie, T. S. Walsh, D. A. Hume, A. Palotie, Y. Xue, V. Colonna, C. Tyler-Smith, J. Dunning, S. B. Gordon, R. L. Smyth, P. J. Openshaw, G. Dougan, A. L. Brass and P. Kellam. IFITM3 restricts the morbidity and mortality associated with influenza. *Nature.* 2012; 484(7395): 519-523.

Feeley, E. M., J. S. Sims, S. P. John, C. R. Chin, T. Pertel, L.-M. Chen, G. D. Gaiha, B. J. Ryan, R. O. Donis, S. J. Elledge and A. L. Brass. IFITM3 Inhibits Influenza A Virus Infection by Preventing Cytosolic Entry. *PLoS Pathog.* 2011; 7(10): e1002337.

Fields, S. and O. Song. A novel genetic system to detect protein-protein interactions. *Nature.* 1989; 340(6230): 245-246.

Fink, J., F. Gu, L. Ling, T. Tolfvenstam, F. Olfat, K. C. Chin, P. Aw, J. George, V. A. Kuznetsov, M. Schreiber, S. G. Vasudevan and M. L. Hibberd. Host Gene Expression Profiling of Dengue Virus Infection in Cell Lines and Patients. *PLoS Negl Trop Dis.* 2007; 1(2): e86.

Fitzgerald, K. A., S. M. McWhirter, K. L. Faia, D. C. Rowe, E. Latz, D. T. Golenbock, A. J. Coyle, S. M. Liao and T. Maniatis. IKKepsilon and TBK1 are essential components of the IRF3 signaling pathway. *Nat Immunol.* 2003; 4(5): 491-496.

Fitzgerald, K. A., D. C. Rowe, B. J. Barnes, D. R. Caffrey, A. Visintin, E. Latz, B. Monks, P. M. Pitha and D. T. Golenbock. LPS-TLR4 signaling to IRF-3/7 and NF-kappaB involves the toll adapters TRAM and TRIF. *J Exp Med.* 2003; 198(7): 1043-1055.

Fredericksen, B. L. and M. Gale. West Nile Virus Evades Activation of Interferon Regulatory Factor 3 through RIG-I-Dependent and -Independent Pathways without Antagonizing Host Defense Signaling. *Journal of Virology.* 2006; 80(6): 2913-2923.

Fujimoto, T., Y. Ohsaki, J. Cheng, M. Suzuki and Y. Shinohara. Lipid droplets: a classic organelle with new outfits. *Histochem Cell Biol.* 2008; 130(2): 263-279.

Furuta, T., L. A. Murao, N. T. Lan, N. T. Huy, V. T. Huong, T. T. Thuy, V. D. Tham, C. T. Nga, T. T. Ha, Y. Ohmoto, M. Kikuchi, K. Morita, M. Yasunami, K. Hirayama and N. Watanabe. Association of mast cell-derived VEGF and proteases in Dengue shock syndrome. *PLoS Negl Trop Dis.* 2012; 6(2): e1505.

Gabilondo, A. M., J. Hegler, C. Krasel, V. Boivin-Jahns, L. Hein and M. J. Lohse. A dileucine motif in the C terminus of the beta2-adrenergic receptor is involved in receptor internalization. *Proc Natl Acad Sci U S A.* 1997; 94(23): 12285-12290.

Galli, S. J., A. M. Dvorak, J. A. Marcum, T. Ishizaka, G. Nabel, H. Der Simonian, K. Pyne, J. M. Goldin, R. D. Rosenberg, H. Cantor and H. F. Dvorak. Mast cell

clones: a model for the analysis of cellular maturation. *J Cell Biol.* 1982; 95(2 Pt 1): 435-444.

Galli, S. J., M. Grimbaldeston and M. Tsai. Immunomodulatory mast cells: negative, as well as positive, regulators of immunity. *Nat Rev Immunol.* 2008; 8(6): 478-486.

Galli, S. J., J. Kalesnikoff, M. A. Grimbaldeston, A. M. Piliponsky, C. M. Williams and M. Tsai. Mast cells as "tunable" effector and immunoregulatory cells: recent advances. *Annu Rev Immunol.* 2005; 23: 749-786.

Galli, S. J., S. Nakae and M. Tsai. Mast cells in the development of adaptive immune responses. *Nat Immunol.* 2005; 6(2): 135-142.

Galli, S. J. and M. Tsai. Mast cells in allergy and infection: versatile effector and regulatory cells in innate and adaptive immunity. *Eur J Immunol.* 2010; 40(7): 1843-1851.

Gassmann, M., B. Grenacher, B. Rohde and J. Vogel. Quantifying Western blots: pitfalls of densitometry. *Electrophoresis.* 2009; 30(11): 1845-1855.

Gifford, C. A., A. M. Assiri, M. C. Satterfield, T. E. Spencer and T. L. Ott. Receptor transporter protein 4 (RTP4) in endometrium, ovary, and peripheral blood leukocytes of pregnant and cyclic ewes. *Biol Reprod.* 2008; 79(3): 518-524.

Gonzalez-Navajas, J. M., J. Lee, M. David and E. Raz. Immunomodulatory functions of type I interferons. *Nat Rev Immunol.* 2012; 12(2): 125-135.

Guha-Thakurta, N. and J. A. Majde. Early induction of proinflammatory cytokine and type I interferon mRNAs following Newcastle disease virus, poly [rI:rC], or low-dose LPS challenge of the mouse. *J Interferon Cytokine Res.* 1997; 17(4): 197-204.

Guhl, S., R. Franke, A. Schielke, R. Johne, D. H. Kruger, M. Babina and A. Rang. Infection of in vivo differentiated human mast cells with hantaviruses. *J Gen Virol.* 2010; 91(Pt 5): 1256-1261.

Gurish, M. F. and J. A. Boyce. Mast cells: ontogeny, homing, and recruitment of a unique innate effector cell. *J Allergy Clin Immunol.* 2006; 117(6): 1285-1291.

Gurish, M. F., H. Tao, J. P. Abonia, A. Arya, D. S. Friend, C. M. Parker and K. F. Austen. Intestinal mast cell progenitors require CD49dbeta7 (alpha4beta7 integrin) for tissue-specific homing. *J Exp Med.* 2001; 194(9): 1243-1252.

Haller, O. and G. Kochs. Interferon-Induced Mx Proteins: Dynamin-Like GTPases with Antiviral Activity. *Traffic.* 2002; 3(10): 710-717.

Hannan, S., M. E. Wilkins, E. Dehghani-Tafti, P. Thomas, S. M. Baddeley and T. G. Smart. Gamma-aminobutyric acid type B (GABA(B)) receptor internalization is regulated by the R2 subunit. *J Biol Chem.* 2011; 286(27): 24324-24335.

Hanyaloglu, A. C. and M. von Zastrow. Regulation of GPCRs by endocytic membrane trafficking and its potential implications. *Annu Rev Pharmacol Toxicol.* 2008; 48: 537-568.

Hayashi, H., H. Matsubara, T. Yokota, I. Kuwabara, M. Kanno, H. Koseki, K. Isono, T. Asano and M. Taniguchi. Molecular cloning and characterization of the gene encoding mouse melanoma antigen by cDNA library transfection. *J Immunol.* 1992; 149(4): 1223-1229.

Hefti, H. P., M. Frese, H. Landis, C. Di Paolo, A. Aguzzi, O. Haller and J. Pavlovic. Human MxA protein protects mice lacking a functional alpha/beta interferon system against La crosse virus and other lethal viral infections. *J Virol.* 1999; 73(8): 6984-6991.

Helbig, K. J., D. T. Lau, L. Semendric, H. A. Harley and M. R. Beard. Analysis of ISG expression in chronic hepatitis C identifies viperin as a potential antiviral effector. *Hepatology.* 2005; 42(3): 702-710.

Hinson, E. R. and P. Cresswell. The antiviral protein, viperin, localizes to lipid droplets via its N-terminal amphipathic alpha-helix. *Proc Natl Acad Sci U S A.* 2009; 106(48): 20452-20457.

Hinson, E. R., N. S. Joshi, J. H. Chen, C. Rahner, Y. W. Jung, X. Wang, S. M. Kaech and P. Cresswell. Viperin is highly induced in neutrophils and macrophages during acute and chronic lymphocytic choriomeningitis virus infection. *J Immunol.* 2010; 184(10): 5723-5731.

Hodges, B. D. and C. C. Wu. Proteomic insights into an expanded cellular role for cytoplasmic lipid droplets. *J Lipid Res.* 2010; 51(2): 262-273.

Honda, K., H. Yanai, A. Takaoka and T. Taniguchi. Regulation of the type I IFN induction: a current view. *Int Immunol.* 2005; 17(11): 1367-1378.

Hornung, V., W. Barchet, M. Schlee and G. Hartmann. RNA recognition via TLR7 and TLR8. *Handb Exp Pharmacol.* 2008; (183): 71-86.

Hornung, V., J. Ellegast, S. Kim, K. Brzozka, A. Jung, H. Kato, H. Poeck, S. Akira, K. K. Conzelmann, M. Schlee, S. Endres and G. Hartmann. 5'-Triphosphate RNA is the ligand for RIG-I. *Science.* 2006; 314(5801): 994-997.

Hu, Y., Y. Jin, D. Han, G. Zhang, S. Cao, J. Xie, J. Xue, Y. Li, D. Meng, X. Fan, L. Q. Sun and M. Wang. Mast cell-induced lung injury in mice infected with H5N1 influenza virus. *J Virol.* 2012; 86(6): 3347-3356.

Hu, Z. Q., W. H. Zhao and T. Shimamura. Regulation of mast cell development by inflammatory factors. *Curr Med Chem.* 2007; 14(28): 3044-3050.

Huang, D. W., B. T. Sherman and R. A. Lempicki. Systematic and integrative analysis of large gene lists using DAVID bioinformatics resources. *Nat. Protocols.* 2008; 4(1): 44-57.

Huang, D. W., B. T. Sherman and R. A. Lempicki. Bioinformatics enrichment tools: paths toward the comprehensive functional analysis of large gene lists. *Nucleic Acids Res.* 2009; 37(1): 1-13.

Inaba, K., M. Inaba, N. Romani, H. Aya, M. Deguchi, S. Ikehara, S. Muramatsu and R. M. Steinman. Generation of large numbers of dendritic cells from mouse bone marrow cultures supplemented with granulocyte/macrophage colony-stimulating factor. *J Exp Med.* 1992; 176(6): 1693-1702.

Ishikawa, H. and G. N. Barber. The STING pathway and regulation of innate immune signaling in response to DNA pathogens. *Cell Mol Life Sci.* 2011; 68(7): 1157-1165.

Iversen, M. B. and S. R. Paludan. Mechanisms of type III interferon expression. *J Interferon Cytokine Res.* 2010; 30(8): 573-578.

Jensen, B. M., J. E. Swindle, S. Iwaki and A. M. Gilfillan. Generation, Isolation and Maintenance of Rodent Mast Cells and Mast Cell Lines. Current Protocols in Immunology. New York, John Wiley & Sons. Inc 2006. 3.23.21 - 23.23.13.

Jiang, D., H. Guo, C. Xu, J. Chang, B. Gu, L. Wang, T. M. Block and J. T. Guo. Identification of three interferon-inducible cellular enzymes that inhibit the replication of hepatitis C virus. *J Virol.* 2008; 82(4): 1665-1678.

Jiang, Z., T. W. Mak, G. Sen and X. Li. Toll-like receptor 3-mediated activation of NF-kappaB and IRF3 diverges at Toll-IL-1 receptor domain-containing adapter inducing IFN-beta. *Proc Natl Acad Sci U S A.* 2004; 101(10): 3533-3538.

Jolly, S., J. Detilleux and D. Desmecht. Extensive mast cell degranulation in bovine respiratory syncytial virus-associated paroxystic respiratory distress syndrome. *Vet Immunol Immunopathol.* 2004; 97(3-4): 125-136.

Juremalm, M. and G. Nilsson. Chemokine receptor expression by mast cells. *Chem Immunol Allergy.* 2005; 87: 130-144.

Karnik, S. S., C. Gogonea, S. Patil, Y. Saad and T. Takezako. Activation of G-protein-coupled receptors: a common molecular mechanism. *Trends Endocrinol Metab.* 2003; 14(9): 431-437.

Kashem, S. W., H. Subramanian, S. J. Collington, P. Magotti, J. D. Lambris and H. Ali. G protein coupled receptor specificity for C3a and compound 48/80-induced degranulation in human mast cells: roles of Mas-related genes MrgX1 and MrgX2. *Eur J Pharmacol.* 2011; 668(1-2): 299-304.

Kato, H., O. Takeuchi, E. Mikamo-Satoh, R. Hirai, T. Kawai, K. Matsushita, A. Hiiragi, T. S. Dermody, T. Fujita and S. Akira. Length-dependent recognition of double-stranded ribonucleic acids by retinoic acid-inducible gene-I and melanoma differentiation-associated gene 5. *J Exp Med.* 2008; 205(7): 1601-1610.

Kato, H., O. Takeuchi, S. Sato, M. Yoneyama, M. Yamamoto, K. Matsui, S. Uematsu, A. Jung, T. Kawai, K. J. Ishii, O. Yamaguchi, K. Otsu, T. Tsujimura, C. S. Koh, C. Reis e Sousa, Y. Matsuura, T. Fujita and S. Akira. Differential roles of MDA5 and RIG-I helicases in the recognition of RNA viruses. *Nature.* 2006; 441(7089): 101-105.

Katritch, V., V. Cherezov and R. C. Stevens. Diversity and modularity of G protein-coupled receptor structures. *Trends Pharmacol Sci.* 2012; 33(1): 17-27.

Kawai, T. and S. Akira. Toll-like receptor and RIG-I-like receptor signaling. *Ann N Y Acad Sci.* 2008; 1143: 1-20.

Kawai, T. and S. Akira. Toll-like receptors and their crosstalk with other innate receptors in infection and immunity. *Immunity.* 2011; 34(5): 637-650.

Kersse, K., M. J. Bertrand, M. Lamkanfi and P. Vandenabeele. NOD-like receptors and the innate immune system: coping with danger, damage and death. *Cytokine Growth Factor Rev.* 2011; 22(5-6): 257-276.

Khaiboullina, S. F., A. A. Rizvanov, M. R. Holbrook and S. St Jeor. Yellow fever virus strains Asibi and 17D-204 infect human umbilical cord endothelial cells and induce novel changes in gene expression. *Virology.* 2005; 342(2): 167-176.

Khattar, S. K., S. Kumar, S. Xiao, P. L. Collins and S. K. Samal. Experimental infection of mice with avian paramyxovirus serotypes 1 to 9. *PLoS One.* 2011; 6(2): e16776.

Kimple, A. J., D. E. Bosch, P. M. Giguere and D. P. Siderovski. Regulators of G-protein signaling and their Galpha substrates: promises and challenges in their use as drug discovery targets. *Pharmacol Rev.* 2011; 63(3): 728-749.

King, C. A., R. Anderson and J. S. Marshall. Dengue virus selectively induces human mast cell chemokine production. *J Virol.* 2002; 76(16): 8408-8419.

Koyama, S., K. J. Ishii, C. Coban and S. Akira. Innate immune response to viral infection. *Cytokine.* 2008; 43(3): 336-341.

Koyama, S., K. J. Ishii, H. Kumar, T. Tanimoto, C. Coban, S. Uematsu, T. Kawai and S. Akira. Differential role of TLR- and RLR-signaling in the immune responses to influenza A virus infection and vaccination. *J Immunol.* 2007; 179(7): 4711-4720.

Krishnaswamy, G., O. Ajitawi and D. S. Chi. The human mast cell: an overview. *Methods Mol Biol.* 2006; 315: 13-34.

Kristiansen, H., H. H. Gad, S. Eskildsen-Larsen, P. Despres and R. Hartmann. The oligoadenylate synthetase family: an ancient protein family with multiple antiviral activities. *J Interferon Cytokine Res.* 2011; 31(1): 41-47.

Kulka, M., L. Alexopoulou, R. A. Flavell and D. D. Metcalfe. Activation of mast cells by double-stranded RNA: evidence for activation through Toll-like receptor 3. *J Allergy Clin Immunol.* 2004; 114(1): 174-182.

Kumar, V. and A. Sharma. Mast cells: emerging sentinel innate immune cells with diverse role in immunity. *Mol Immunol.* 2010; 48(1-3): 14-25.

Lee, M. S., J. M. Roos, L. C. McGuigan, K. A. Smith, N. Cormier, L. K. Cohen, B. E. Roberts and L. G. Payne. Molecular attenuation of vaccinia virus: mutant generation and animal characterization. *J Virol.* 1992; 66(5): 2617-2630.

Lee, S. M. Y., J. L. Gardy, C. Y. Cheung, T. K. W. Cheung, K. P. Y. Hui, N. Y. Ip, Y. Guan, R. E. W. Hancock and J. S. M. Peiris. Systems-Level Comparison of Host-Responses Elicited by Avian H5N1 and Seasonal H1N1 Influenza Viruses in Primary Human Macrophages. *PLoS One.* 2009; 4(12): e8072.

Levy, D. E., R. A. Lerner and M. C. Wilson. The Gv-1 locus coordinately regulates the expression of multiple endogenous murine retroviruses. *Cell.* 1985; 41(1): 289-299.

Li, Z., K. C. Wolff and C. E. Samuel. RNA adenosine deaminase ADAR1 deficiency leads to increased activation of protein kinase PKR and reduced vesicular stomatitis virus growth following interferon treatment. *Virology.* 2010; 396(2): 316-322.

Lilley, K. S. and D. B. Friedman. All about DIGE: quantification technology for differential-display 2D-gel proteomics. *Expert Rev Proteomics.* 2004; 1(4): 401-409.

Lin, R. J., H. P. Yu, B. L. Chang, W. C. Tang, C. L. Liao and Y. L. Lin. Distinct antiviral roles for human 2',5'-oligoadenylate synthetase family members against dengue virus infection. *J Immunol.* 2009; 183(12): 8035-8043.

Liu, Y. J. IPC: professional type 1 interferon-producing cells and plasmacytoid dendritic cell precursors. *Annu Rev Immunol.* 2005; 23: 275-306.

Loo, Y. M. and M. Gale, Jr. Immune signaling by RIG-I-like receptors. *Immunity.* 2011; 34(5): 680-692.

Lu, X., T. M. Tumpey, T. Morken, S. R. Zaki, N. J. Cox and J. M. Katz. A mouse model for the evaluation of pathogenesis and immunity to influenza A (H5N1) viruses isolated from humans. *J Virol.* 1999; 73(7): 5903-5911.

Luckhardt, T. R., S. M. Coomes, G. Trujillo, J. S. Stoolman, K. M. Vannella, U. Bhan, C. A. Wilke, T. A. Moore, G. B. Toews, C. Hogaboam and B. B. Moore. TLR9-induced interferon beta is associated with protection from gammaherpesvirus-induced exacerbation of lung fibrosis. *Fibrogenesis Tissue Repair.* 2011; 4: 18.

MacLachlan, N. J. and E. J. Dubovi. Fenner's Veterinary Virology. 2010. Academic Press.

Magalhaes, A. C., H. Dunn and S. S. G. Ferguson. Regulation of GPCR activity, trafficking and localization by GPCR-interacting proteins. *British Journal of Pharmacology.* 2012; 165(6): 1717-1736.

Marshall, J. S. Mast-cell responses to pathogens. *Nat Rev Immunol.* 2004; 4(10): 787-799.

Matsui, K., Y. Kumagai, H. Kato, S. Sato, T. Kawagoe, S. Uematsu, O. Takeuchi and S. Akira. Cutting edge: Role of TANK-binding kinase 1 and inducible IkappaB kinase in IFN responses against viruses in innate immune cells. *J Immunol.* 2006; 177(9): 5785-5789.

Matsushima, H., N. Yamada, H. Matsue and S. Shimada. TLR3-, TLR7-, and TLR9-mediated production of proinflammatory cytokines and chemokines from murine connective tissue type skin-derived mast cells but not from bone marrow-derived mast cells. *J Immunol.* 2004; 173(1): 531-541.

McAlpine, S. M., T. B. Issekutz and J. S. Marshall. Virus stimulation of human mast cells results in the recruitment of CD56(+) T cells by a mechanism dependent on CCR5 ligands. *FASEB J.* 2012; 26(3): 1280-1289.

McCartney, S. A., W. Vermi, S. Lonardi, C. Rossini, K. Otero, B. Calderon, S. Gilfillan, M. S. Diamond, E. R. Unanue and M. Colonna. RNA sensor-induced type I IFN prevents diabetes caused by a beta cell-tropic virus in mice. *J Clin Invest.* 2011; 121(4): 1497-1507.

McFerran, J. B. and R. Nelson. Some properties of an avirulent Newcastle disease virus. *Arch Gesamte Virusforsch.* 1971; 34(1): 64-74.

McGinnes, L. W., H. Pantua, J. Reitter and T. G. Morrison. Newcastle disease virus: propagation, quantification, and storage. *Curr Protoc Microbiol.* 2006; Chapter 15: Unit 15F 12.

Melchjorsen, J., J. Rintahaka, S. Soby, K. A. Horan, A. Poltajainen, L. Ostergaard, S. R. Paludan and S. Matikainen. Early innate recognition of herpes simplex virus in human primary macrophages is mediated via the MDA5/MAVS-dependent and MDA5/MAVS/RNA polymerase III-independent pathways. *J Virol.* 2010; 84(21): 11350-11358.

Metcalfe, D. D., D. Baram and Y. A. Mekori. Mast cells. *Physiol Rev.* 1997; 77(4): 1033-1079.

Metz, M., M. A. Grimbaldeston, S. Nakae, A. M. Piliponsky, M. Tsai and S. J. Galli. Mast cells in the promotion and limitation of chronic inflammation. *Immunol Rev.* 2007; 217: 304-328.

Mihalich, A., P. Viganò, D. Gentilini, M. O. Borghi, M. Vignali, M. Busacca and A. Di Blasio. Interferon-inducible genes, TNF-related apoptosis-inducing ligand (TRAIL) and interferon inducible protein 27 (IFI27) are negatively regulated in leiomyomas: implications for a role of the interferon pathway in leiomyoma development. *Gynecological Endocrinology.* 2012; 28(3): 216-219.

Miller, A. L., T. L. Bowlin and N. W. Lukacs. Respiratory syncytial virus-induced chemokine production: linking viral replication to chemokine production in vitro and in vivo. *J Infect Dis.* 2004; 189(8): 1419-1430.

Murphy, K. M., P. Travers, M. Walport and C. Janeway. Janeway's Immunobiology. 2011. Garland Science.

Muzio, M., D. Bosisio, N. Polentarutti, G. D'Amico, A. Stoppacciaro, R. Mancinelli, C. van't Veer, G. Penton-Rol, L. P. Ruco, P. Allavena and A. Mantovani. Differential expression and regulation of toll-like receptors (TLR) in human leukocytes: selective expression of TLR3 in dendritic cells. *J Immunol.* 2000; 164(11): 5998-6004.

Nakai, K. and P. Horton. PSORT: a program for detecting sorting signals in proteins and predicting their subcellular localization. *Trends Biochem Sci.* 1999; 24(1): 34-36.

Nasr, N., S. Maddocks, S. G. Turville, A. N. Harman, N. Woolger, K. J. Helbig, J. Wilkinson, C. R. Bye, T. K. Wright, D. Rambukwelle, H. Donaghy, M. R. Beard and A. L. Cunningham. HIV-1 infection of human macrophages directly induces viperin which inhibits viral production. *Blood.* 2012; 120(4): 778-788.

Newton, K. and V. M. Dixit. Signaling in innate immunity and inflammation. *Cold Spring Harb Perspect Biol.* 2012; 4(3).

Noppert, S. J., K. A. Fitzgerald and P. J. Hertzog. The role of type I interferons in TLR responses. *Immunol Cell Biol.* 2007; 85(6): 446-457.

Oganesyan, G., S. K. Saha, B. Guo, J. Q. He, A. Shahangian, B. Zarnegar, A. Perry and G. Cheng. Critical role of TRAF3 in the Toll-like receptor-dependent and -independent antiviral response. *Nature.* 2006; 439(7073): 208-211.

Onoguchi, K., M. Yoneyama, A. Takemura, S. Akira, T. Taniguchi, H. Namiki and T. Fujita. Viral infections activate types I and III interferon genes through a common mechanism. *J Biol Chem.* 2007; 282(10): 7576-7581.

Opitz, B., A. Rejaibi, B. Dauber, J. Eckhard, M. Vinzing, B. Schmeck, S. Hippenstiel, N. Suttorp and T. Wolff. IFNbeta induction by influenza A virus is mediated by RIG-I which is regulated by the viral NS1 protein. *Cell Microbiol.* 2007; 9(4): 930-938.

Orinska, Z., E. Bulanova, V. Budagian, M. Metz, M. Maurer and S. Bulfone-Paus. TLR3-induced activation of mast cells modulates CD8+ T-cell recruitment. *Blood.* 2005; 106(3): 978-987.

Oyoshi, M. K., A. Elkhal, L. Kumar, J. E. Scott, S. Koduru, R. He, D. Y. Leung, M. D. Howell, H. C. Oettgen, G. F. Murphy and R. S. Geha. Vaccinia virus inoculation in sites of allergic skin inflammation elicits a vigorous cutaneous IL-17 response. *Proc Natl Acad Sci U S A.* 2009; 106(35): 14954-14959.

Penno, M. A., M. Klingler-Hoffmann, J. A. Brazzatti, A. Boussioutas, T. Putoczki, M. Ernst and P. Hoffmann. 2D-DIGE analysis of sera from transgenic mouse models reveals novel candidate protein biomarkers for human gastric cancer. *J Proteomics.* 2012.

Pfaffl, M. W. A new mathematical model for relative quantification in real-time RT-PCR. *Nucleic Acids Res.* 2001; 29(9): e45.

Pichlmair, A., C. Lassnig, C. A. Eberle, M. W. Gorna, C. L. Baumann, T. R. Burkard, T. Burckstummer, A. Stefanovic, S. Krieger, K. L. Bennett, T. Rulicke, F. Weber, J. Colinge, M. Muller and G. Superti-Furga. IFIT1 is an antiviral protein that recognizes 5'-triphosphate RNA. *Nat Immunol.* 2011; 12(7): 624-630.

Pichlmair, A., O. Schulz, C. P. Tan, T. I. Näslund, P. Liljeström, F. Weber and C. Reis e Sousa. RIG-I-Mediated Antiviral Responses to Single-Stranded RNA Bearing 5'-Phosphates. *Science.* 2006; 314(5801): 997-1001.

Ploegh, H. L. A lipid-based model for the creation of an escape hatch from the endoplasmic reticulum. *Nature.* 2007; 448(7152): 435-438.

Preisser, L., N. Ancellin, L. Michaelis, C. Creminon, A. Morel and B. Corman. Role of the carboxyl-terminal region, di-leucine motif and cysteine residues in signalling and internalization of vasopressin V1a receptor. *FEBS Lett.* 1999; 460(2): 303-308.

Rathinam, V. A., S. K. Vanaja and K. A. Fitzgerald. Regulation of inflammasome signaling. *Nat Immunol.* 2012; 13(4): 333-332.

Razin, E., J. N. Ihle, D. Seldin, J. M. Mencia-Huerta, H. R. Katz, P. A. LeBlanc, A. Hein, J. P. Caulfield, K. F. Austen and R. L. Stevens. Interleukin 3: A differentiation and growth factor for the mouse mast cell that contains chondroitin sulfate E proteoglycan. *J Immunol.* 1984; 132(3): 1479-1486.

Reder, A. T., S. Velichko, K. D. Yamaguchi, K. Hamamcioglu, K. Ku, J. Beekman, T. C. Wagner, H. D. Perez, H. Salamon and E. Croze. IFN-beta1b induces transient and variable gene expression in relapsing-remitting multiple sclerosis patients independent of neutralizing antibodies or changes in IFN receptor RNA expression. *J Interferon Cytokine Res.* 2008; 28(5): 317-331.

Ritchie, K. J., C. S. Hahn, K. I. Kim, M. Yan, D. Rosario, L. Li, J. C. de la Torre and D. E. Zhang. Role of ISG15 protease UBP43 (USP18) in innate immunity to viral infection. *Nat Med.* 2004; 10(12): 1374-1378.

Robenek, H., O. Hofnagel, I. Buers, M. J. Robenek, D. Troyer and N. J. Severs. Adipophilin-enriched domains in the ER membrane are sites of lipid droplet biogenesis. *Journal of Cell Science.* 2006; 119(20): 4215-4224.

Robenek, M. J., N. J. Severs, K. Schlattmann, G. Plenz, K. P. Zimmer, D. Troyer and H. Robenek. Lipids partition caveolin-1 from ER membranes into lipid droplets: updating the model of lipid droplet biogenesis. *FASEB J.* 2004; 18(7): 866-868.

Rommel, C., M. Camps and H. Ji. PI3K delta and PI3K gamma: partners in crime in inflammation in rheumatoid arthritis and beyond? *Nat Rev Immunol.* 2007; 7(3): 191-201.

Rosenbaum, D. M., S. G. Rasmussen and B. K. Kobilka. The structure and function of G-protein-coupled receptors. *Nature.* 2009; 459(7245): 356-363.

Rothenfusser, S., N. Goutagny, G. DiPerna, M. Gong, B. G. Monks, A. Schoenemeyer, M. Yamamoto, S. Akira and K. A. Fitzgerald. The RNA helicase Lgp2 inhibits TLR-independent sensing of viral replication by retinoic acid-inducible gene-I. *J Immunol.* 2005; 175(8): 5260-5268.

Sadler, A. J. and B. R. Williams. Interferon-inducible antiviral effectors. *Nat Rev Immunol.* 2008; 8(7): 559-568.

Saito, H., M. Kubota, R. W. Roberts, Q. Chi and H. Matsunami. RTP family members induce functional expression of mammalian odorant receptors. *Cell.* 2004; 119(5): 679-691.

Saito, T., R. Hirai, Y. M. Loo, D. Owen, C. L. Johnson, S. C. Sinha, S. Akira, T. Fujita and M. Gale, Jr. Regulation of innate antiviral defenses through a shared repressor domain in RIG-I and LGP2. *Proc Natl Acad Sci U S A.* 2007; 104(2): 582-587.

Saito, T., D. M. Owen, F. Jiang, J. Marcotrigiano and M. Gale, Jr. Innate immunity induced by composition-dependent RIG-I recognition of hepatitis C virus RNA. *Nature.* 2008; 454(7203): 523-527.

Salerno, A., M. Albanese and P. Byfield. Effects of Newcastle disease virus (NDV) on infection of adult mice with the Thogoto-like Ar-126 arbovirus. *Pathol Microbiol (Basel).* 1975; 43(4): 299-306.

Sanda, C., P. Weitzel, T. Tsukahara, J. Schaley, H. J. Edenberg, M. A. Stephens, J. N. McClintick, L. M. Blatt, L. Li, L. Brodsky and M. W. Taylor. Differential gene induction by type I and type II interferons and their combination. *J Interferon Cytokine Res.* 2006; 26(7): 462-472.

Sarasin-Filipowicz, M., E. J. Oakeley, F. H. Duong, V. Christen, L. Terracciano, W. Filipowicz and M. H. Heim. Interferon signaling and treatment outcome in chronic hepatitis C. *Proc Natl Acad Sci U S A.* 2008; 105(19): 7034-7039.

Sasai, M., M. Matsumoto and T. Seya. The kinase complex responsible for IRF-3-mediated IFN-beta production in myeloid dendritic cells (mDC). *J Biochem.* 2006; 139(2): 171-175.

Schoggins, J. W., S. J. Wilson, M. Panis, M. Y. Murphy, C. T. Jones, P. Bieniasz and C. M. Rice. A diverse range of gene products are effectors of the type I interferon antiviral response. *Nature.* 2011; 472(7344): 481-485.

Seo, J. Y., R. Yaneva and P. Cresswell. Viperin: a multifunctional, interferon-inducible protein that regulates virus replication. *Cell Host Microbe.* 2011; 10(6): 534-539.

Serebriiskii, I. G. and E. A. Golemis. Uses of lacZ to study gene function: evaluation of beta-galactosidase assays employed in the yeast two-hybrid system. *Anal Biochem.* 2000; 285(1): 1-15.

Shinya, K., T. Okamura, S. Sueta, N. Kasai, M. Tanaka, T. E. Ginting, A. Makino, A. J. Eisfeld and Y. Kawaoka. Toll-like receptor pre-stimulation protects mice against lethal infection with highly pathogenic influenza viruses. *Virol J.* 2011; 8: 97.

Shirato, K. and F. Taguchi. Mast cell degranulation is induced by A549 airway epithelial cell infected with respiratory syncytial virus. *Virology.* 2009; 386(1): 88-93.

St John, A. L., A. P. Rathore, H. Yap, M. L. Ng, D. D. Metcalfe, S. G. Vasudevan and S. N. Abraham. Immune surveillance by mast cells during dengue infection promotes natural killer (NK) and NKT-cell recruitment and viral clearance. *Proc Natl Acad Sci U S A.* 2011; 108(22): 9190-9195.

Stelekati, E. (2007). The role of mast cells in CD8+ T cell-mediated immune responses. PhD, Christian-Albrecht-Universität zu Kiel.

Stelekati, E., R. Bahri, O. D'Orlando, Z. Orinska, H. W. Mittrucker, R. Langenhaun, M. Glatzel, A. Bollinger, R. Paus and S. Bulfone-Paus. Mast cell-mediated antigen presentation regulates CD8+ T cell effector functions. *Immunity.* 2009; 31(4): 665-676.

Stetson, D. B. and R. Medzhitov. Type I interferons in host defense. *Immunity.* 2006; 25(3): 373-381.

Suh, W. K., M. F. Cohen-Doyle, K. Fruh, K. Wang, P. A. Peterson and D. B. Williams. Interaction of MHC class I molecules with the transporter associated with antigen processing. *Science.* 1994; 264(5163): 1322-1326.

Sun, Q., D. Wang, R. She, W. Li, S. Liu, D. Han, Y. Wang and Y. Ding. Increased mast cell density during the infection with velogenic Newcastle disease virus in chickens. *Avian Pathol.* 2008; 37(6): 579-585.

Sundstrom, J. B., D. M. Little, F. Villinger, J. E. Ellis and A. A. Ansari. Signaling through Toll-like receptors triggers HIV-1 replication in latently infected mast cells. *J Immunol.* 2004; 172(7): 4391-4401.

Szretter, K. J., A. L. Balish and J. M. Katz. Influenza: propagation, quantification, and storage. *Curr Protoc Microbiol.* 2006; Chapter 15: Unit 15G 11.

Takaoka, A., Z. Wang, M. K. Choi, H. Yanai, H. Negishi, T. Ban, Y. Lu, M. Miyagishi, T. Kodama, K. Honda, Y. Ohba and T. Taniguchi. DAI (DLM-1/ZBP1) is a cytosolic DNA sensor and an activator of innate immune response. *Nature.* 2007; 448(7152): 501-505.

Takaoka, A. and H. Yanai. Interferon signalling network in innate defence. *Cell Microbiol.* 2006; 8(6): 907-922.

Takeuchi, O. and S. Akira. Recognition of viruses by innate immunity. *Immunol Rev.* 2007; 220: 214-224.

Tan, C. M., A. E. Brady, H. H. Nickols, Q. Wang and L. E. Limbird. Membrane trafficking of G protein-coupled receptors. *Annu Rev Pharmacol Toxicol.* 2004; 44: 559-609.

Taylor, A. R., D. G. Sharp, D. Beard, J. W. Beard, J. H. Dingle and A. E. Feller. Isolation and Characterization of Influenza A Virus (PR8 Strain). *The Journal of Immunology.* 1943; 47(3): 261-282.

Thompson, M. R., J. J. Kaminski, E. A. Kurt-Jones and K. A. Fitzgerald. Pattern recognition receptors and the innate immune response to viral infection. *Viruses.* 2011; 3(6): 920-940.

Tracey, L., I. Spiteri, P. Ortiz, M. Lawler, M. A. Piris and R. Villuendas. Transcriptional response of T cells to IFN-alpha: changes induced in IFN-alpha-sensitive and resistant cutaneous T cell lymphoma. *J Interferon Cytokine Res.* 2004; 24(3): 185-195.

Ueta, M., T. Kawai, N. Yokoi, S. Akira and S. Kinoshita. Contribution of IPS-1 to polyI:C-induced cytokine production in conjunctival epithelial cells. *Biochem Biophys Res Commun.* 2011; 404(1): 419-423.

Unal, H. and S. S. Karnik. Domain coupling in GPCRs: the engine for induced conformational changes. *Trends Pharmacol Sci.* 2012; 33(2): 79-88.

Uthaiah, R. C., G. J. Praefcke, J. C. Howard and C. Herrmann. IIGP1, an interferon-gamma-inducible 47-kDa GTPase of the mouse, showing cooperative enzymatic activity and GTP-dependent multimerization. *J Biol Chem.* 2003; 278(31): 29336-29343.

Venter, M., T. G. Myers, M. A. Wilson, T. J. Kindt, J. T. Paweska, F. J. Burt, P. A. Leman and R. Swanepoel. Gene expression in mice infected with West Nile virus strains of different neurovirulence. *Virology.* 2005; 342(1): 119-140.

Vestal, D. J. and J. A. Jeyaratnam. The guanylate-binding proteins: emerging insights into the biochemical properties and functions of this family of large interferon-induced guanosine triphosphatase. *J Interferon Cytokine Res.* 2011; 31(1): 89-97.

Vines, C. M. and E. R. Prossnitz. Mechanisms of G protein-coupled receptor-mediated degranulation. *FEMS Microbiol Lett.* 2004; 236(1): 1-6.

Vosskuhl, K., T. F. Greten, M. P. Manns, F. Korangy and J. Wedemeyer. Lipopolysaccharide-mediated mast cell activation induces IFN-gamma secretion by NK cells. *J Immunol.* 2010; 185(1): 119-125.

Waibler, Z., M. Anzaghe, H. Ludwig, S. Akira, S. Weiss, G. Sutter and U. Kalinke. Modified Vaccinia Virus Ankara Induces Toll-Like Receptor-Independent Type I Interferon Responses. *Journal of Virology.* 2007; 81(22): 12102-12110.

Walsh, M. C., G. K. Kim, P. L. Maurizio, E. E. Molnar and Y. Choi. TRAF6 autoubiquitination-independent activation of the NFkappaB and MAPK pathways in response to IL-1 and RANKL. *PLoS One.* 2008; 3(12): e4064.

Wang, D., Y. Liu, R. She, J. Xu, L. Liu, J. Xiong, Y. Yang, Q. Sun and K. Peng. Reduced mucosal injury of SPF chickens by mast cell stabilization after infection with very virulent infectious bursal disease virus. *Vet Immunol Immunopathol.* 2009; 131(3-4): 229-237.

Wang, D., J. Xiong, R. She, L. Liu, Y. Zhang, D. Luo, W. Li, Y. Hu, Y. Wang, Q. Zhang and Q. Sun. Mast cell mediated inflammatory response in chickens after infection with very virulent infectious bursal disease virus. *Vet Immunol Immunopathol.* 2008; 124(1-2): 19-28.

Wang, X., E. R. Hinson and P. Cresswell. The interferon-inducible protein viperin inhibits influenza virus release by perturbing lipid rafts. *Cell Host Microbe.* 2007; 2(2): 96-105.

Wang, Z., M. K. Choi, T. Ban, H. Yanai, H. Negishi, Y. Lu, T. Tamura, A. Takaoka, K. Nishikura and T. Taniguchi. Regulation of innate immune responses by DAI (DLM-1/ZBP1) and other DNA-sensing molecules. *Proceedings of the National Academy of Sciences.* 2008; 105(14): 5477-5482.

Wang, Z., Y. Lai, J. J. Bernard, D. T. Macleod, A. L. Cogen, B. Moss and A. Di Nardo. Skin mast cells protect mice against vaccinia virus by triggering mast cell receptor S1PR2 and releasing antimicrobial peptides. *J Immunol.* 2012; 188(1): 345-357.

Weischenfeldt, J. and B. Porse. Bone Marrow-Derived Macrophages (BMM): Isolation and Applications. *Cold Spring Harbor Protocols.* 2008; 2008(12): pdb.prot5080.

Whitworth, G. B. An introduction to microarray data analysis and visualization. *Methods Enzymol.* 2010; 470: 19-50.

Wilden, H., P. Fournier, R. Zawatzky and V. Schirrmacher. Expression of RIG-I, IRF3, IFN-beta and IRF7 determines resistance or susceptibility of cells to infection by Newcastle Disease Virus. *Int J Oncol.* 2009; 34(4): 971-982.

Wiley, S. R., K. Schooley, P. J. Smolak, W. S. Din, C.-P. Huang, J. K. Nicholl, G. R. Sutherland, T. D. Smith, C. Rauch, C. A. Smith and R. G. Goodwin. Identification and characterization of a new member of the TNF family that induces apoptosis. *Immunity.* 1995; 3(6): 673-682.

Wu, C., C. Orozco, J. Boyer, M. Leglise, J. Goodale, S. Batalov, C. L. Hodge, J. Haase, J. Janes, J. W. Huss, 3rd and A. I. Su. BioGPS: an extensible and customizable portal for querying and organizing gene annotation resources. *Genome Biol.* 2009; 10(11): R130.

Xia, Z. P., L. Sun, X. Chen, G. Pineda, X. Jiang, A. Adhikari, W. Zeng and Z. J. Chen. Direct activation of protein kinases by unanchored polyubiquitin chains. *Nature.* 2009; 461(7260): 114-119.

Xu, Y., M. Johansson and A. Karlsson. Human UMP-CMP kinase 2, a novel nucleoside monophosphate kinase localized in mitochondria. *J Biol Chem.* 2008; 283(3): 1563-1571.

Yoneyama, M., M. Kikuchi, T. Natsukawa, N. Shinobu, T. Imaizumi, M. Miyagishi, K. Taira, S. Akira and T. Fujita. The RNA helicase RIG-I has an essential function in double-stranded RNA-induced innate antiviral responses. *Nat Immunol.* 2004; 5(7): 730-737.

Zarember, K. A. and P. J. Godowski. Tissue expression of human Toll-like receptors and differential regulation of Toll-like receptor mRNAs in leukocytes in response to microbes, their products, and cytokines. *J Immunol.* 2002; 168(2): 554-561.

Zaslavsky, E., U. Hershberg, J. Seto, A. M. Pham, S. Marquez, J. L. Duke, J. G. Wetmur, B. R. Tenoever, S. C. Sealfon and S. H. Kleinstein. Antiviral response dictated by choreographed cascade of transcription factors. *J Immunol.* 2010; 184(6): 2908-2917.

Zawatzky, R., H. Wurmbaeck, W. Falk and A. Homfeld. Endogenous interferon specifically regulates Newcastle disease virus-induced cytokine gene expression in mouse macrophages. *J Virol.* 1991; 65(9): 4839-4846.

Zhang, Z., B. Yuan, M. Bao, N. Lu, T. Kim and Y. J. Liu. The helicase DDX41 senses intracellular DNA mediated by the adaptor STING in dendritic cells. *Nat Immunol.* 2011; 12(10): 959-965.

Zinchuk, V., O. Zinchuk and T. Okada. Quantitative colocalization analysis of multicolor confocal immunofluorescence microscopy images: pushing pixels to explore biological phenomena. *Acta Histochem Cytochem.* 2007; 40(4): 101-111.

A. Appendix: Bioinformatic analysis of RTP4 sequence for identifying signal peptides and sorting signals

Input Sequence

```
QUERY (249 aa)

MLFPDDFSTW EQTFQELMQE EKPGAKWSLH LDKNIVPDGA ALGWRQHQQT
VLGRFQCSRC CRSWTSAQVM ILCHMYPDTL KSQGQARMRI FGQKCQKCFG
CQFETPKFST EIIKRILNNL VNYILQRYYG HRKIALTSNA SLGEKVTLDG
PHDTRNCEAC SLNSHGRCAL AHKVKPPRSP SPLPNSSSPS KSCPPPPQTR
NTDFGNKTLQ DFGNRTFQGC REPPQREIEP PLFLFLSIAA FALFSLFTR
```

Results of Subprograms

```
PSG:  a new signal peptide prediction method
      N-region:  length 11;  pos.chg 0;  neg.chg 3
      H-region:  length 4;  peak value   0.00
      PSG score:  -4.40

GvH:  von Heijne's method for signal seq. recognition
      GvH score (threshold: -2.1):  -7.05
      possible cleavage site: between 60 and 61

>>> Seems to have no N-terminal signal peptide

ALOM: Klein et al's method for TM region allocation
      Init position for calculation: 1
      Tentative number of TMS(s) for the threshold  0.5:   1
      Number of TMS(s) for threshold  0.5:   1
      INTEGRAL    Likelihood = -7.27   Transmembrane  232 - 248
      PERIPHERAL  Likelihood =  9.02 (at 60)
      ALOM score:  -7.27  (number of TMSs: 1)

MTOP: Prediction of membrane topology (Hartmann et al.)
      Center position for calculation: 239
      Charge difference:  1.0   C( 1.0) - N( 0.0)
      C > N: C-terminal side will be inside
```

```
>>> Single TMS is located near the C-terminus

>>> membrane topology: type Nt  (cytoplasmic tail 1 to 231)

MITDISC: discrimination of mitochondrial targeting seq
      R content:        0       Hyd Moment(75):   8.44
      Hyd Moment(95):   5.54    G content:        0
      D/E content:      2       S/T content:      0
      Score: -6.79

Gavel: prediction of cleavage sites for mitochondrial preseq
      cleavage site motif not found

NUCDISC: discrimination of nuclear localization signals
      pat4: none
      pat7: none
      bipartite: none
      content of basic residues:  12.4%
      NLS Score: -0.47

KDEL: ER retention motif in the C-terminus: none

ER Membrane Retention Signals: none

SKL: peroxisomal targeting signal in the C-terminus: none

SKL2: 2nd peroxisomal targeting signal:  none

VAC: possible vacuolar targeting motif: none

RNA-binding motif: none

Actinin-type actin-binding motif:
      type 1: none
      type 2: none

NMYR: N-myristoylation pattern : none

Prenylation motif: none

memYORL: transport motif from cell surface to Golgi: none

Tyrosines in the tail: too long tail

Dileucine motif in the tail: none

checking 63 PROSITE DNA binding motifs:  none

checking 71 PROSITE ribosomal protein motifs:  none

checking 33 PROSITE prokaryotic DNA binding motifs:  none
```

```
NNCN: Reinhardt's method for Cytplasmic/Nuclear discrimination
      Prediction: nuclear
      Reliability: 94.1

COIL: Lupas's algorithm to detect coiled-coil regions
```

Results of the *k*-NN Prediction

$k = 9/23$

```
         26.1 %: cytoplasmic
         21.7 %: nuclear
         13.0 %: vesicles of secretory system
         13.0 %: endoplasmic reticulum
          8.7 %: Golgi
          4.3 %: extracellular, including cell wall
          4.3 %: cytoskeletal
          4.3 %: plasma membrane
          4.3 %: mitochondrial

>> prediction for QUERY is cyt (k=23)
```

The RTP4 protein sequence of *M. musculus* was analyzed using the bioinformatic tool PSORT II (http://psort.hgc.jp/form2.html) that predicts protein localization sites in cells, based on the presence of signal peptides and sorting signals in the sequence of a given protein (Nakai *et al.*, 1999).

B. Appendix: Analysis of RTP4 sequences for determining the presence of di-leucine motifs

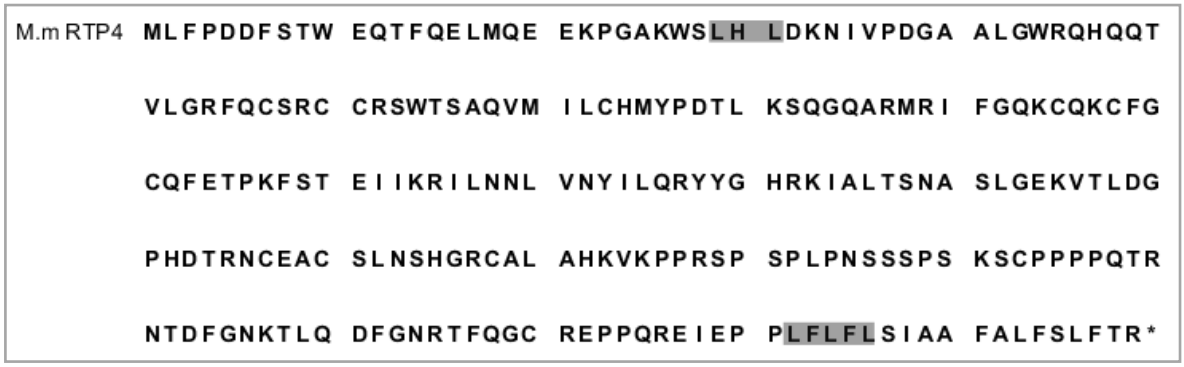

Presence of three dileucine motifs “LXL” in the sequence of murine RTP4 protein.

9. Acknowledgements

Foremost, I want to thank to “El Creador” that has given me the opportunity to achieve this goal.

My special thanks to Prof. Dr. Dr. Silvia Bulfone-Paus for the opportunity to prepare my doctoral thesis in the Immunobiology lab at FZB and for her scientific and personal support, critical discussions, for being always so optimistic, for showing me a good example of “strength” and in general for all the help I received during my work.

I am deeply grateful with Prof. Dr. Hafez Mohamed Hafez for his immense help and support that make of this dream to come true and with PD. Dr. Holger Heine for the supervision of this work. Special thanks to Annette Wallisch for the proof reading of this work.

I would like to thanks Dr. Zane Orinska for critical points of views and for all the brilliant ideas. Equally grateful with Dr. Farhad Mirghomizadeh, who taught me how to be creative in the field of molecular biology. Thanks for the scientific, personal and political talks. Special thanks to the members of the LG Immunobiology Rajia Bahri, Anne Katrin Brückner, Orietta D’Orlando, Hanno Ewers, Frauke Koops, Julia Polansky-Biskup, Gesine Rode, Katrin Streek, and Katrin Westphal.

I am also very thankful for the fruitful cooperation with Prof. Dr. Rainer Zawatzky, who kindly provided the anti-RTP4 antibody.

I also want to thank Gudrun Lehwark for her care and all the friends from the “Ausländerbande”, for great moments, for the cultural exchange that without doubt have enormously enriched my life.

And finally I would like to thank my “moms” for all their love and support throughout my stay in Borstel. Equally important and grateful with “Moni” that has been my ground and support during the last years of my PhD. This wouldn't be possible without you!

10. Eidesstattliche Erklärung

Hiermit bestätige ich, dass ich die vorliegende Arbeit selbständig angefertigt habe. Ich versichere, dass ich ausschließlich die angegebenen Quellen und Hilfen Anspruch genommen habe.